NATIONAL ADVISORY COMMITTEE FOR AERONAUTICS

WARTIME REPORT

ORIGINALLY ISSUED
September 1944 as
Memorandum Report

TESTS OF A 0.30-SCALE SEMISPAN MODEL OF THE DOUGLAS XTB2D-1 AIRPLANE WING AND FUSELAGE COMBINATION IN THE NACA 19-FOOT PRESSURE TUNNEL

I - FULL-SPAN FLAP AND AIR-BRAKE INVESTIGATION

By C. Dixon Ashworth, Stanley H. Spooner, and Robert T. Russell

Langley Memorial Aeronautical Laboratory
Langley Field, Va.

NACA

WASHINGTON

NATIONAL ADVISORY COMMITTEE FOR AERONAUTICS

MEMORANDUM REPORT

for the

Bureau of Aeronautics, Navy Department

TESTS OF A 0.30-SCALE SEMISPAN MODEL OF THE DOUGLAS XTB2D-1 AIRPLANE WING AND FUSELAGE COMBINATION IN THE NACA 19-FOOT PRESSURE TUNNEL

I - FULL-SPAN FLAP AND AIR-BRAKE INVESTIGATION

By C. Dixon Ashworth, Stanley H. Spooner, and Robert T. Russell

SUMMARY

Tests have been conducted in the NACA 19-foot pressure tunnel of a 0.30-scale semispan model of the XTB2D-1 airplane wing and fuselage combination. The purpose of the full-span flap and air-brake investigation was to determine the optimum position of the double-slotted flap, the characteristics of the full-span flaps at various deflections in their fully extended position, the effectiveness of deflecting the full-span flaps to small positive angles as a camber changing feature, the stalling characteristics of the wing, and the effectiveness of the flap as a brake when deflected to negative angles.

The data indicate that on the airplane any one flap parameter could be moved 3/16 inch from its optimum position and not appreciably affect the value of the maximum lift coefficient. A loss of flap effectiveness was encountered between 30° and 55° flap deflection due to a stall condition on the flap for nearly every configuration tested. The effective camber changing feature produced no drag reduction except above a lift coefficient of approximately 1.1. The stalling characteristics of the wing were, in general, satisfactory. For braking in a dive, decelerating, and evasive maneuvering, the brakes produced a drag coefficient increment of 0.077 at a deflection of -54° which appeared satisfactory from some preliminary calculations.

INTRODUCTION

The XTB2D-1 airplane is a proposed single-engine torpedo bomber designed by the Douglas Aircraft Corporation to operate from aircraft carriers and capable of carrying a large disposable load. Design information for this airplane has been previously obtained on a relatively small scale model of the airplane in the Guggenheim Aeronautical Laboratory, California Institute of Technology, and on a simplified model of the XA-26 airplane in the NACA 19-foot pressure tunnel. In order to obtain additional information at large values of Reynolds number, a 0.30-scale semispan model of the XTB2D-1 airplane was tested in the NACA 19-foot pressure tunnel.

To adapt the tunnel for the semispan model a large end plate was installed to serve as a reflection plane to maintain the lift distribution at the root section.

The model was equipped with a full-span, double-slotted flap arrangement. The inboard section of the full-span flap (the flap) was designed to act either as a high lift device or as an air brake. The outboard section (the roll flap) was designed to provide additional lift and to serve as a lateral-control device.

The data from the tests are presented in two separate reports. This report (part I) presents the results of tests made to determine the optimum position of the flap, the effectiveness of the flap and roll flap as high lift devices, the stalling characteristics of the model, the air-brake characteristics, the flap and roll-flap hinge moments and loads, and the effectiveness of a camber changing feature. Part II (reference 1) presents the roll-flap positioning tests and the lateral control characteristics.

COEFFICIENTS AND SYMBOLS

The coefficients and symbols used herein are defined as follows:

C_L lift coefficient (L/qS)

C_D drag coefficient (D/qS)

C_m pitching-moment coefficient (M/qSc)

C_{h_f} flap hinge-moment coefficient (H_f/qS_fc_f)

C_{N_f} flap normal-force coefficient (N_f/qS_f)

C_{C_f} flap chord-force coefficient (C_f/qS_f)

C_{h_a} roll-flap hinge-moment coefficient $(H_a/qb_a\bar{c}_a^2)$

C_{N_a} roll-flap normal-force coefficient (N_a/qS_a)

C_{C_a} roll-flap chord-force coefficient (C_a/qS_a)

where

L lift

D drag

M pitching moment about 0.25 mean aerodynamic chord

H_f flap hinge moment about 0.30 flap chord

N_f flap normal force

C_f flap chord force

H_a roll-flap hinge moment about 0.26 roll-flap chord

N_a roll-flap normal force

C_a roll-flap chord force

q dynamic pressure of free stream $\left(\frac{1}{2}\rho V^2\right)$

S semispan wing area (27.24 square feet)

c mean aerodynamic chord (2.696 feet)

S_f flap area (3.243 square feet)

c_f total flap chord (0.744 foot)

$b_a\bar{c}_a^2$ product of roll-flap span and square of root-mean-square chord of roll flap aft of hinge axis (0.832 foot^3)

S_a	roll-flap area (2.654 feet^2)
V	airspeed
ρ	mass density of air
and	
α	corrected angle of attack of wing reference line
δ_f	flap deflection, degrees
δ_a	roll-flap deflection, degrees
δ_{v_f}	flap vane angle, degrees
δ_{v_a}	roll-flap vane angle, degrees
δ_{c_f}	flap cut-off angle, degrees
δ_{c_a}	roll-flap cut-off angle, degrees
E_f	extension of flap, percent of maximum flap extension
E_a	extension of roll flap, percent of maximum roll-flap extension
c_w	wing chord at any spanwise station (35.7 inches from wing root to wing fold line; 34.3 inches at inboard end of roll flap; 18.6 inches at outboard end of roll flap)
g_1	radial distance from wing lip to vane
l_1	distance from wing lip to leading edge of vane parallel to wing reference line
g_2	radial distance from vane trailing edge to flap
l_2	distance from vane trailing edge to leading edge of flap parallel to wing reference line
R	Reynolds number ($\rho Vc/\mu$)
M	Mach number (V/V_c)
μ	coefficient of viscosity
V_c	sonic velocity

APPARATUS AND TESTS

The 0.30-scale semispan model of the XTB2D-1 airplane wing and fuselage combination, constructed by the Douglas Aircraft Corporation, is shown in figure 1. The arrangement of the end plate furnished by the NACA and the location of the model with respect to the tunnel is shown in figures 2 and 3.

Figure 1 shows that the wing, which was built around modified NACA low-drag sections, has rectangular center sections and the outer panels are tapered 2:1. The leading edge of the wing is straight and there is 12° geometric dihedral in the outer panels. The model fuselage did not exactly conform to the shape of the prototype but was similar in size to a scaled model of the airplane fuselage.

The wing and flaps were constructed of mahogany reinforced with steel; whereas, the vanes were made of solid steel. The surfaces were kept aerodynamically smooth by filling surface discontinuities with crack filler and glazing putty and finishing with carborundum paper.

The end plate was constructed of a basic steel framework to which was fastened $\frac{3}{4}$-inch plywood. The gap between the fuselage and the end plate was held at approximately 3/8 inch.

Figure 4 shows the following items that were attached to the model for various tests: vane-bracket covers, wing-fuselage fillet, partial end-plate seal, and a flap wedge which either moved with the flap or was held in a retracted position.

Figures 5 and 6 show the inner and outer sections of the 25-percent chord, full-span, double-slotted flap. Also included in these figures are the small and large chord flap and roll-flap vanes which were supplied with the model.

Figures 7 and 8 show the various attitudes of the Douglas "all-purpose full-span flaps" which were tested on the semispan model. For take-off, landing, maneuvering, and attitude control, the flap and roll flap operate in

their fully extended position; the deflection of the flap may be anywhere between 7° and 55° and the neutral deflection of the roll flap (from which it operates as a lateral-control device) is between 7° and 30°. The flap and roll flap deflect together from 7° to 30°. At 30° the roll flap has reached its maximum deflection as a high lift device; whereas, the flap may continue to a deflection of 55°. The existing design is such that the deflection of the flap and roll flap shall be dictated by the hinge moments acting on the surface.

In order to provide for braking in a dive, decelerating, and evasive maneuvering, the flap may be deflected to negative angles in its fully extended position. For this flap configuration the roll flap may be either in its retracted or extended position.

In an attempt to extend the low profile-drag range by increasing the wing camber, the full-span flaps could be deflected to 10° in their retracted position.

To obtain the optimum position of the flap, studies were made with the flap deflected 55° in its fully extended position. The six parameters, which were independently varied in obtaining the best lip-vane-flap location, are shown in figure 9.

The characteristics of the flaps were investigated for the following three conditions:

1. Deflection of the flap and roll flap to positive angles for the landing and take-off attitude

2. Deflection of the flap to negative angles for the air-brake condition

3. Deflection of the flap and roll flap to positive angles, in their retracted position, to obtain effective camber change.

To facilitate further discussion a "standard-model configuration" is set up which consists of the following component parts:

1. Wing and fuselage

2. Small chord vanes

3. Flap wedge moving with flap

The model was altered from the standard configuration during the investigation by

1. A partial end-plate seal which extended around the front portion of the fuselage from the leading edge of the wing on the top of the fuselage to the trailing edge of the wing on the bottom of the fuselage

2. A complete end-plate seal which was similar to the partial seal but extended aft of the wing on both the top and bottom of the fuselage

3. Large chord vanes

4. Flap wedge held in a retracted position

5. Wing-fuselage fillet

6. Vane-bracket covers

7. A spoiler on the leading edge of the flap

Stall studies of the complete semispan model were made with the flaps retracted and fully extended. These studies were recorded by visual observation, still pictures, and moving pictures of tufts located at approximately 20, 30, 40, 50, 60, 70, 80, and 90 percent of the wing chord and spaced about every 2 inches spanwise.

The majority of the tests were made at a Reynolds number and Mach number of approximately 5,200,000 and 0.12, respectively. All tests were made through a suitable angle-of-attack range with the air in the tunnel compressed to approximately $2\frac{1}{3}$ atmospheres. These tests are outlined in detail in table I.

The aerodynamic forces and moments were measured by means of a six-component simultaneous recording balance system. The flap and roll-flap forces and moments were measured by electrical resistance-type strain gages.

REDUCTION OF DATA

All results were reduced to standard nondimensional coefficients converted so that the coefficients apply to

the complete wing. The pitching moment applies to a center-of-gravity location in the plane of symmetry at 25 percent of the mean aerodynamic chord and is referred to the wind axis.

No corrections were made to the data for the effects of drag and interference of the model support system. Therefore, the values of lift, drag, and pitching-moment coefficients include the amount caused by such effects. However, the increments in these coefficients due to flap deflection may be taken to be correct, neglecting the small increments in the tare values due to the flap deflections.

Corrections were made to the drag coefficients to account for jet-boundary effects. The corrections made to the angle of attack were air-flow misalinement and jet boundary (including streamline curvature). No corrections were applied to the lift coefficient, the pitching-moment coefficient, and the flap or roll-flap hinge moment or force coefficients.

The magnitude and sign of the complete corrections to the gross data are given in the following equations:

$$C_D = C_{D_{gross}} + 0.01203C_L^2$$

$$\alpha = \alpha \text{ tunnel} + 0.788C_L + 0.3^\circ$$

RESULTS AND DISCUSSION

Full-Span Flap Positioning

Flap positioning.- The lift and pitching-moment characteristics of the model, obtained by varying each flap parameter (fig. 9) independently, are shown in figure 10. For this investigation the flap was deflected 55° and the roll flap 30°. It is appreciated that the method of positioning the flap and vane, whereby the parameters are varied only once, might not give the optimum arrangement; but due to time limitations, the method used was considered sufficiently accurate.

In figure 11 the maximum lift coefficient is plotted against each of the parameters. It is indicated

that the maximum lift coefficient does not decrease more than 0.01 from the optimum value if the parameters remain within the following ranges:

g_1	$0.012c_w$	to	$0.023c_w$
l_1	$0.014c_w$	to	$0.017c_w$
g_2	$0.012c_w$	to	$0.017c_w$
l_2	$0.033c_w$	to	$0.038c_w$
δ_{vf}	29°	to	39°

where $c_w = 35.7$ inches. The cut-off angle δ_{cf} does not appear critical but, as the curve is based on only two points, it is best to limit the optimum position to a single angle, 38°.

The data indicate that any one flap parameter on the airplane could be changed at least 3/16 inch from its optimum position and not decrease the value of the maximum lift coefficient by more than 0.01.

Effect of roll-flap positioning.- The results of positioning the roll flap for highest lift coefficient compatible with optimum rolling effectiveness are presented in reference 1. These positioning tests were made with the roll flap deflected 30° in its fully extended position. Figure 12 shows a comparison of the aerodynamic characteristics of the model for the roll flap located in its predetermined and optimum positions. In both cases the flap was deflected 55° and the flap parameters were located in their optimum position. The results show that the maximum lift coefficient was only slightly increased and the drag coefficient was slightly decreased when the roll flap was changed from its predetermined setting to the optimum setting arrived at from this investigation.

Effects of Miscellaneous Items

Scale effect.- The effect of change of Reynolds and Mach number on the lift, drag, and pitching-moment characteristics of the model with the flap and roll flap deflected 55° and 30°, respectively, is shown in figure 13. It may be seen that there was practically no scale effect over the range tested.

Effect of vane-bracket covers.- Covers (fig. 4) were installed over the vane brackets for the flap positioning runs. The effect of these covers is shown in figure 14. It is indicated that their only important effect was to improve the lift characteristics near $C_{L_{max}}$.

Effect of wing-fuselage fillet.- In an attempt to improve the lift characteristics of the wing, a fillet (fig. 4) was installed at the wing-fuselage juncture. The effect of the fillet on the aerodynamic characteristics of the model is presented in figure 15. The fillet increased the angle of stall 2.5° and $C_{L_{max}}$ by 0.05. It also slightly increased the drag throughout the lift range.

Effect of end-plate seal.- The effect of a partial and complete end-plate seal with the full-span flaps in their fully extended position and a complete end-plate seal with the flaps retracted is shown in figures 16(a), 16(b), and 16(c). With the flaps extended either seal increased the maximum lift coefficient by approximately 0.1. In the flaps-retracted condition, the addition of the seal did not appreciably affect the lift characteristics.

No aerodynamic characteristics except the lift coefficient are presented when the seal was installed because of excessive friction between the rubber seal and the end plate.

Full-Span Flap Investigation

Presentation of data.- The results of the flap investigation are presented herein for various positions of the full-span flaps during the extension cycle (figs. 7 and 8) for the following model conditions:

1. Standard model configuration (figs. 17 and 18)

2. Standard model configuration with a complete end-plate seal and wing-fuselage fillet (fig. 19)

3. Standard model configuration with a complete end-plate seal and flap spoiler (fig. 20)

4. Standard model configuration with a complete end-plate seal, flap spoiler, and large chord vanes (fig. 21)

The aerodynamic characteristics of the wing, flap and roll flap are presented for the following full-span flap positions with the model in its standard configuration:

E_f and E_a (percent)	δ_f (deg)	δ_a (deg)
0	0	0
30	0	0
50	0	0
70	7	0
100	7	7
100	10	10
100	15	15
100	20	20
100	25	25
100	30	30
100	40	30
100	50	30
100	55	30

Less complete data are presented for the other three model conditions. It was believed that no extensive program should be carried out when the end-plate seal was installed because of the excessive friction between the seal and the end plate.

It will be noted that in conditions 3 and 4 the standard model configuration was altered by the addition of a flap spoiler (fig. 5). The spoiler was found advantageous during the dive-brake investigation; consequently, the effect of the spoiler was checked during the full-span flap investigation.

Maximum lift coefficient.- The following table lists the value of the maximum lift coefficient for the four different model conditions ($\delta_f = 55°$, $\delta_a = 30°$):

Condition	Variation from standard model configuration	Maximum lift coefficient ($C_{L_{max}}$)
1	----------	2.81
2	Complete end-plate seal and wing-fuselage fillet	2.90
3	Complete end-plate seal and flap spoiler	2.85
4	Complete end-plate seal, flap spoiler, and large chord vanes	2.95

Thus, it is seen that when the end-plate seal or the large chord vane were installed, an increase in maximum lift coefficient is obtained; whereas, the flap spoiler decreases the maximum lift coefficient.

From the pitching-moment data presented in figure 18(c), it is estimated that trimming the airplane will decrease these maximum lift coefficients approximately 0.14.

Flap effectiveness.- The variation of the lift coefficient with full-span flap deflection at $\alpha = 0^\circ$ for the four model conditions is shown in figure 22. It is apparent that there is a loss in flap effectiveness between 30° and 55° flap deflection for all model conditions, except when the model was equipped with large-chord vanes. It was indicated from some unpublished studies of the flap stalling characteristics that the loss in flap effectiveness might be caused by the flap partially stalling.

Effect of spoiler.- Figure 23 shows that the effect of the flap spoiler on the aerodynamic characteristics of the wing, with the flaps in their high lift attitude, was to decrease the lift throughout the angle-of-attack range. This decrease in lift was accompanied by a decrease in the magnitude of the pitching moment. The addition of the spoiler also decreased the magnitude of the flap normal force and chord force but slightly increased the magnitude of the flap hinge moment.

Effect of flap wedge.- The effect of the flap wedge in its retracted and extended position with the flap and roll flap deflected 55° and 30°, respectively, in their fully extended position is shown in figure 24. An increase in drag, with the flap wedge extended and at 55°, was the only marked effect that occurred.

Effective camber changing feature.- The aerodynamic characteristics of the wing, flap, and roll flap are presented in figure 25 for the cases where the full-span flaps were deflected to approximately 0°, 5°, and 10° in their retracted position. It was desired that the small flap deflections would effectively increase the wing camber and thus reduce the drag at the lift coefficient for best climb, ceiling, and range. It is shown that no drag reduction was obtained except above a lift coefficient of approximately 1.1.

Stalling characteristics.- The stalling characteristics for the conditions of flap neutral and full-span flaps deflected are presented in figure 26. In general, the stalling characteristics of the semispan model may be adjudged satisfactorily. The stall starts near the wing-fuselage juncture at the trailing edge and spreads forward and outboard on the inner panel of the wing. Over the range tested, the roll flap showed no indication of stalling. With the full-span flaps deflected, a portion of the flap remains stalled until the wing starts to stall. This accounts for the hook in the lift curve close to the stall.

These stalling characteristics were obtained by observing wool tufts attached to the model. The presence of the tufts had a detrimental effect on the lift coefficient. It is believed, however, that the stall progression noted with tufts on is indicative of the stall which would occur when there were no tufts attached to the wing.

Air-Brake Investigation

The specifications, for the brakes on the XTB2D-1 airplane, supplied by the Douglas Aircraft Corporation, state that the brakes shall limit the speed to 425 miles per hour indicated airspeed in a 50° dive. Reference 2 indicates that a torpedo bomber should lose speed as rapidly as possible until a speed of approximately 165 miles per hour is reached during a torpedo attack.

Other airplane characteristics caused by the application of the air brake which require consideration are (1) that attitude and trim changes shall be small and (2) the hinge-moment characteristics shall tend to keep the brakes in a closed position and progressively increase the force necessary to open the brakes. From the structural standpoint of the airplane it was desired that the air-brake cycle produce (1) no decrease in lift at a particular angle of attack or increase in angle of attack at a particular lift coefficient in order to insure that the aerodynamic loads do not shift from the inner to the outer wing panel, (2) no increase in the magnitude of the pitching moment to prevent the down loads on the horizontal tail from becoming excessive, and (3) flow separation on the lower surface of the flap to reduce the magnitude of the loads on the flap.

The characteristics of the wing and the air brake for several flap deflections at various points in the brake extension cycle (fig. 7) are presented in figures 27 through 35. Results are shown for two cases: (a) normal flap configuration and (b) flap equipped with a spoiler.

A comparison of these two cases, in the fully extended position of the brake, showed that the addition of the spoiler reduced the normal forces acting on the flap by causing the flow over the lower surface of the flap to separate. The effect of Reynolds number on the characteristics of the air brake, deflected -15° in its fully extended position with the leading-edge spoiler off, is shown in figures 30(a) and 30(b). These results indicated the desirability of obtaining all further data relative to the air brakes for this airplane at the highest possible Reynolds number and with the spoiler attached to the flap.

For the condition of zero lift coefficient, the variation of increment of pitching-moment coefficient, drag coefficient, and angle of attack with flap deflection during the brake cycle is shown in figure 36. With the spoiler on the flap the drag coefficient is increased 0.077 at a flap deflection of -54°. If the flap follows its design path (fig. 36) to a deflection of -54°, there is a maximum change of 2° in the angle of attack and 0.063 in the pitching-moment coefficient.

Figure 36 also shows that at -11.5° flap deflection there is a negative pitching-moment coefficient change which further increases the down load on the tail and that above a flap deflection of approximately -11.5° there is a positive change in the angle of attack which would indicate that the aerodynamic loads are shifting to the outer wing panel. Both of these changes are structurally disadvantageous and the design path of the flap may have to be altered.

The hinge-moment characteristics shown in figure 35(b) indicate that the brakes would tend to remain closed in the high-speed condition and that if there was no appreciable change in the attitude of the airplane during the brake cycle a progressively increasing force is necessary to open the brakes.

The effect of the large chord-flap vane on the characteristics of the wing and flap when the flap is in its fully extended air-brake attitude is presented in figure 37. The information available is insufficient to predict what effect the large chord vanes would have on the complete dive-brake characteristics but it is apparent that they would increase the drag increment.

Preliminary calculations have been made of the effectiveness of the brake for application to the XTB2D-1 airplane. Two conditions have been analyzed: (1) the level approach to a target at sea level and (2) a 50° dive approach from various altitudes up to 20,000 feet. The first condition was analyzed by methods described in reference 3 and for the second condition reference 4 was utilized. The results of these calculations and the assumptions made for the calculations are presented with the following tables:

LEVEL APPROACH AT SEA LEVEL

Wing loading, pounds per square foot	56
Initial velocity, miles per hour	300
Brake drag increment	0.077

Assume throttle setting remains constant

Time after applying brake (sec)	Distance traveled (yd)	Velocity (mph)
0	0	300
5	690	270
10	1320	245
15	1870	225
20	2415	205
25	2890	190
30	3340	175
35	3770	165

These calculations indicate that with the brakes set at -54° it would take 35 seconds to decrease the speed of the airplane from 300 to 165 miles per hour. In this time interval the airplane would have traveled 2 miles.

50° DIVE APPROACH

Wing loading, pounds per square foot	56
Initial velocity, miles per hour	200
Brake drag increment	0.077
Assumed airplane drag	0.035
Drag available for braking	0.112

It was assumed that the variation of airplane profile drag with Mach number for the XTB2D-1 airplane was the same as airplane B of reference 3.

Height, h, at which dive is started (ft)	True velocity at h = 0 (mph)
8,000	375
12,000	400
16,000	415
20,000	425

These results indicate that in a 50° dive started at 20,000 feet with the brakes deflected -54° the speed of the airplane would not exceed 425 miles per hour at sea level.

CONCLUSIONS

This investigation of the characteristics of the full-span flap and air brake on the 0.30-scale semispan model of the XTB2D-1 airplane wing and fuselage combination indicate that:

1. On the airplane any one flap parameter could be moved at least 3/16 inch from its optimum setting and not decrease $C_{L_{max}}$ by more than 0.01.

2. A maximum lift coefficient of 2.95 was obtained when the model was equipped with a complete end-plate seal, flap spoiler, and large chord vanes. $C_{L_{max}}$ was decreased 0.10 when the small chord vanes were installed. It is estimated that trimming the airplane will cause an additional decrease in $C_{L_{max}}$ of approximately 0.14.

3. Nearly every model configuration showed a loss of flap effectiveness between 30° and 55° due to a stall condition on the flap.

4. The effective camber changing feature produced no drag reduction except above a lift coefficient of approximately 1.1.

5. The stalling characteristics of the model appear to be satisfactory either with the flaps retracted or with the flaps fully extended.

6. For braking in a dive, decelerating, and evasive maneuvering, the brakes produced a drag coefficient increment of 0.077 at -54° flap deflection. During the brake cycle from fully retracted to -54° deflection, a maximum change of 2° angle of attack and 0.063 change in pitching-moment coefficient was encountered. Estimates of the airplane performance with the brakes deflected -54° indicate that, in a 50° dive started at 200 miles per hour at 20,000 feet, the indicated airspeed will not exceed 425 miles per hour; it is also indicated

that, at sea-level altitude, the time required to decrease the speed of the airplane from 300 to 165 miles per hour would be 35 seconds. During this time interval, the airplane would have traveled 2 miles.

Langley Memorial Aeronautical Laboratory
National Advisory Committee for Aeronautics
Langley Field, Va., September 7, 1944

REFERENCES

1. Spooner, Stanley H., Ashworth, C. Dixon, and Russell, Robert T.: Tests of a 0.30-Scale Semi-span Model of the Douglas XTB2D-1 Airplane Wing and Fuselage Combination in the NACA 19-Foot Pressure Tunnel. II - Roll-Flap Positioning and Lateral-Control Investigation. NACA MR, Sept. 7, 1944.

2. Davies, H., and Kirk, F. N.: A Résumé of Aerodynamic Data on Air Brakes. Rep. No. Aero 1756, British R.A.E., June 1942.

3. Lowell, Arthur L.: Fighter Airbrakes. Introductory Investigation of Means for Improving the Tactical Effectiveness of Combat Aircraft by Making Provisions for Rapid Decelerations in Flight. A.C.T.R. No. 4772, Materiel Div., Air Corps, May 15, 1942..

4. Pearson, H. A.: Time-Velocity-Altitude Relations for an Airplane Diving in a Standard Atmosphere. NACA ARR, March 1943.

TABLE I.- TESTS AND FIGURES

Figure	Presentation	Plot	Approximate dynamic pressure (lb/sq ft)	Variation from standard model configuration	R_f (percent)	R_a (percent)	δ_f (deg)	δ_a (deg)	Remarks
10	Flap positioning	C_L vs α, C_m	50	Vane-bracket covers	100	100	55	30	Roll-flap not in its optimum position
11	Summary of flap positioning	$C_{L_{max}}$ vs s_1, l_1, s_2, l_2, δ_{vr}, δ_{cf}	50	------do.-----	100	100	55	30	Do.
12	Effect of positioning roll-flap	C_L vs C_D, α, C_m	50	Wing-fuselage fillet	100	100	55	30	----------
13	Effect of Reynolds number	C_L vs C_D, α, C_m	Vary	Vane-bracket covers	100	100	55	30	Roll-flap not in its optimum position
14	Effect of vane-bracket covers	---do.---	50	------do.-----	100	100	55	30	Do.
15	Effect of wing-fuselage fillet	---do.---	50	Wing-fuselage fillet	100	100	55	30	Do.
16	Effect of partial and complete end-plate seals	C_L vs α	50	Partial and complete end-plate seals	Vary	Vary	Vary	Vary	Roll-flap not in its optimum position (fig. 16(a))
17	Flap Characteristics	C_L vs C_D, α, C_m; C_L vs C_{h_f}, C_{H_f}, C_{C_f}; C_L vs C_{h_a}, C_{H_a}, C_{C_f}	50	----------	Vary	Vary	Vary	0	----------
18	-------do.--------	---do.---	50	----------	100	100	Vary	Vary	----------
19	-------do.--------	C_L vs α	50	Complete end-plate seal and wing-fuselage fillet	100	100	Vary	Vary	----------
20	-------do.--------	C_L vs α; C_L vs C_{h_f}, C_{H_f}, C_{C_f}	50	Complete end-plate seal and flap spoiler	100	100	Vary	Vary	----------
21	-------do.--------	C_L vs α; C_L vs C_{h_f}, C_{H_f}, C_{C_f}; C_L vs C_{h_a}, C_{H_a}, C_{C_a}	50	Complete end-plate seal, flap spoiler, and large chord vanes	100	100	Vary	Vary	----------
22	Summary of flap characteristics	C_L at $\alpha = 0°$ vs δ_f and δ_a	50	Complete end-plate seal, wing-fuselage fillet, flap spoiler, and large chord vanes	100	100	Vary	Vary	----------
23	Effect of spoiler	C_L vs C_D, α, C_m; C_L vs C_{h_f}, C_{H_f}, C_{C_f}	50	Flap spoiler	100	100	55	30	----------
24	Effect of flap wedge	C_L vs C_D, α, C_m	50	Flap wedge retracted and flap spoiler	100	100	55	30	----------
25	Effective camber changing feature	C_L vs C_D, α, C_m; C_L vs C_{h_f}, C_{H_f}, C_{C_f}; C_L vs C_{h_a}, C_{H_a}, C_{C_a}	50	----------	0	0	Vary	Vary	----------
26	Stall characteristics	---------	50	Wing-fuselage fillet	Vary	Vary	Vary	Vary	----------
27	Air-brake characteristics	C_L vs C_D, α, C_m; C_L vs C_{h_f}, C_{H_f}, C_{C_f}	50	Flap wedge retracted	Vary	0	Vary	0	----------
28	-------do.--------	---do.---	50	------do.-----	40	0	Vary	0	----------
29	-------do.--------	---do.---	50	------do.-----	60	0	Vary	0	----------
30	-------do.--------	---do.---	Vary	------do.-----	100	0	Vary	0	----------
31	-------do.--------	---do.---	75	Flap wedge retracted and flap spoiler	Vary	0	Vary	0	----------
32	-------do.--------	---do.---	75	------do.-----	40	0	Vary	0	----------
33	-------do.--------	---do.---	75	------do.-----	60	0	Vary	0	----------
34	-------do.--------	---do.---	75	------do.-----	80	0	Vary	0	----------
35	-------do.--------	---do.---	75	------do.-----	100	0	Vary	0	----------
36	Summary of air-brake characteristics	ΔC_m, $\Delta\alpha$, ΔC_D at $C_L = 0$ vs δ_f	Vary	------do.-----	Vary	0	Vary	0	----------
37	Air-brake characteristics	C_L vs C_D, α, C_m; C_L vs C_{h_f}, C_{H_f}, C_{C_f}	75	Flap wedge retracted, flap spoiler and large chord vanes	100	0	Vary	0	----------

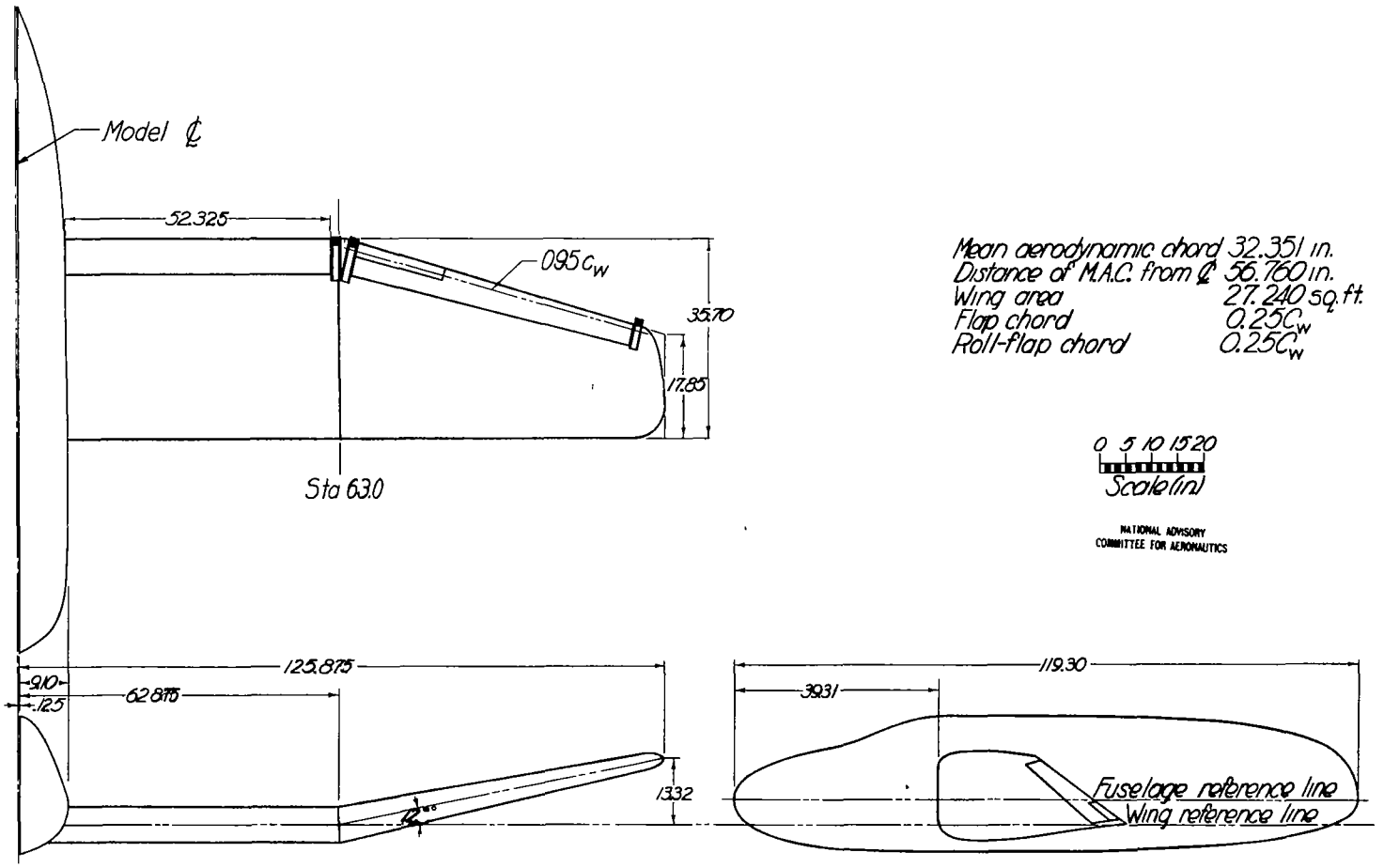

Figure 1.- Three view drawing of the 0.30-scale semispan model of the Douglas XTB2D-1 Airplane.

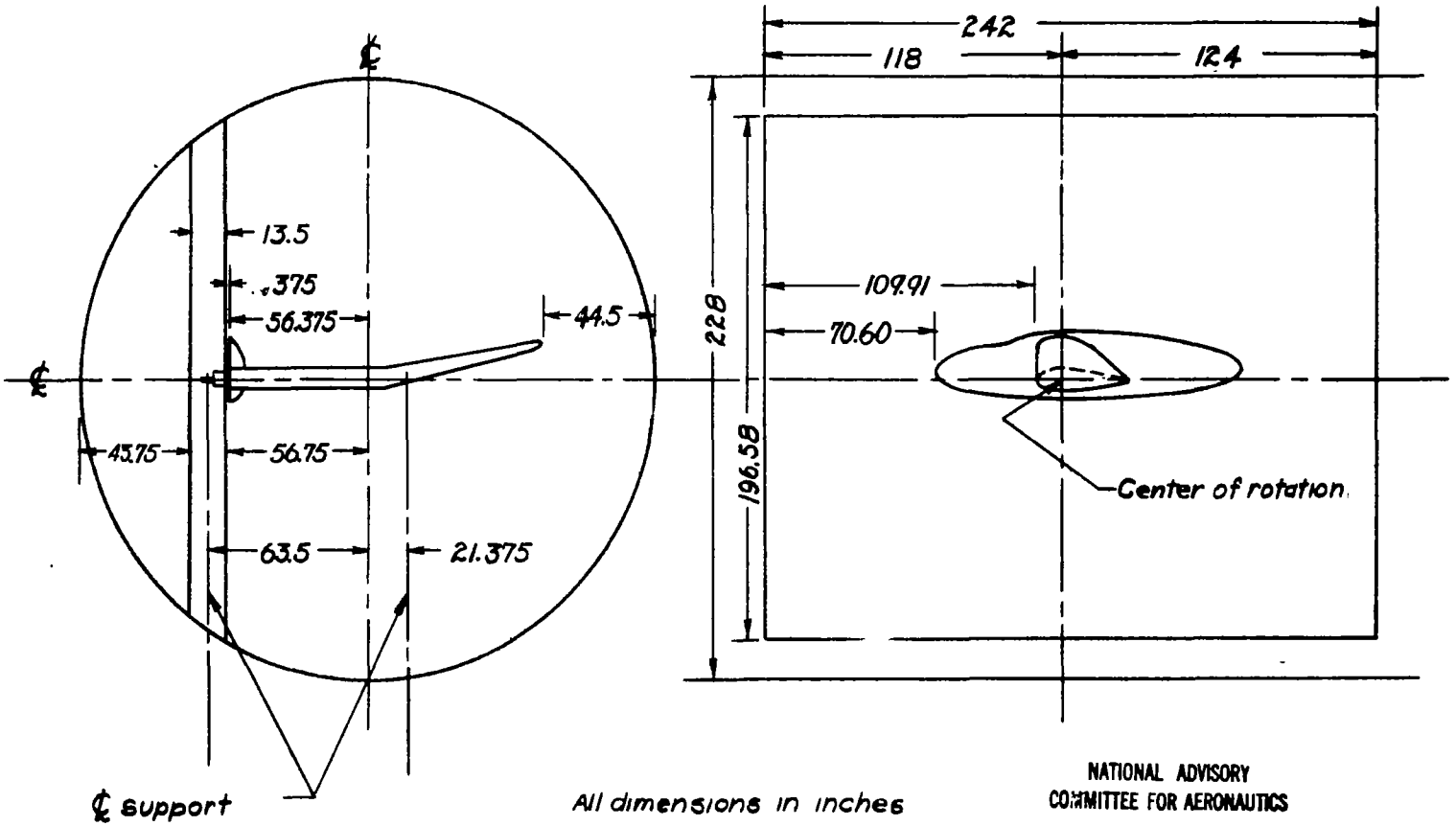

Figure 2.— Arrangement of the 0.30-scale XTB2D-1 semispan model and end-plate in the 19-foot pressure tunnel.

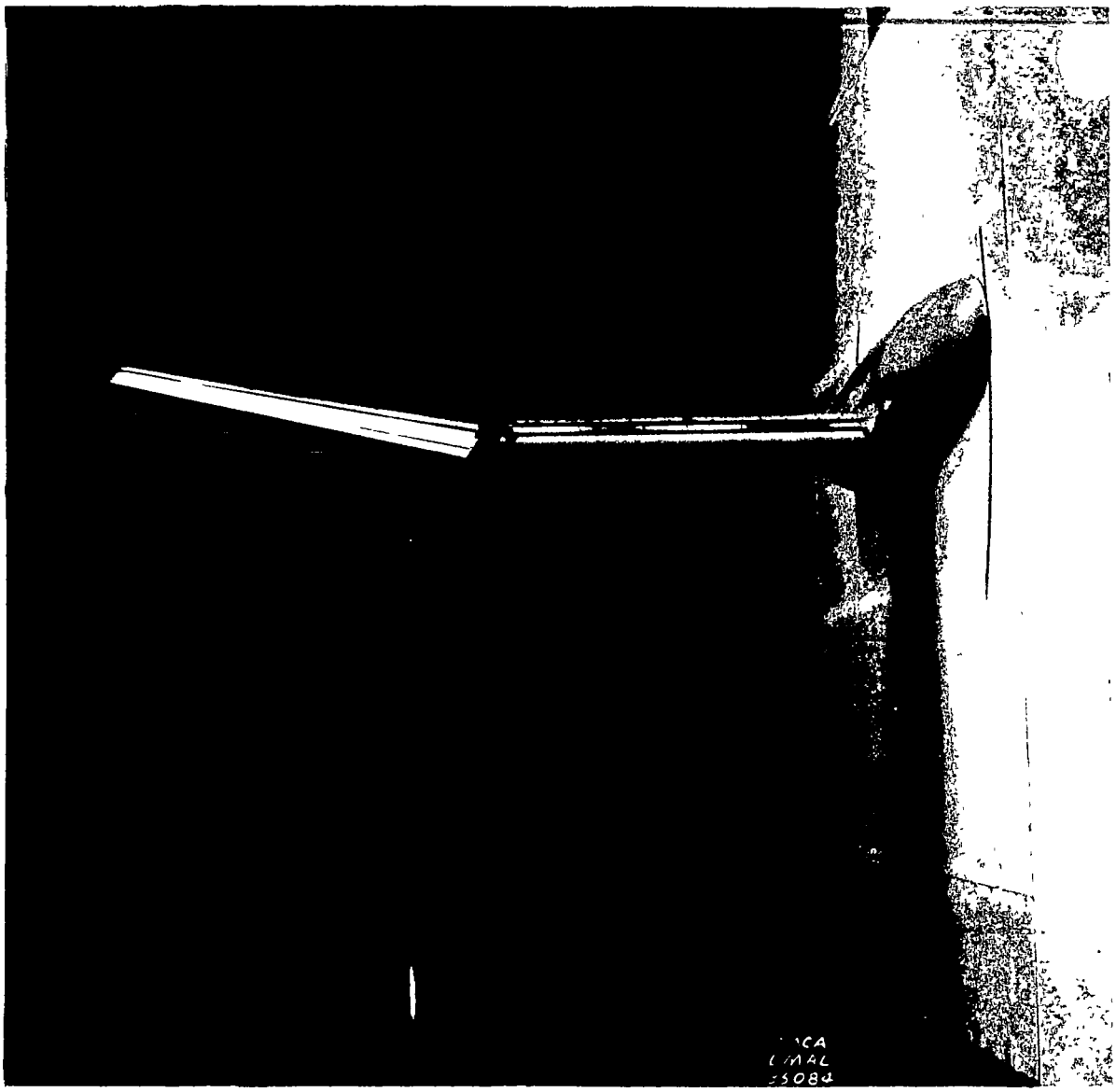

Figure 3.- 0.30-scale XTB2D-1 semispan model mounted in the 19-foot pressure tunnel.

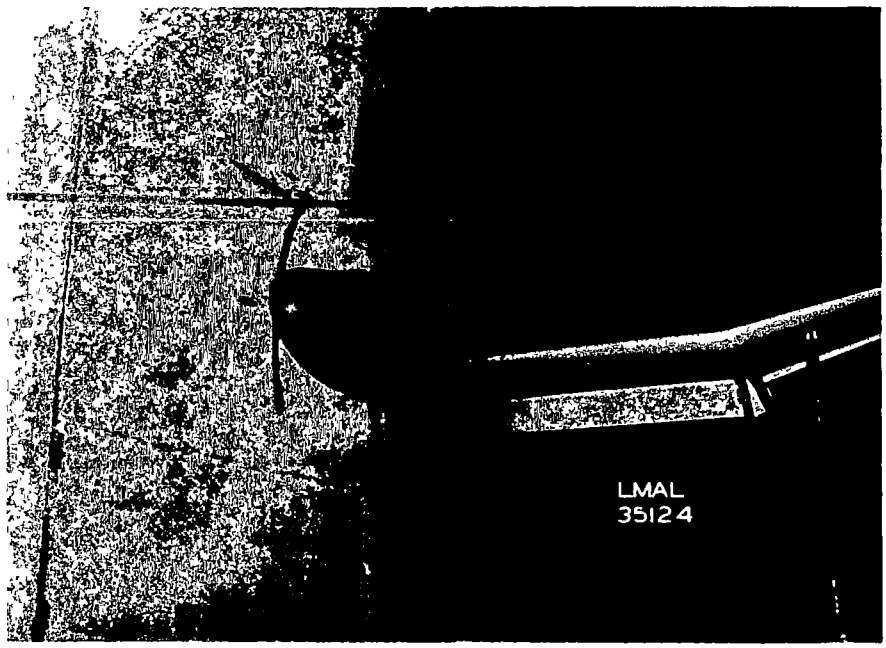

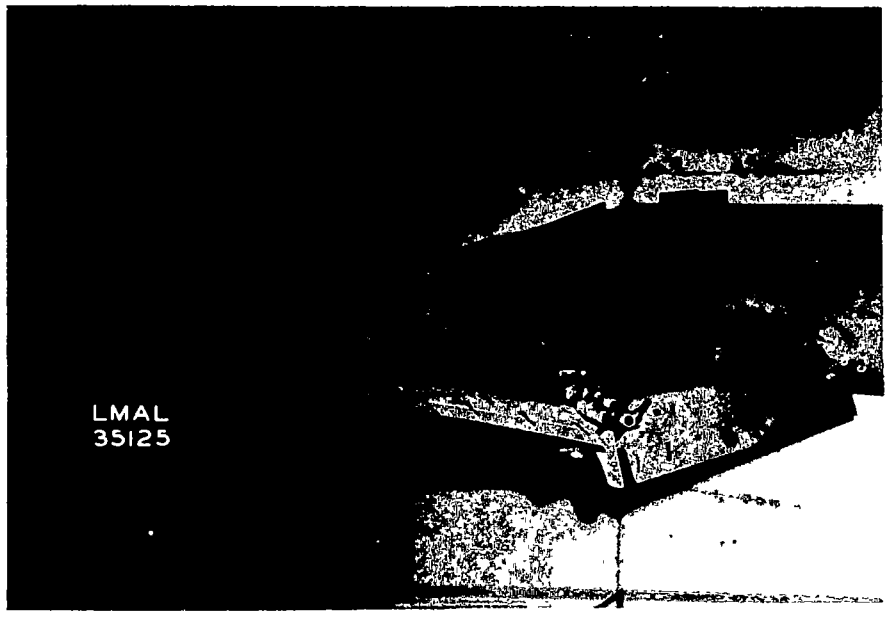

(a) Partial end-plate seal, flap wedge, wing-fuselage fillet.

Figure 4.- Detail photographs of the 0.30-scale XTB2D-1 semispan model.

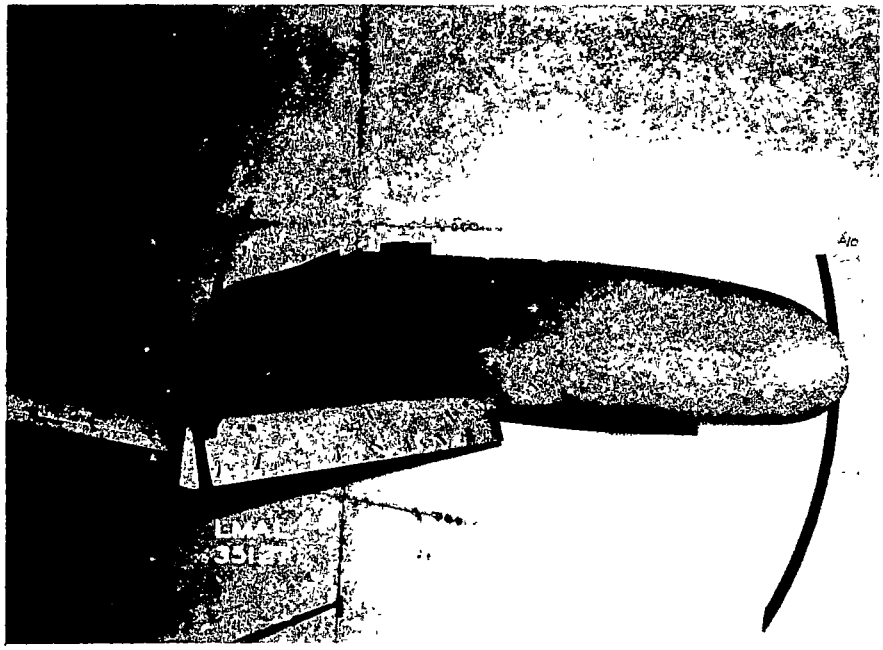

(b) Vane-bracket covers.

Figure 4.- Concluded.

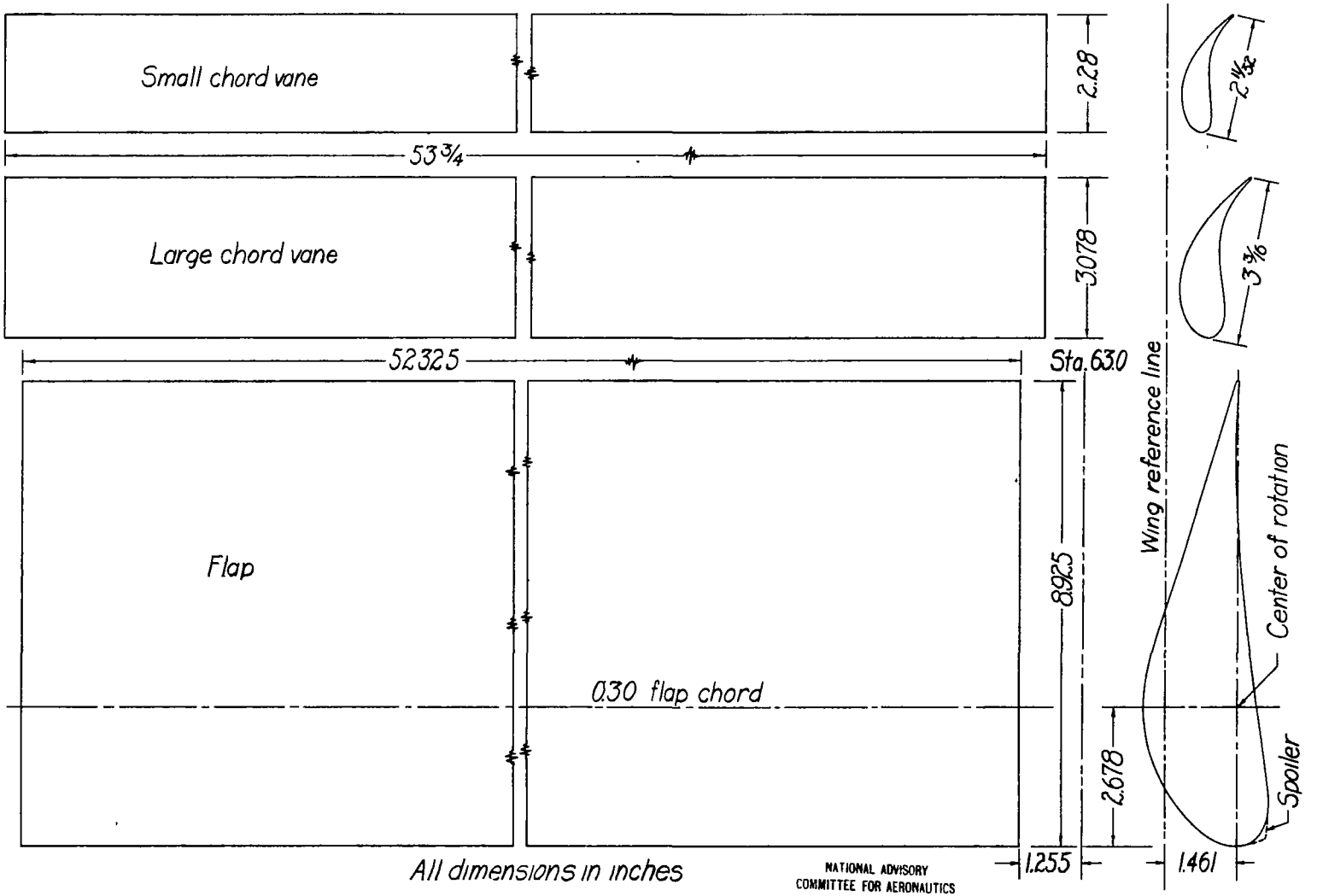

Figure 5.—Flap and vanes of the 0.30-scale XTB2D-1 semispan model.

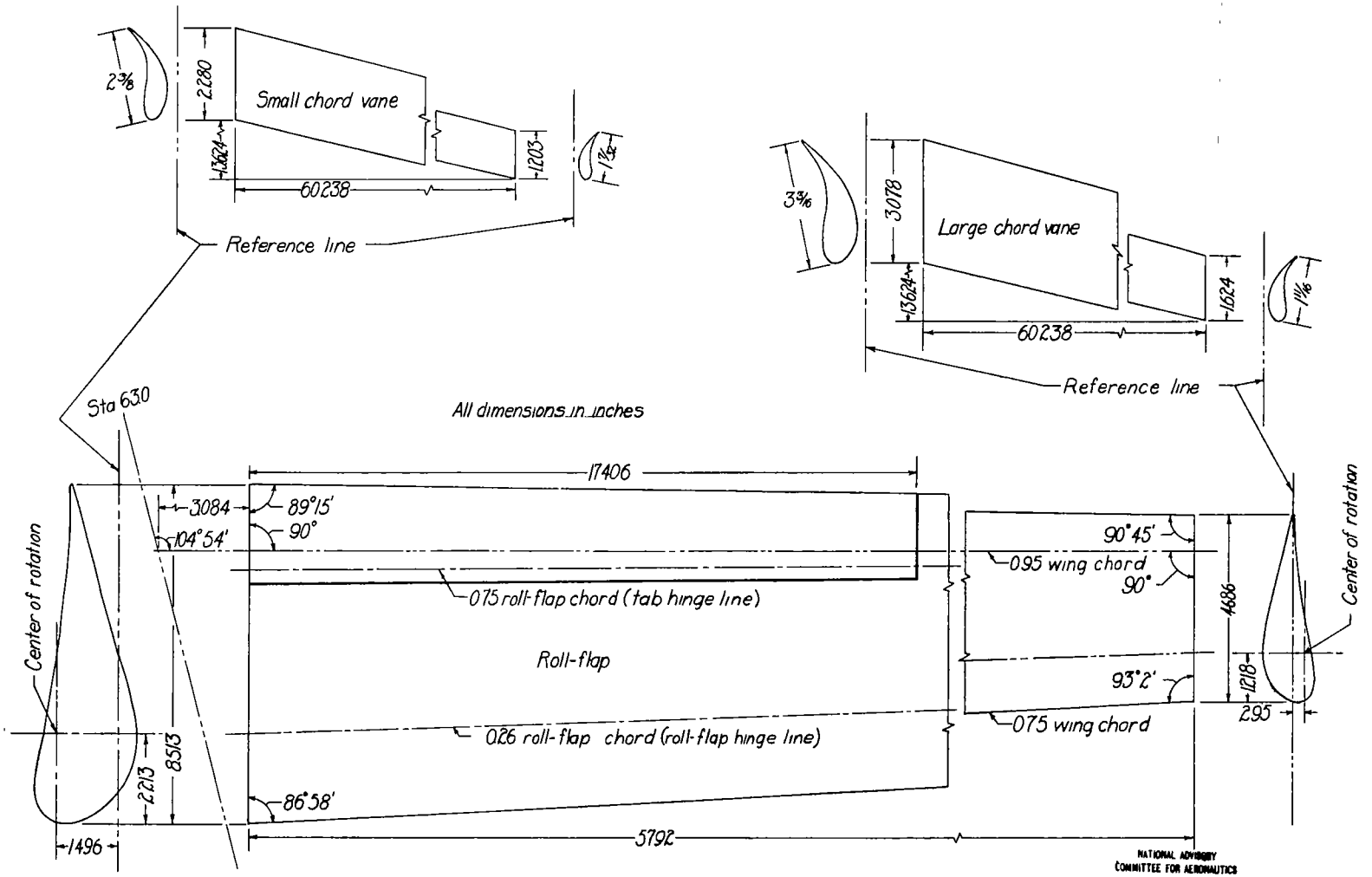

Figure 6.—Roll-flap and vanes of the 0.30-scale XTB2D-1 semispan model.

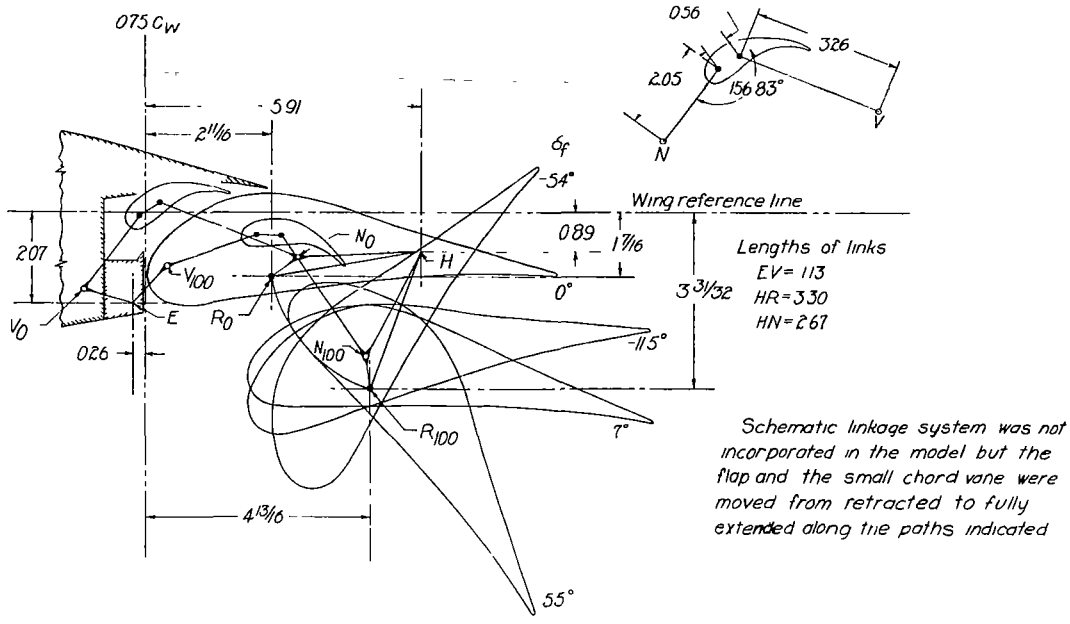

Path of flap and vane from retracted to fully extended

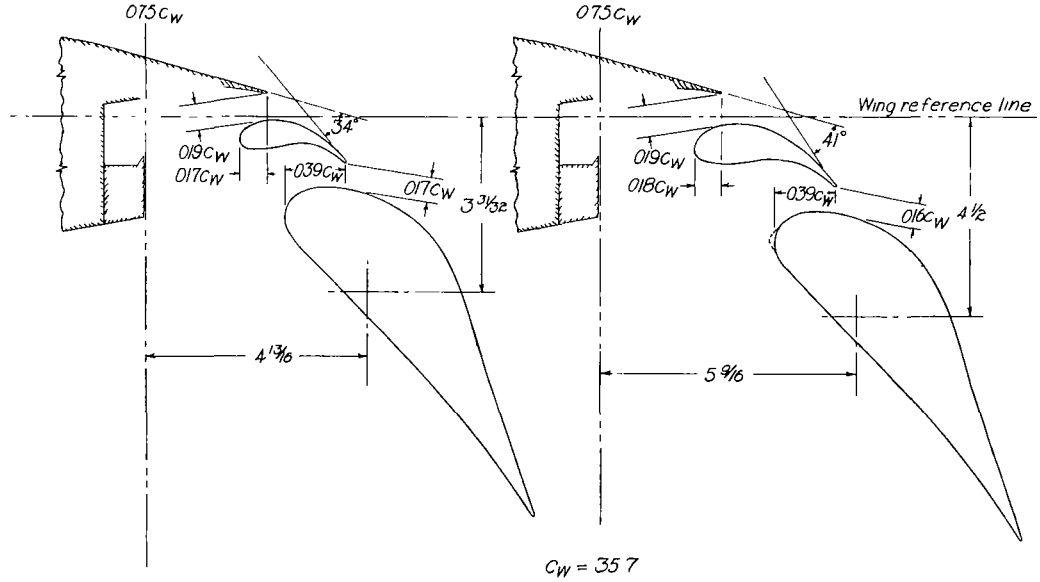

Small chord vane

Large chord vane

Approximate magnitude of wing-vane-flap parameters, δ_f=55°.

All dimensions in inches

NATIONAL ADVISORY COMMITTEE FOR AERONAUTICS

Figure 7 – Vane and flap location for the 030-scale XTB2D-1 semispan model.

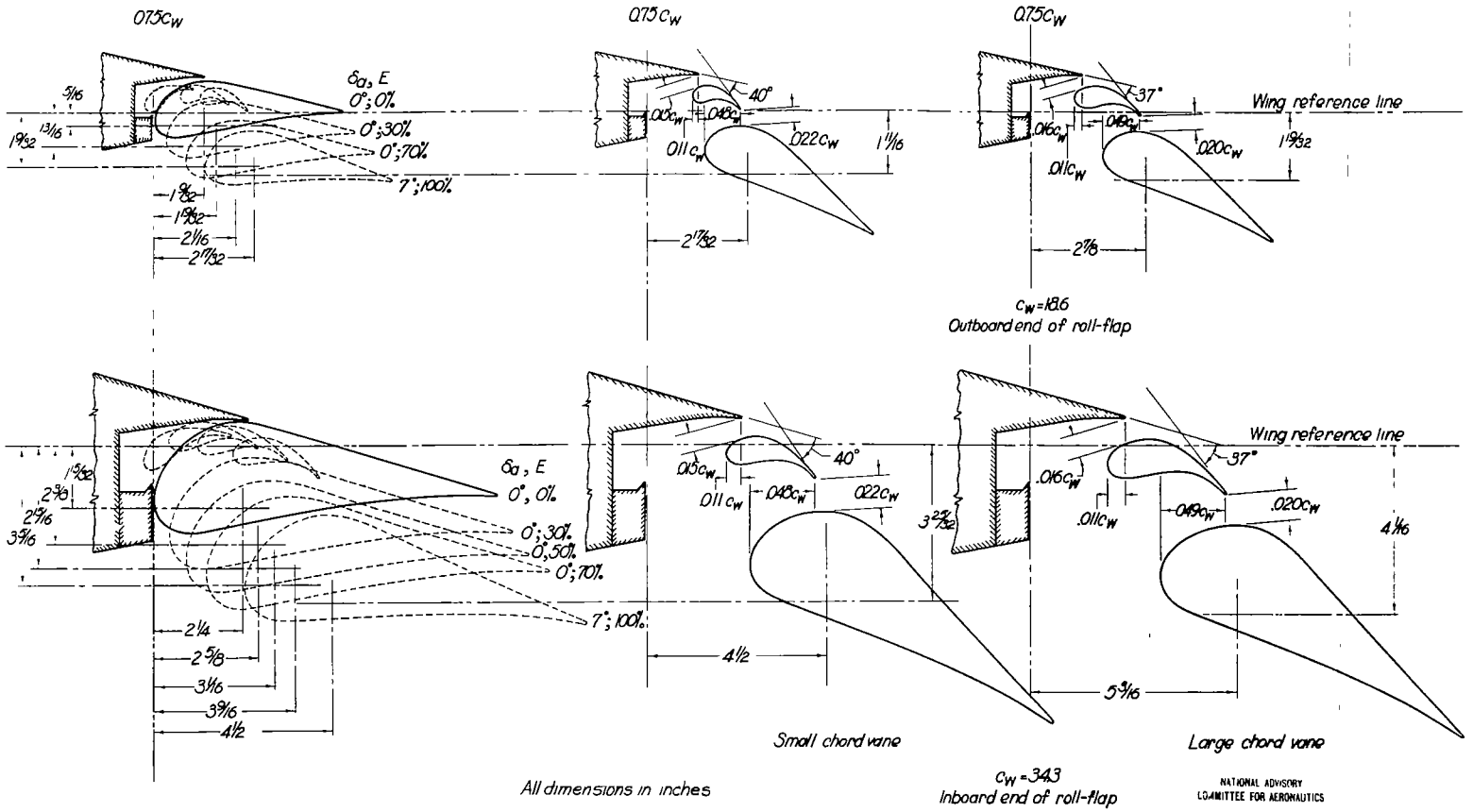

Figure 8.-Vane and roll-flap location for the XTB2D-1 semispan model.

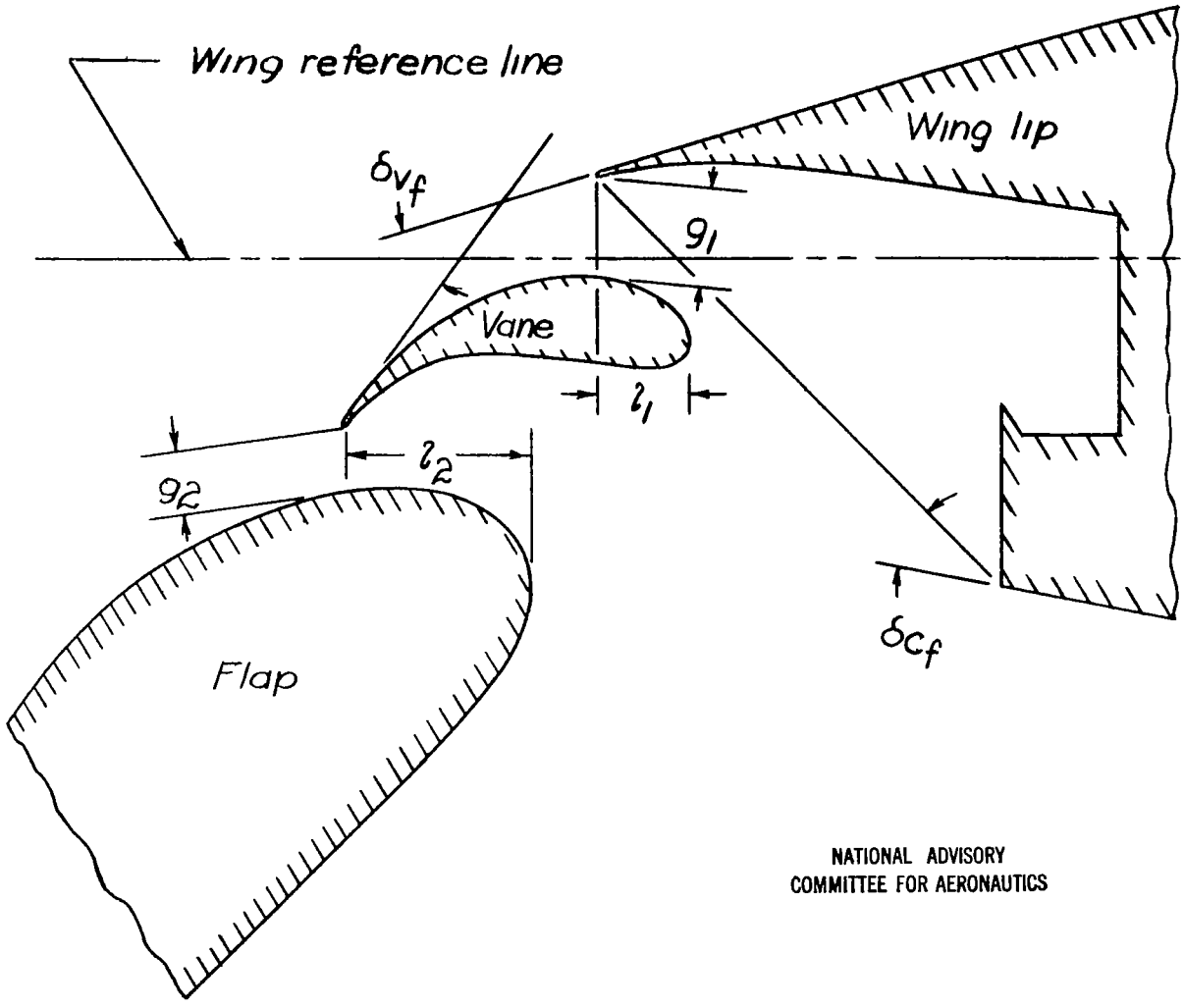

Figure 9 .– Wing-vane-flap parameters .

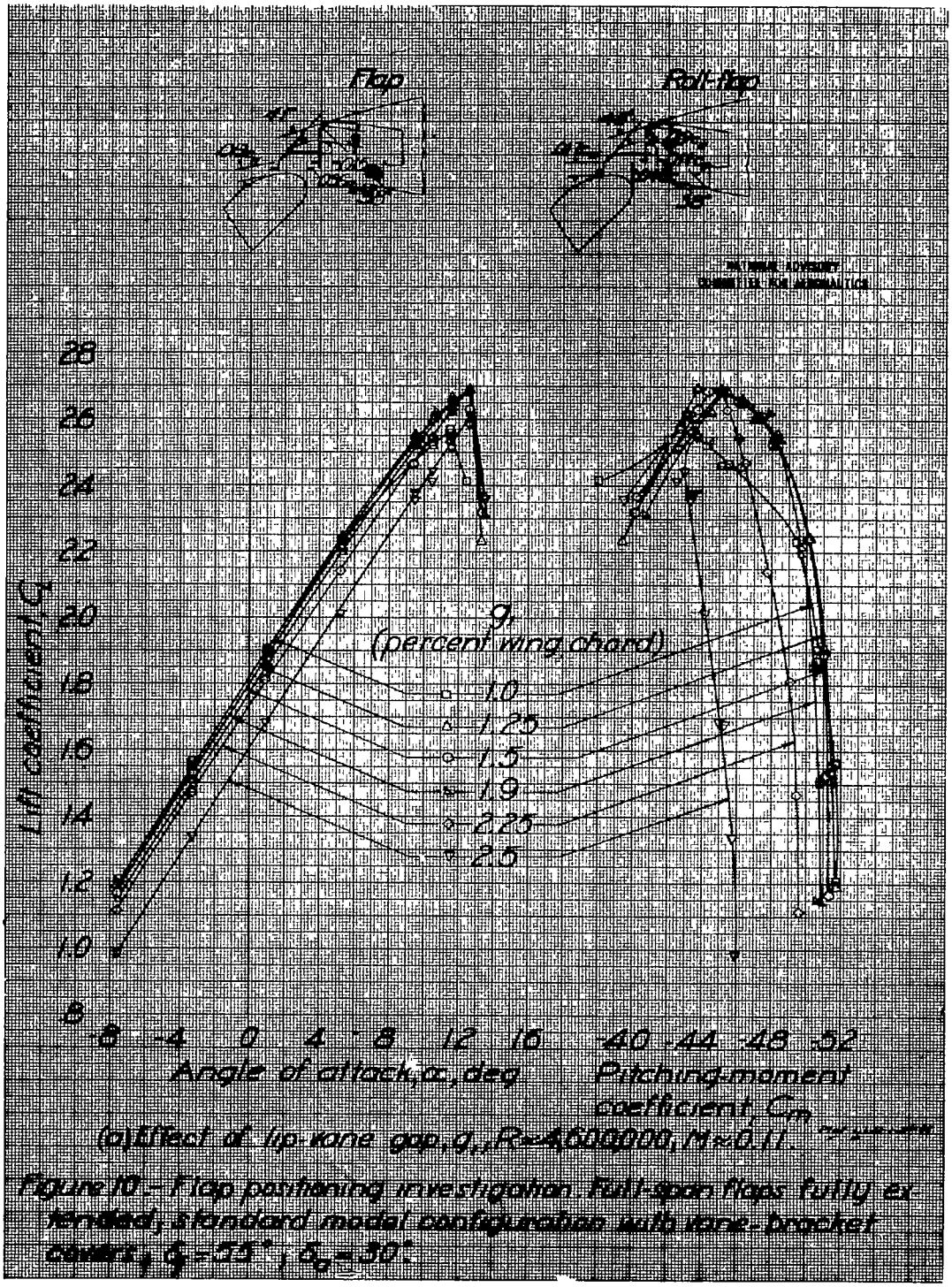

(a) Effect of lip-cone gap, g_f; $R = 4,600,000$, $M = 0.11$.

Figure 10.- Flap positioning investigation. Full-span flaps fully extended; standard model configuration with cove-bracket covers; $\delta_f = 25°$; $\delta_e = 30°$.

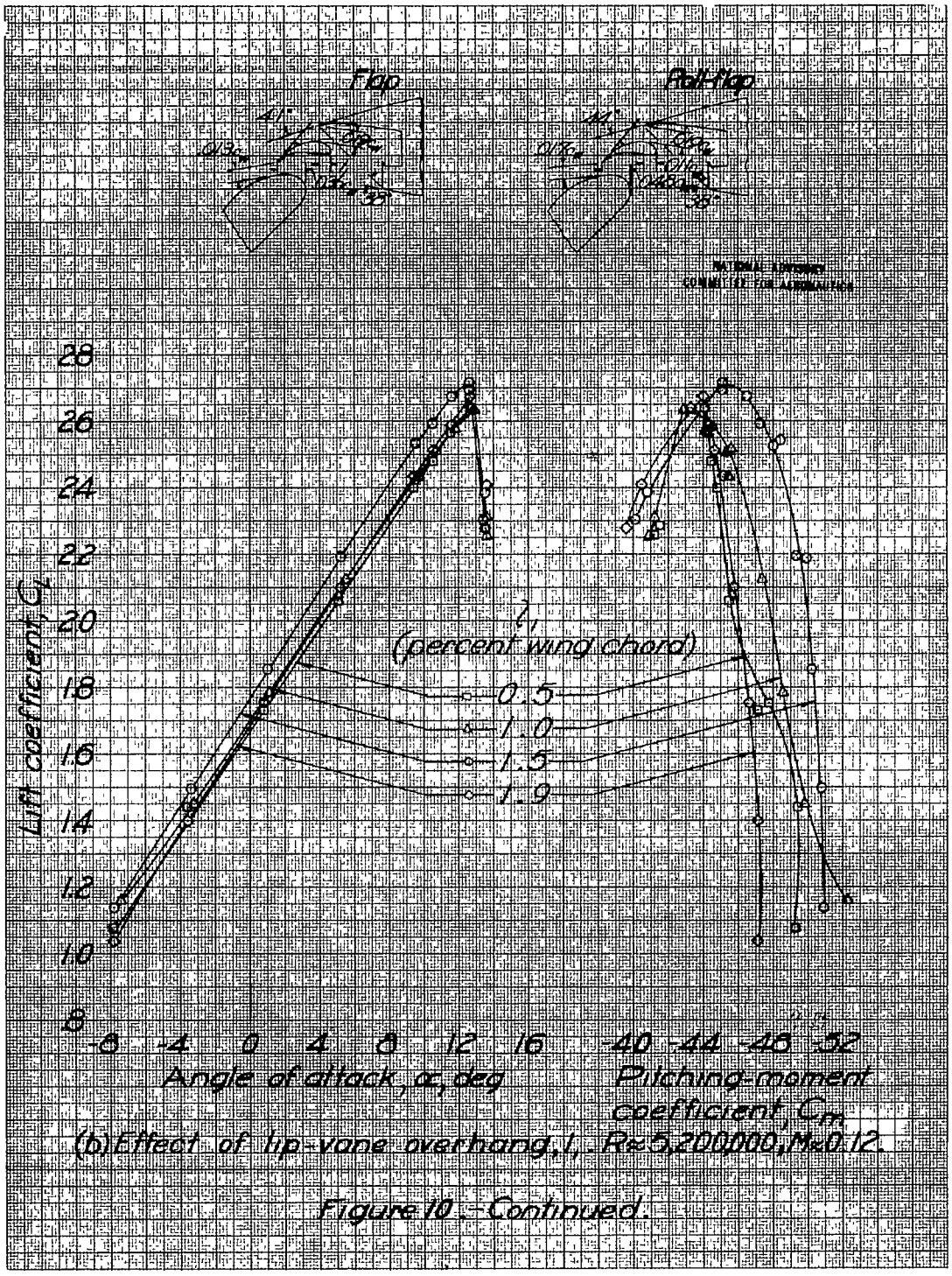

(b) Effect of lip-vane overhang, l_1. R_c 5,200000, M_c 0.12.

Figure 10.- Continued.

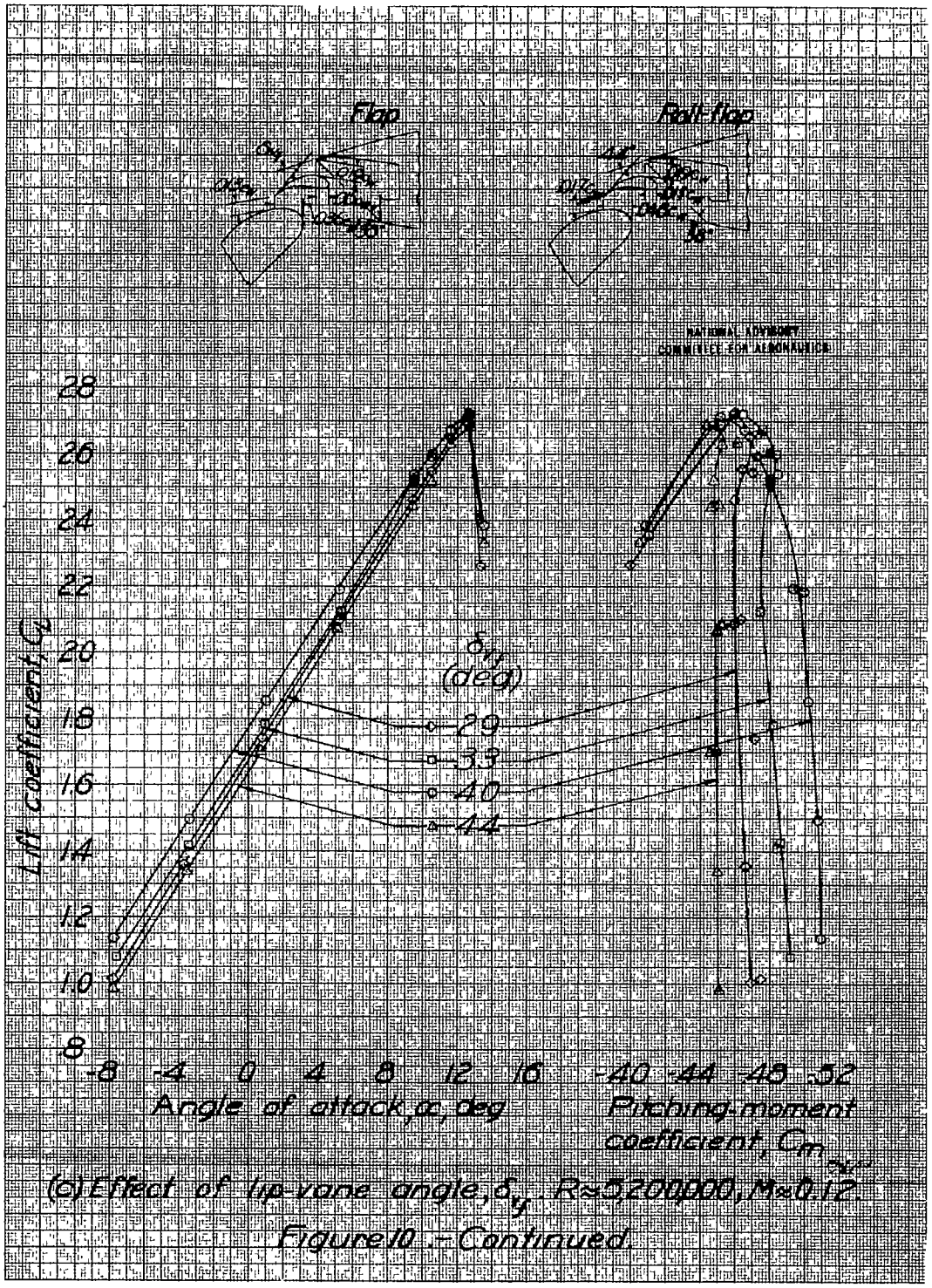

(c) Effect of lip-vane angle, δ_{lf}. $R \approx 5{,}200{,}000$, $M \approx 0.12$

Figure 10. - Continued.

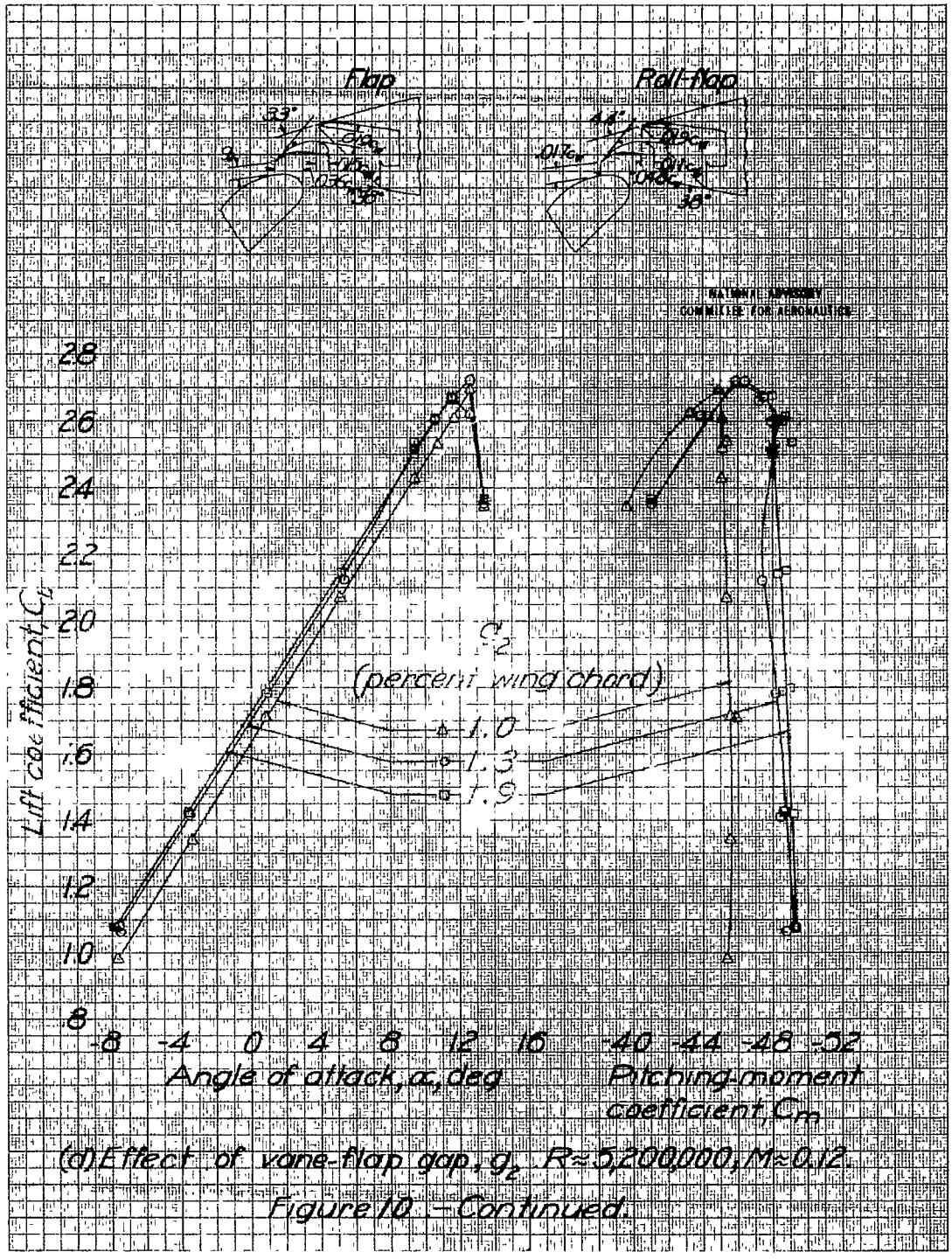

(d) Effect of vane-flap gap, C_2. $R \approx 5,200,000$, $M \approx 0.12$.

Figure 10.—Continued.

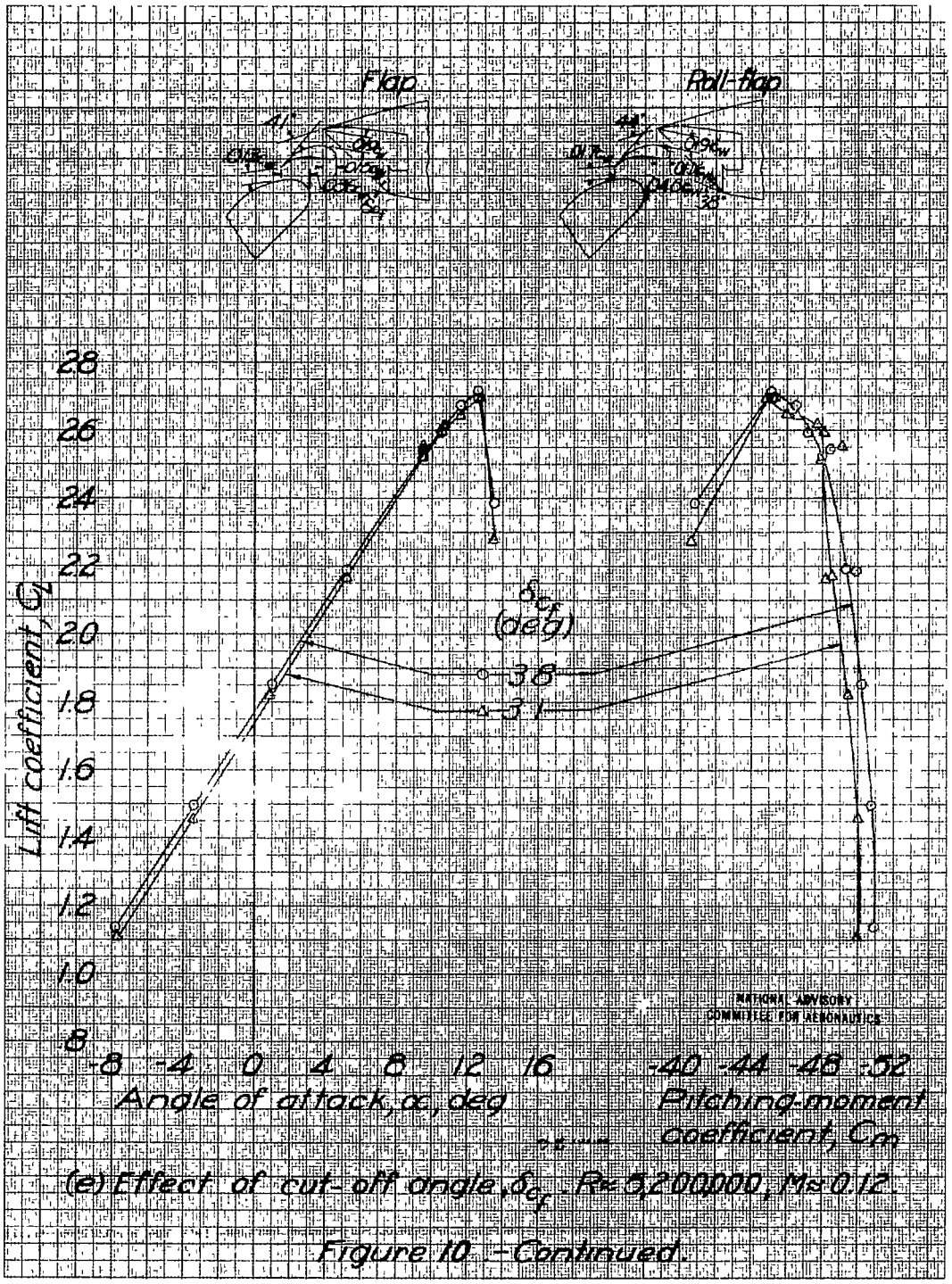

(e) Effect of cut-off angle, δ_{c_f}. $R \approx 5,200,000$, $M \approx 0.12$.

Figure 10.—Continued.

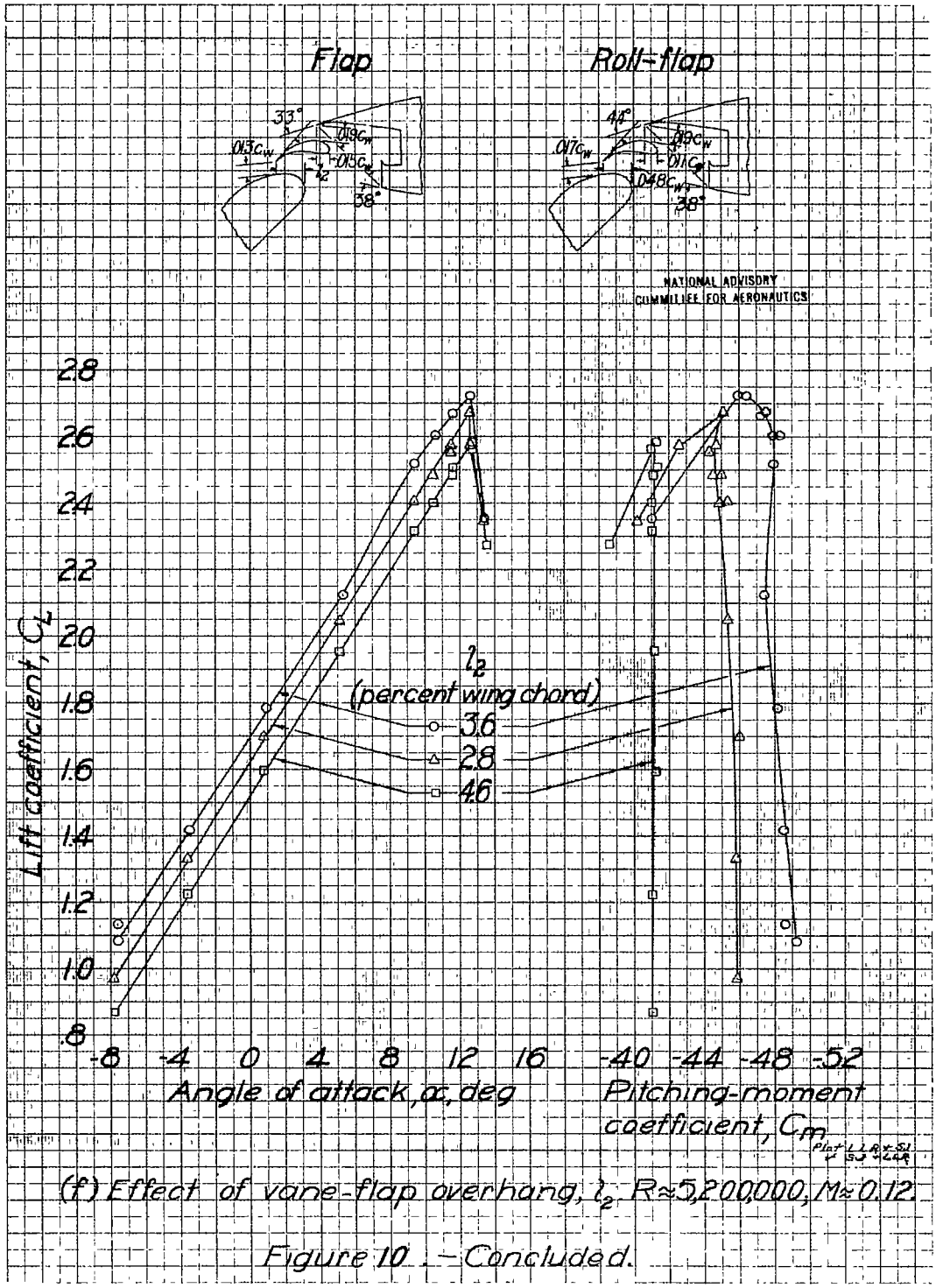

(f) Effect of vane-flap overhang, l_2. $R \approx 5,200,000$, $M \approx 0.12$

Figure 10.—Concluded.

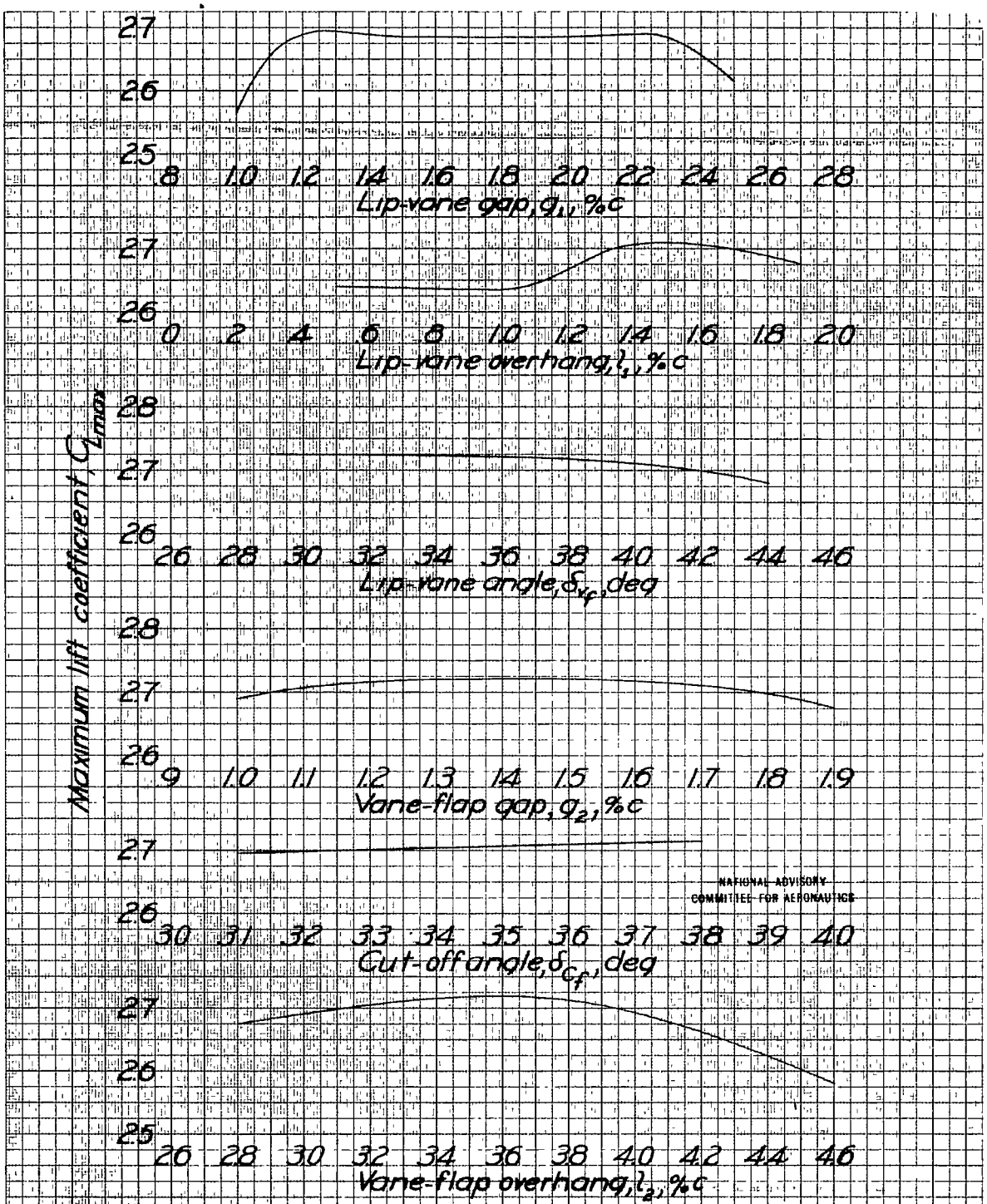

Figure 11.- Variation of $C_{L_{max}}$ with lip-vane-flap parameters. Full-span flaps fully extended; standard model configuration with vane-bracket covers, $\delta_f = 55°$; $\delta_a = 30°$

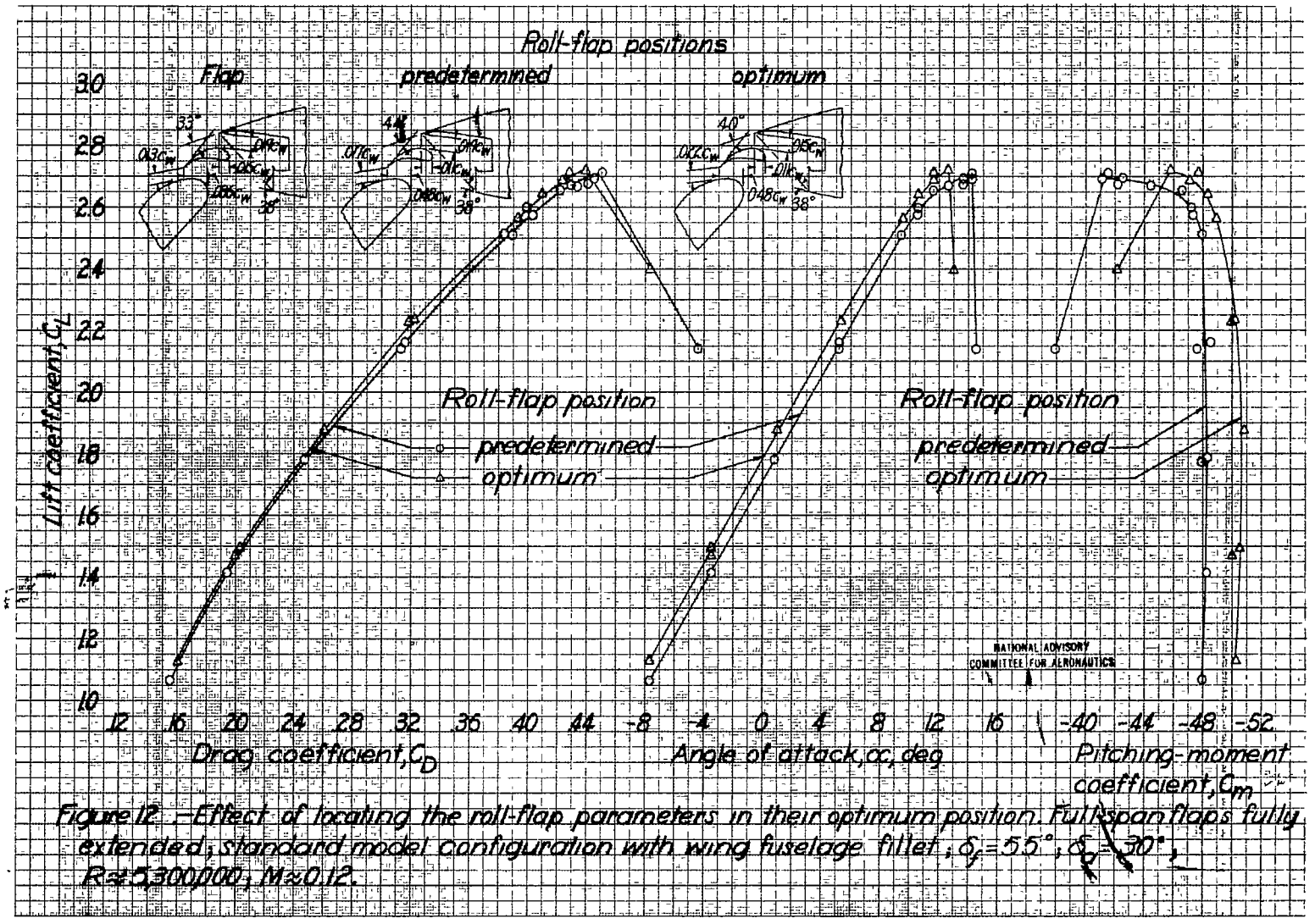

Figure 12.–Effect of locating the roll-flap parameters in their optimum position. Full-span flaps fully extended; standard model configuration with wing fuselage fillet; $\delta_f = 55°$; $\delta_D = 30°$; $R \approx 5{,}300{,}000$; $M \approx 0.12$.

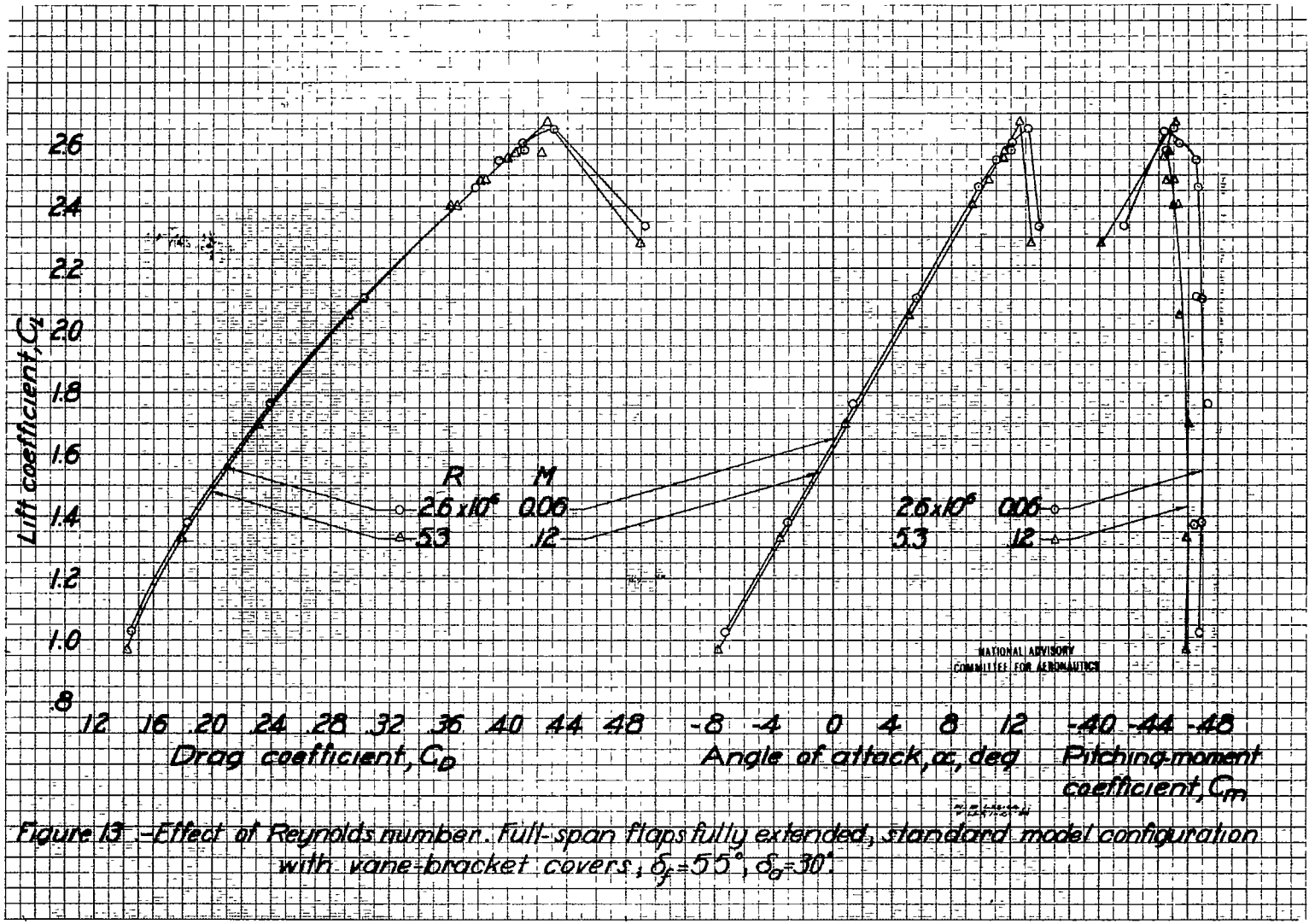

Figure 13.–Effect of Reynolds number. Full-span flaps fully extended, standard model configuration with vane-bracket covers; $\delta_f = 55°$, $\delta_o = 30°$.

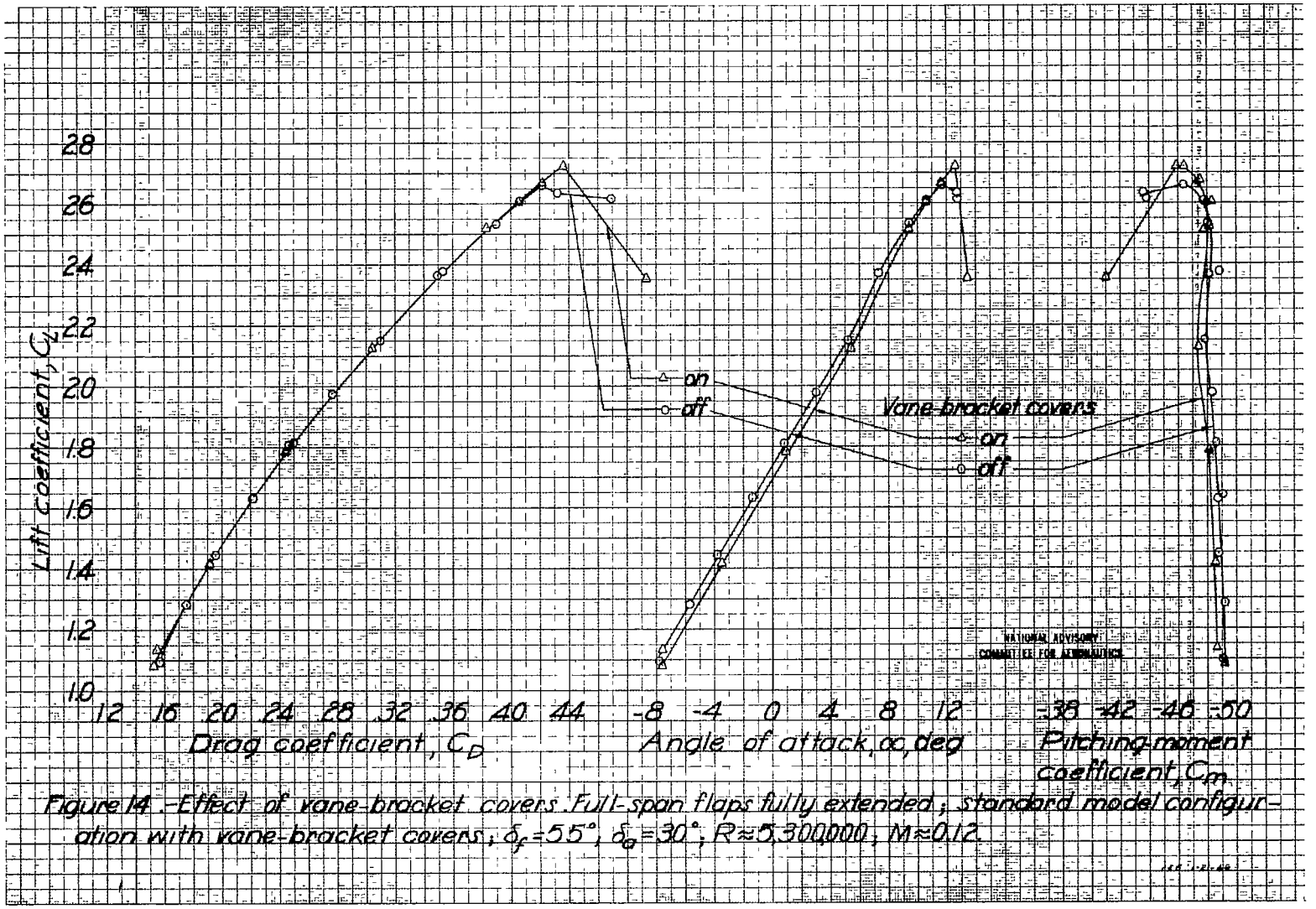

Figure 14.- Effect of vane-bracket covers. Full-span flaps fully extended; standard model configuration with vane-bracket covers; $\delta_f = 55°$, $\delta_a = 30°$; $R \approx 5,300,000$; $M \approx 0.12$.

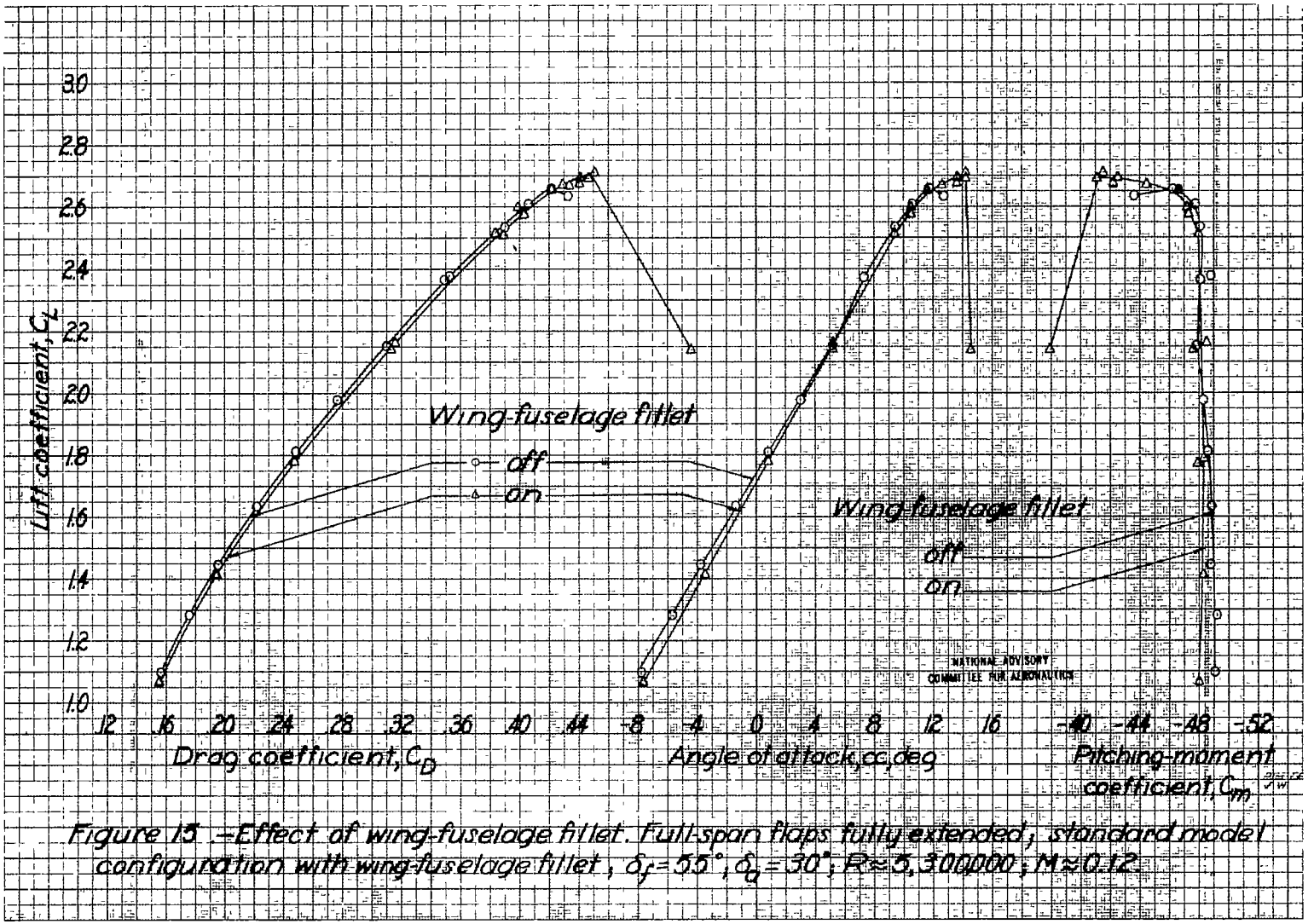

Figure 15.—Effect of wing-fuselage fillet. Full-span flaps fully extended; standard model configuration with wing-fuselage fillet; $\delta_f = 55°$; $\delta_a = 30°$; $R \approx 3,300,000$; $M \approx 0.12$.

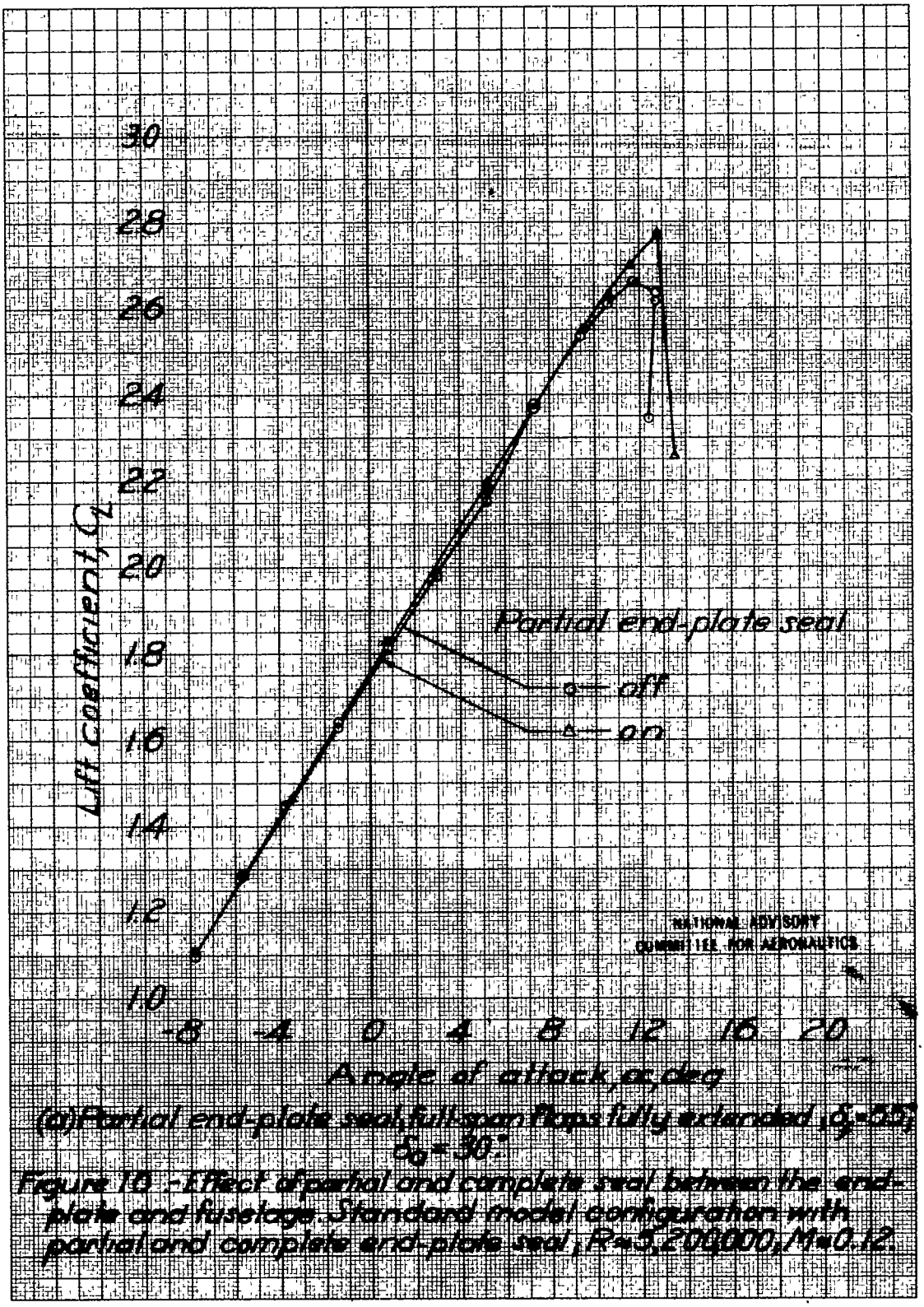

(a) Partial end-plate seal, full-span flaps fully extended (δ_f=50), δ_e=30°.

Figure 10.- Effect of partial and complete seal between the end-plate and fuselage. Standard model configuration with partial and complete end-plate seal; R=5,200,000, M=0.12.

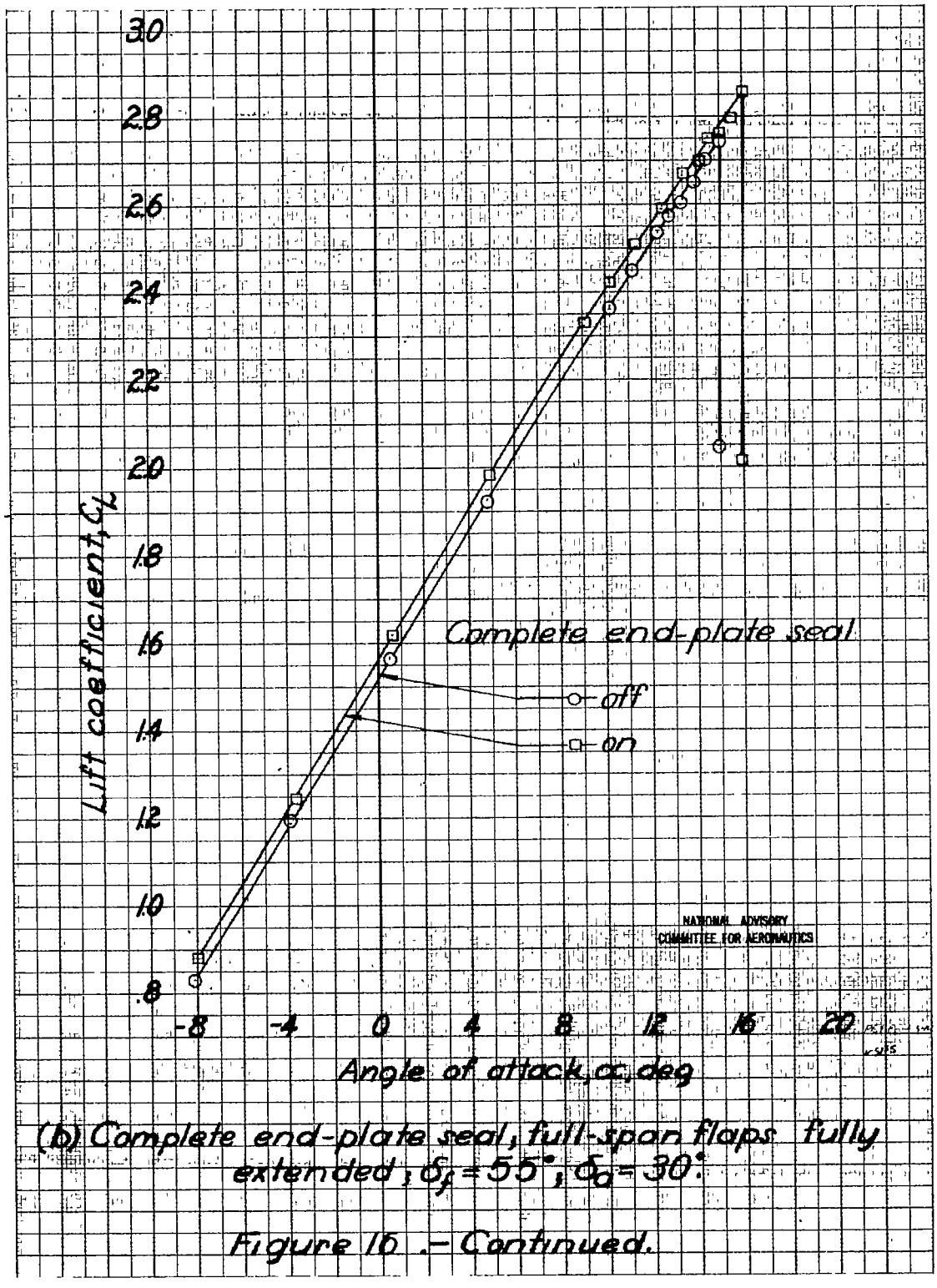

(b) Complete end-plate seal; full-span flaps fully extended; $\delta_f = 55°$; $\delta_a = 30°$.

Figure 16 .- Continued.

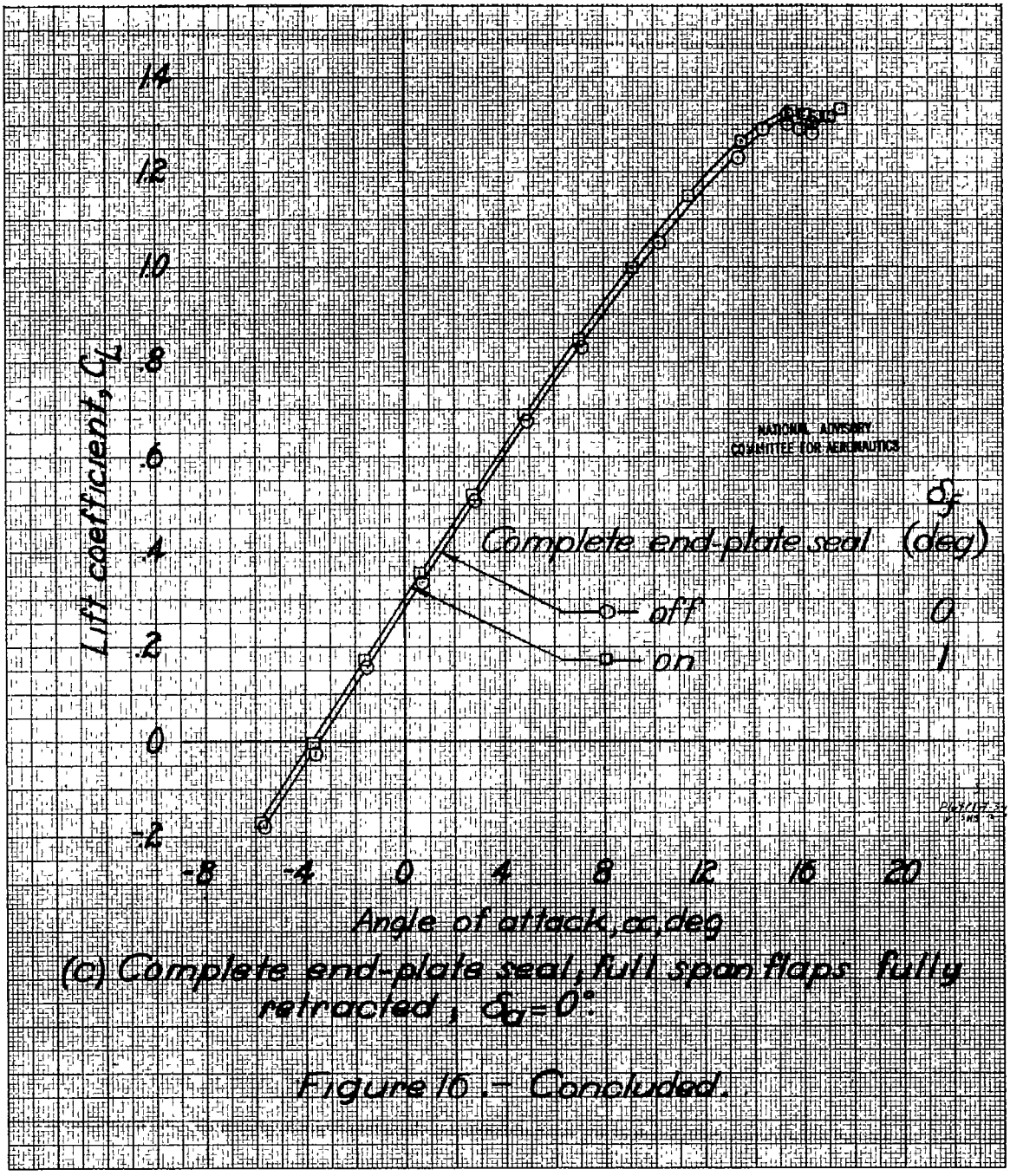

(c) Complete end-plate seal, full span flaps fully retracted; $\delta_f = 0°$.

Figure 16.- Concluded.

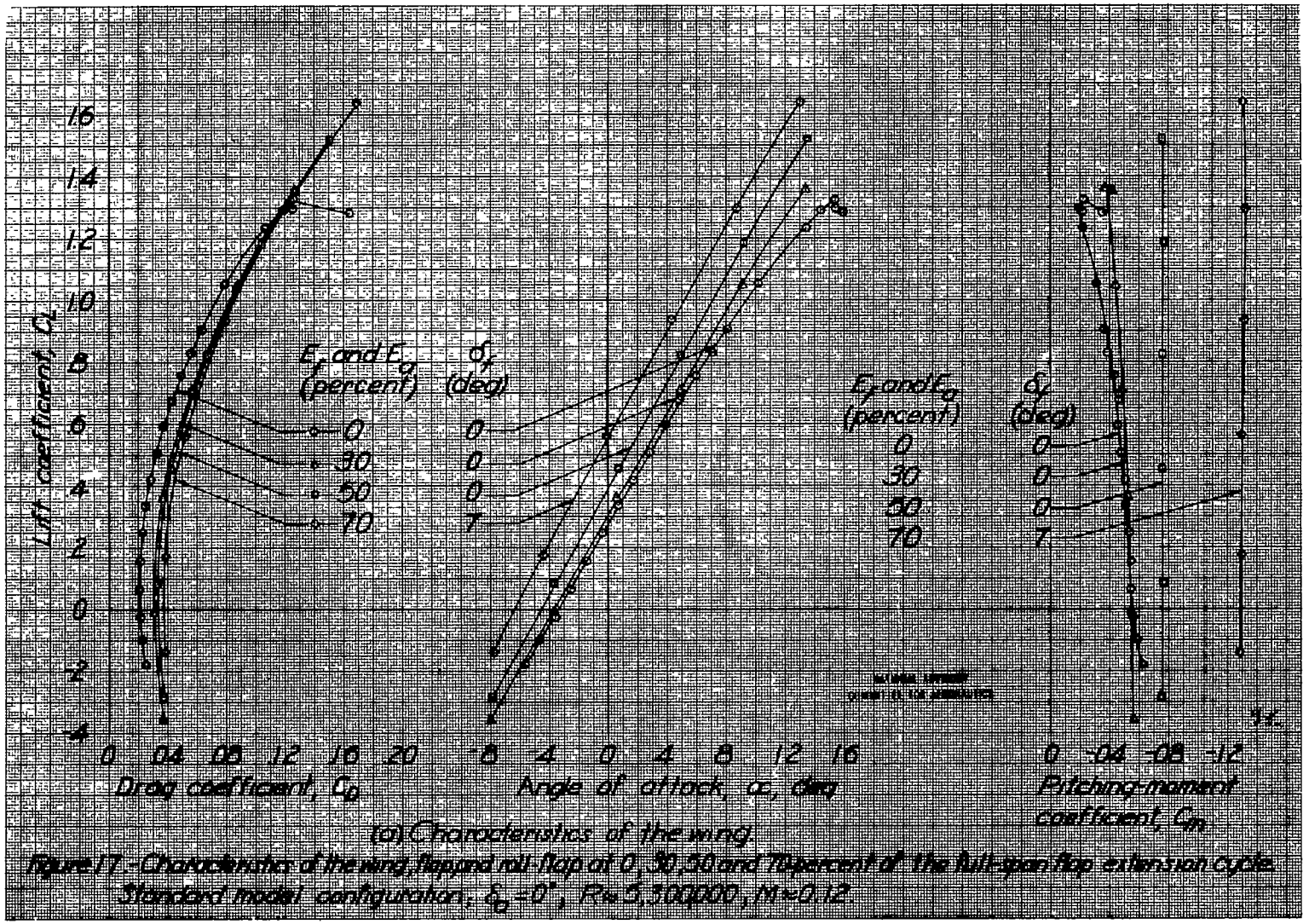

(a) Characteristics of the wing.

Figure 17.- Characteristics of the wing, flap, and roll flap at 0, 30, 50, and 70 percent of the full-span flap extension cycle. Standard model configuration, $\delta_a = 0°$; $R \approx 5,300,000$; $M \approx 0.12$.

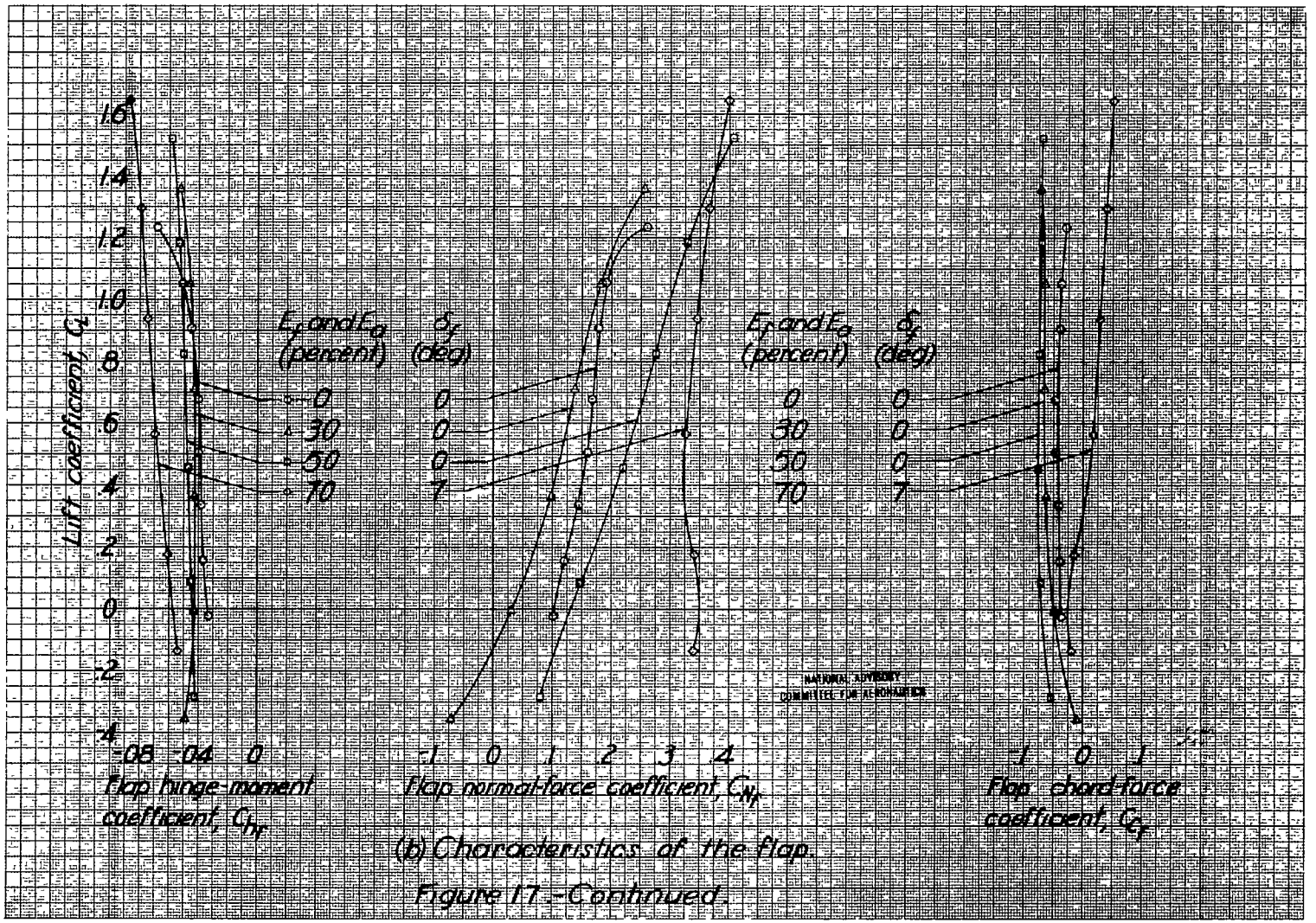

(b) Characteristics of the flap.

Figure 17.- Continued.

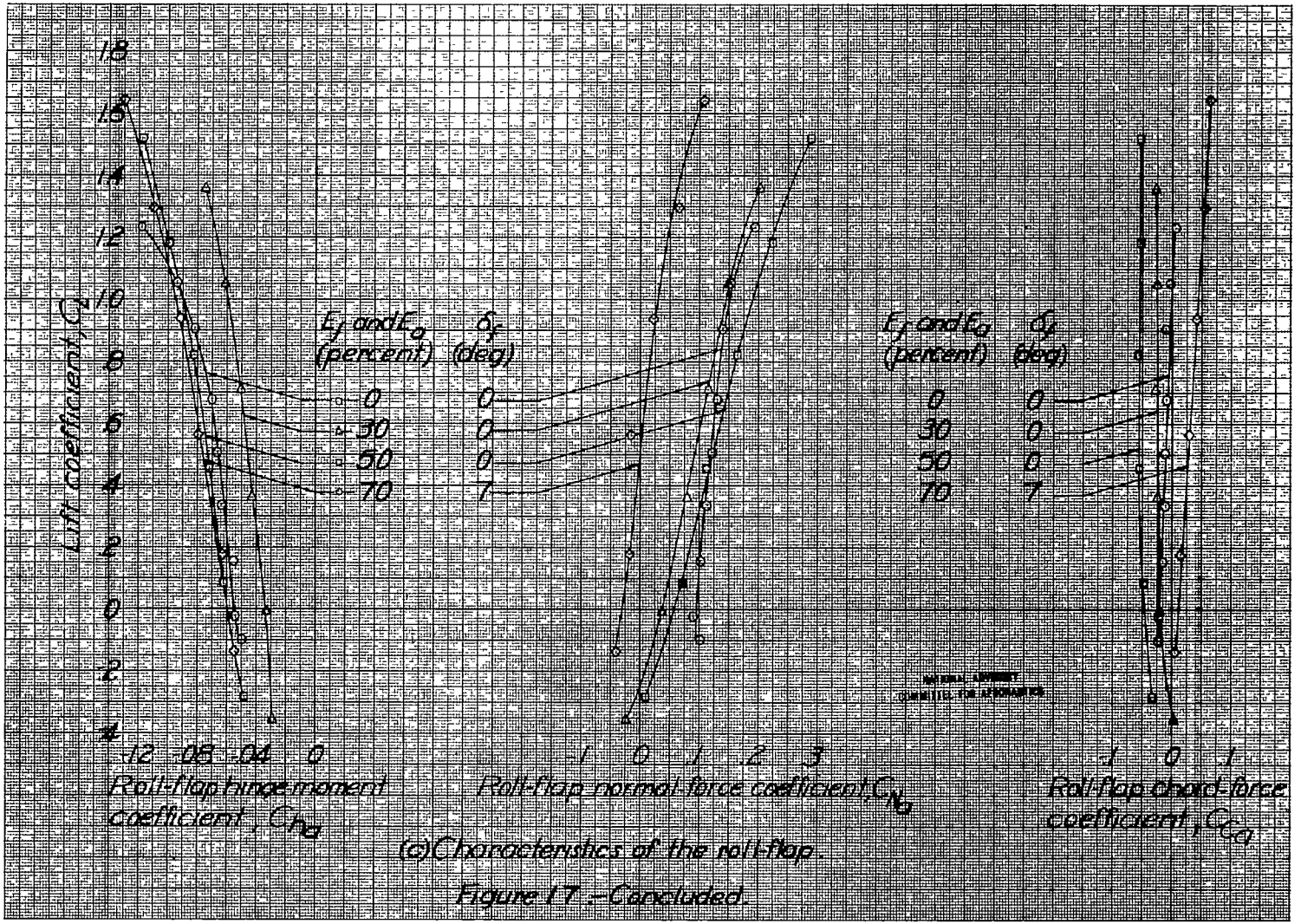

(c) Characteristics of the roll flap.

Figure 17.- Concluded.

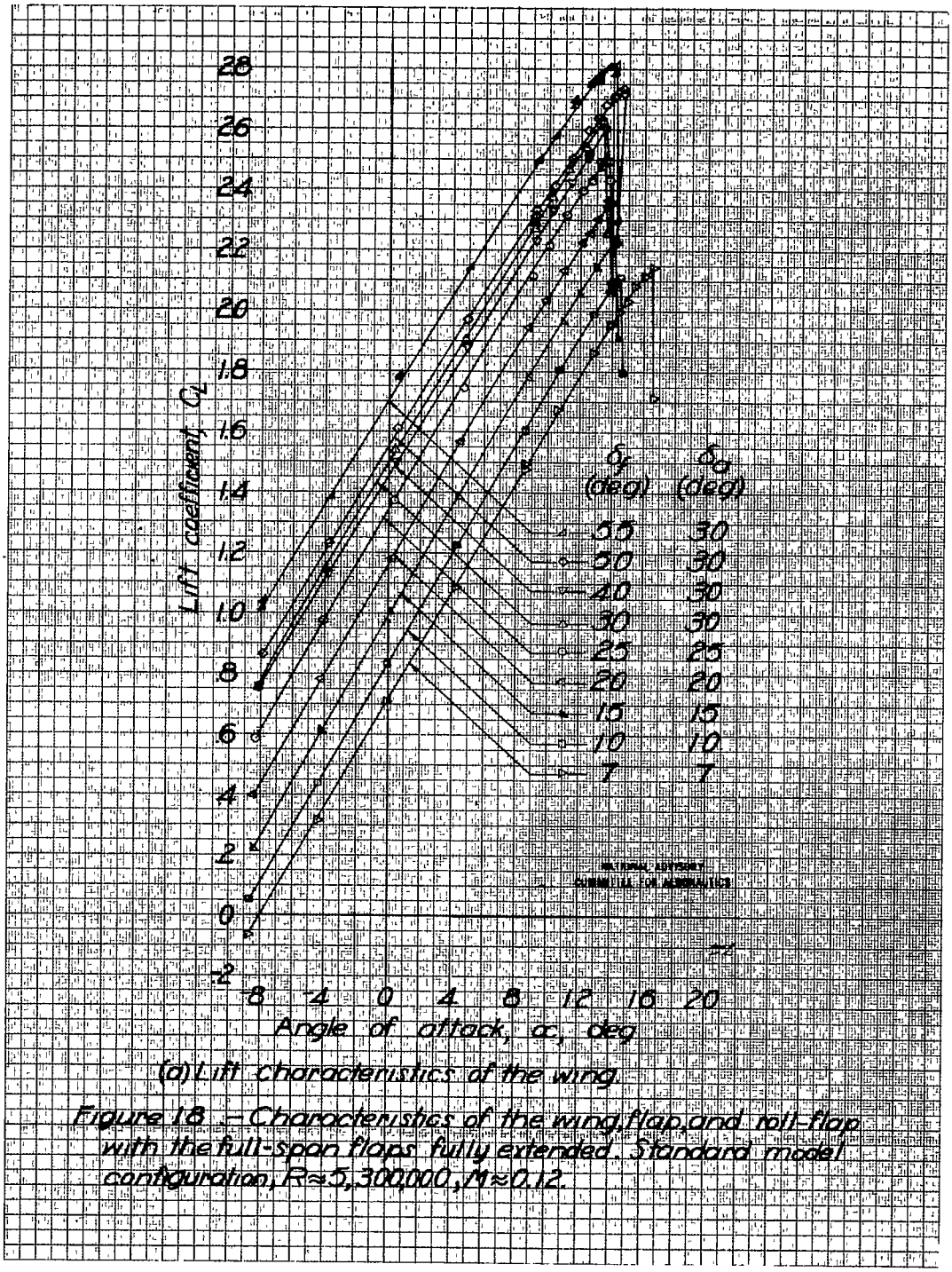

(a) Lift characteristics of the wing.

Figure 18.- Characteristics of the wing flap and roll-flap with the full-span flaps fully extended. Standard model configuration, $R \approx 5,300,000$, $M \approx 0.12$.

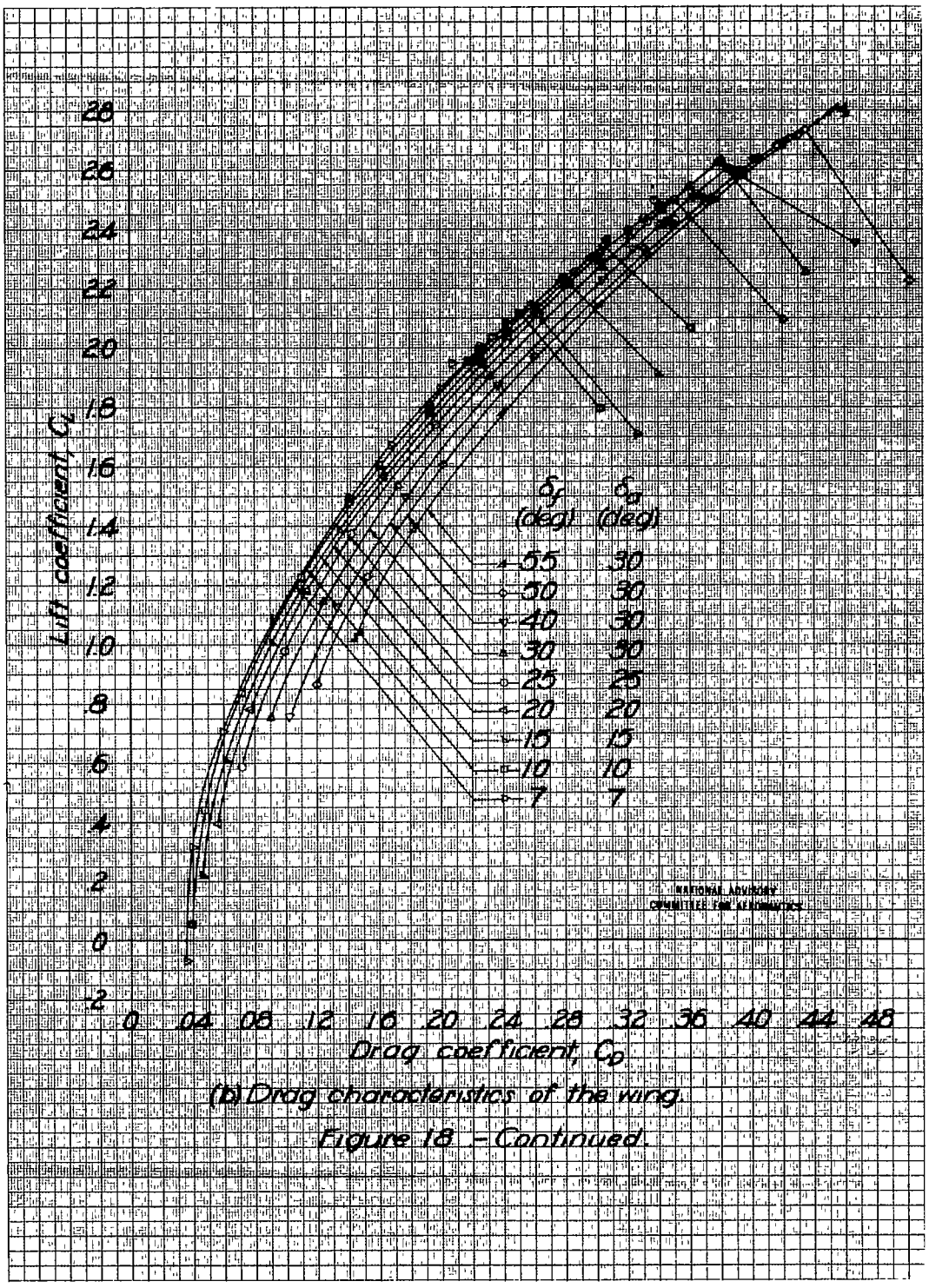

(b) Drag characteristics of the wing.

Figure 18 – Continued.

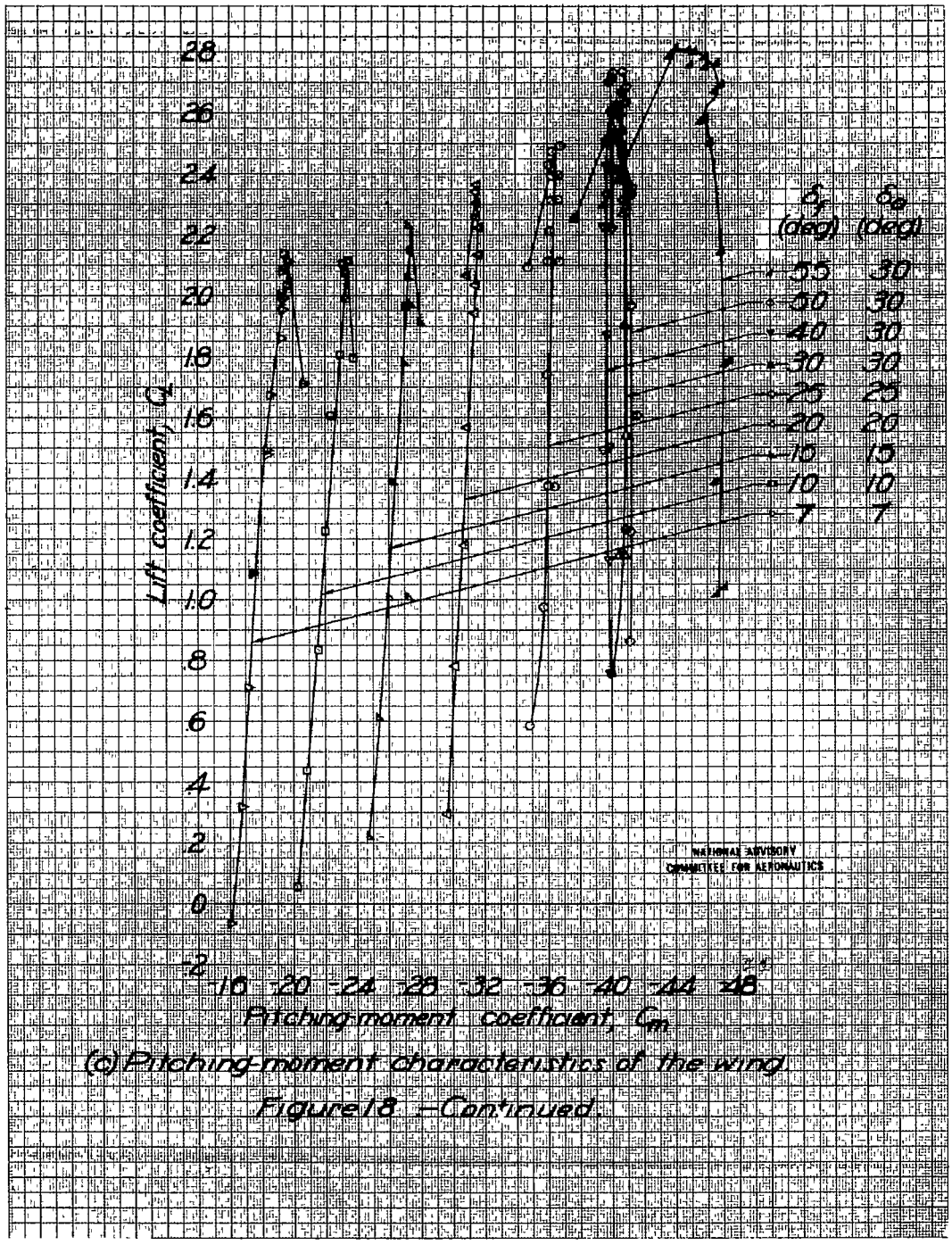

(c) Pitching-moment characteristics of the wing.

Figure 18.—Continued.

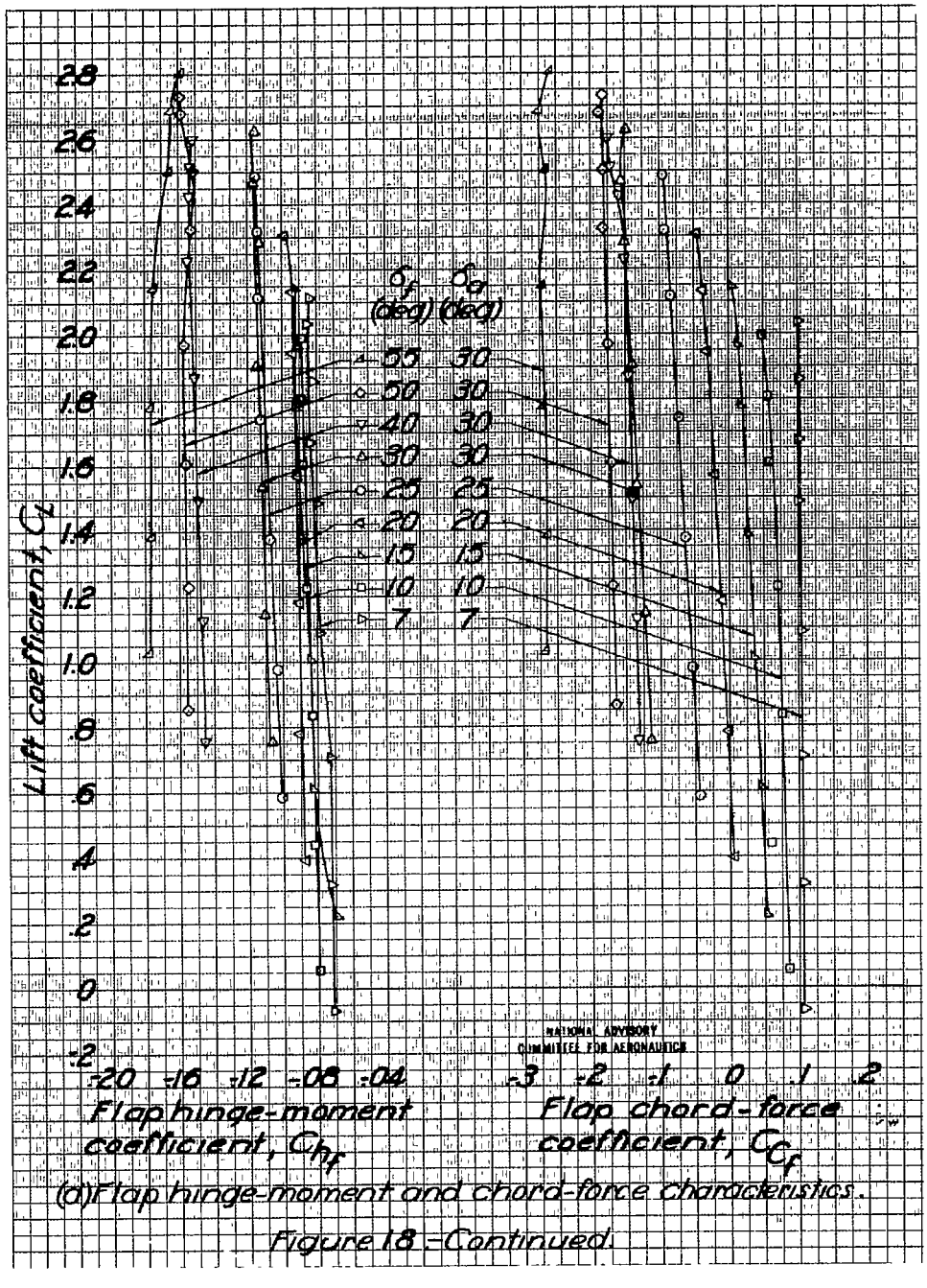

(d) Flap hinge-moment and chord-force characteristics.

Figure 18.—Continued.

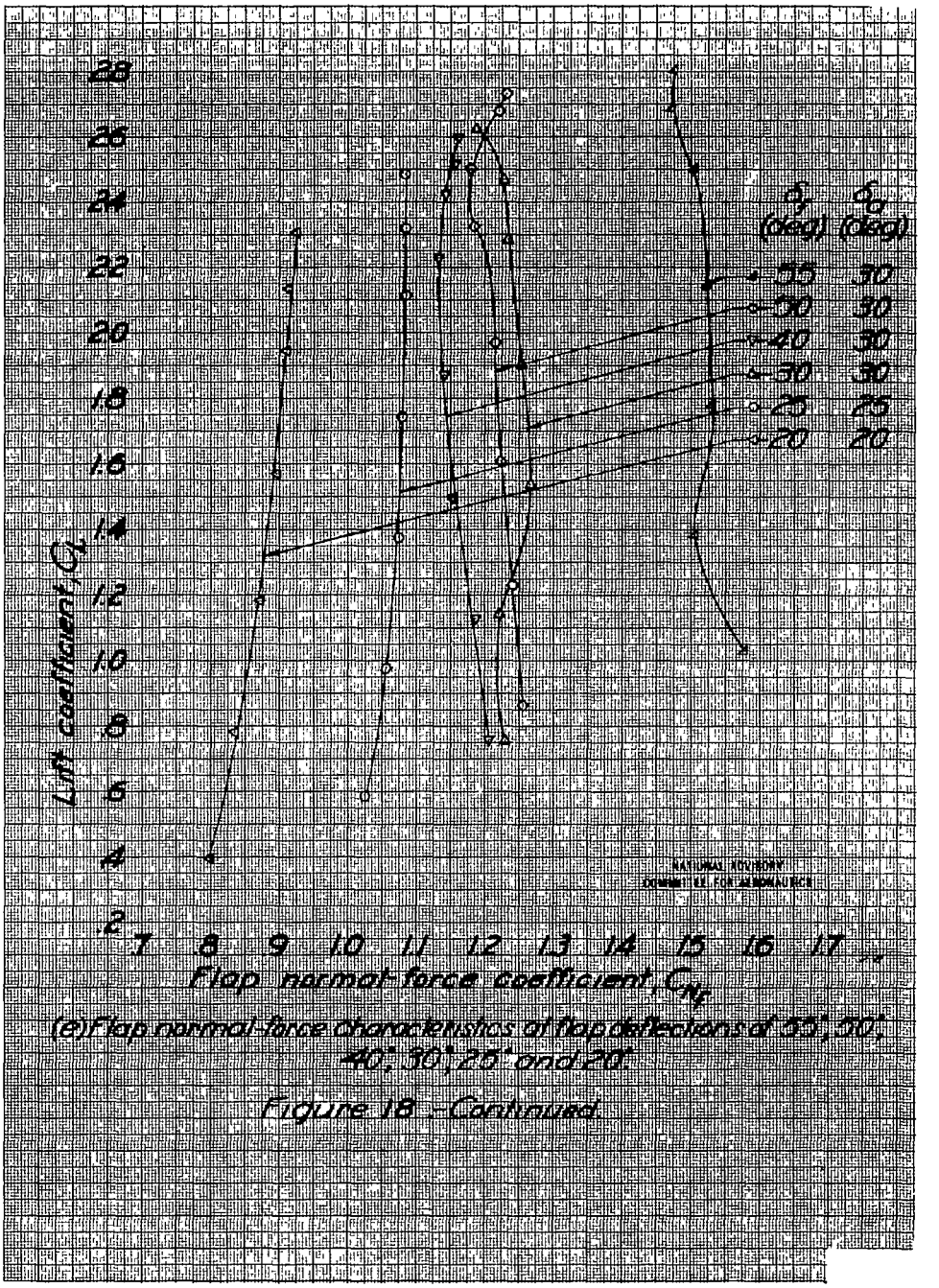

(e) Flap normal-force characteristics of flap deflections of 55°, 50°, 40°, 30°, 25° and 20°.

Figure 18.—Continued.

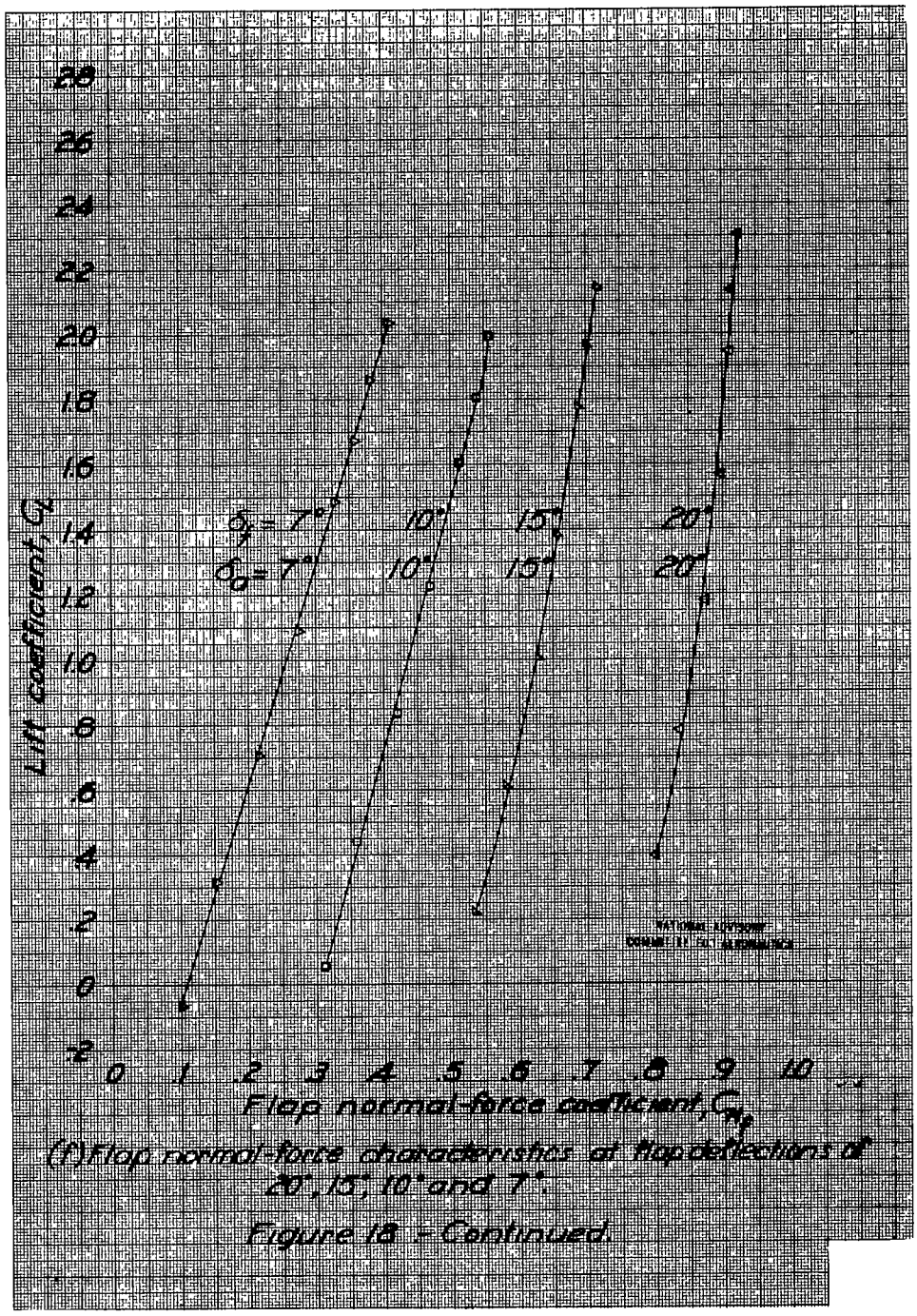

(f) Flap normal-force characteristics at flap deflections of 20°, 15°, 10° and 7°.

Figure 18 - Continued.

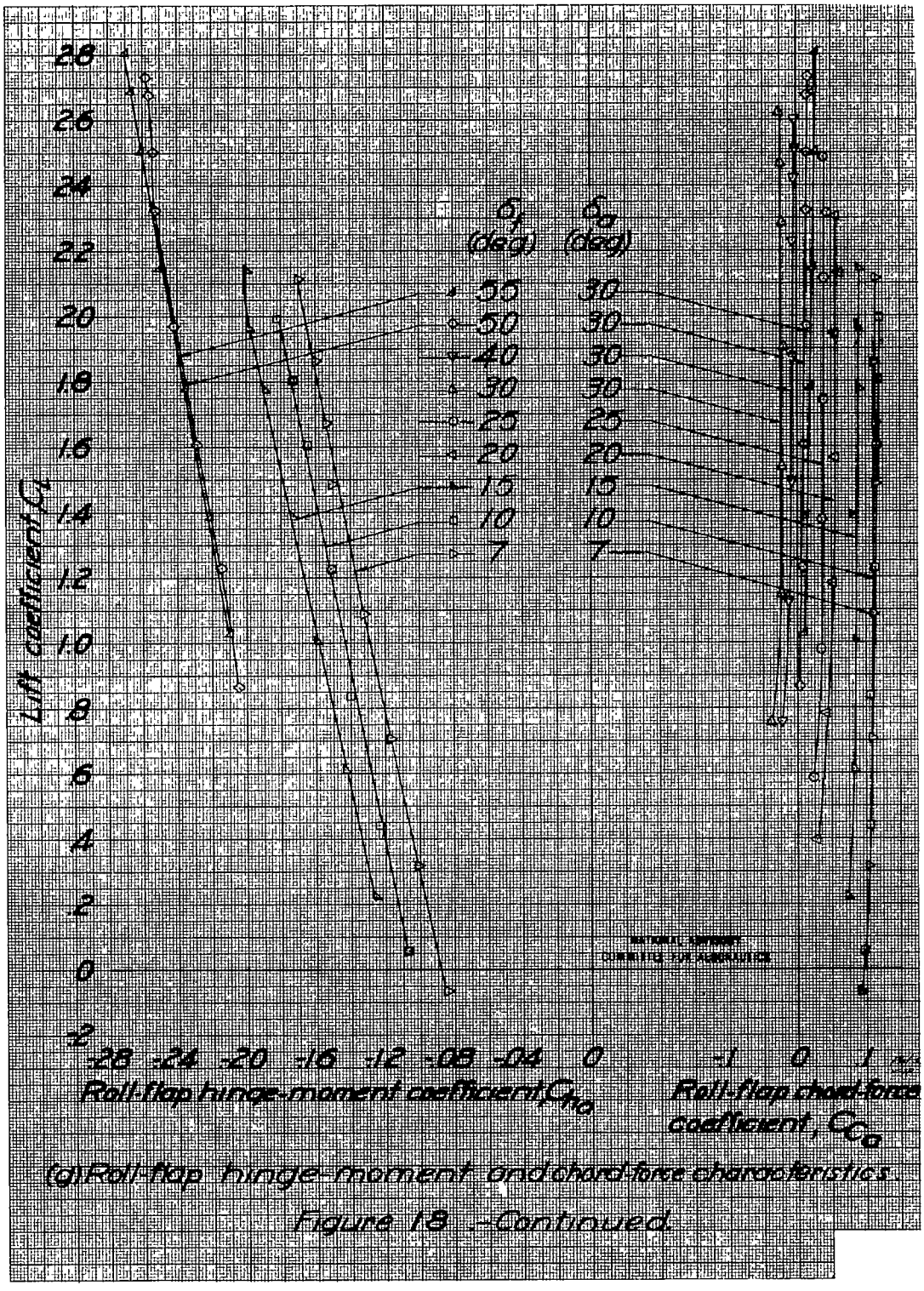

(a) Roll-flap hinge-moment and chord-force characteristics.

Figure 18.--Continued.

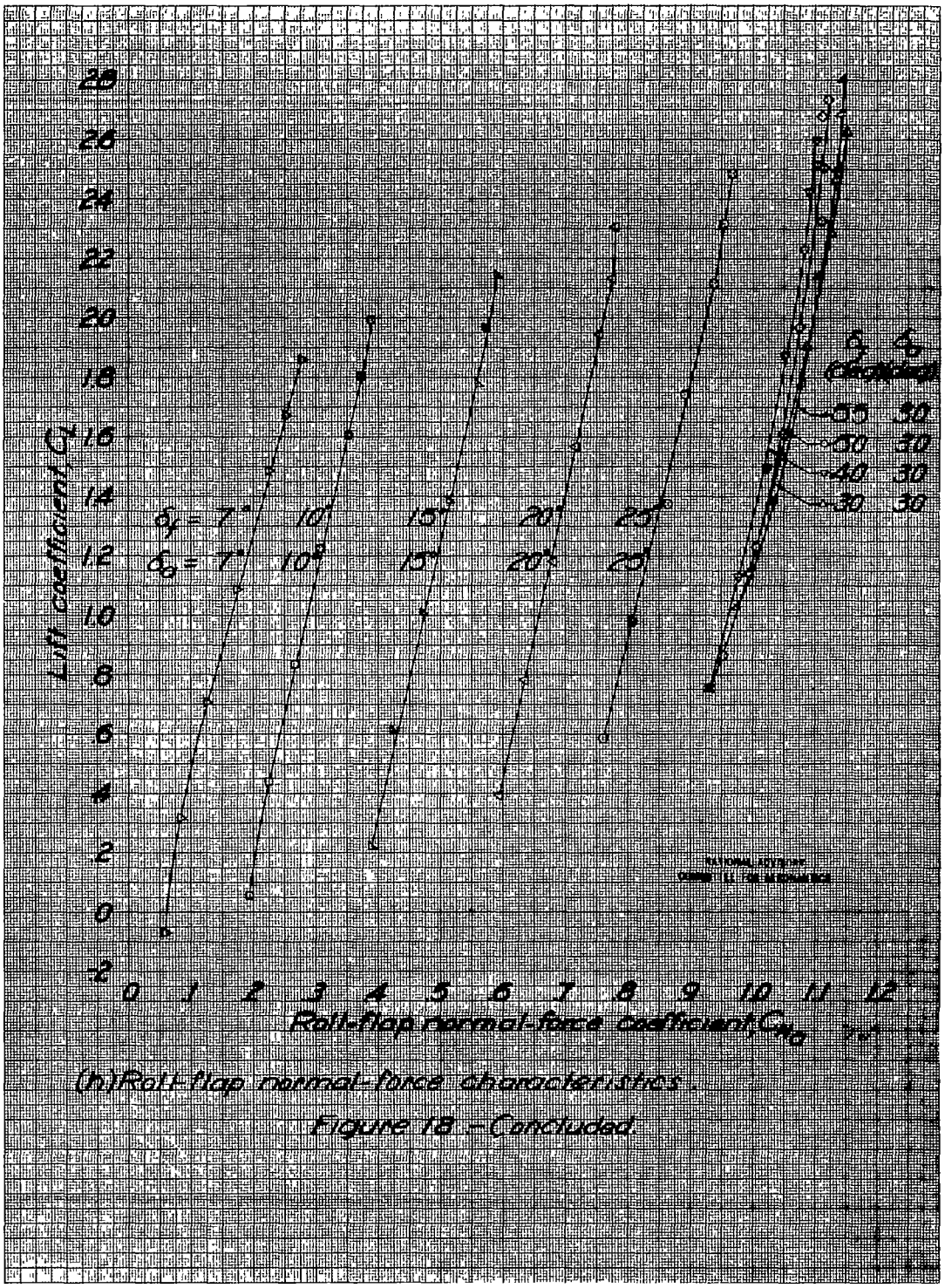

(h) Roll-flap normal-force characteristics.

Figure 18 – Concluded.

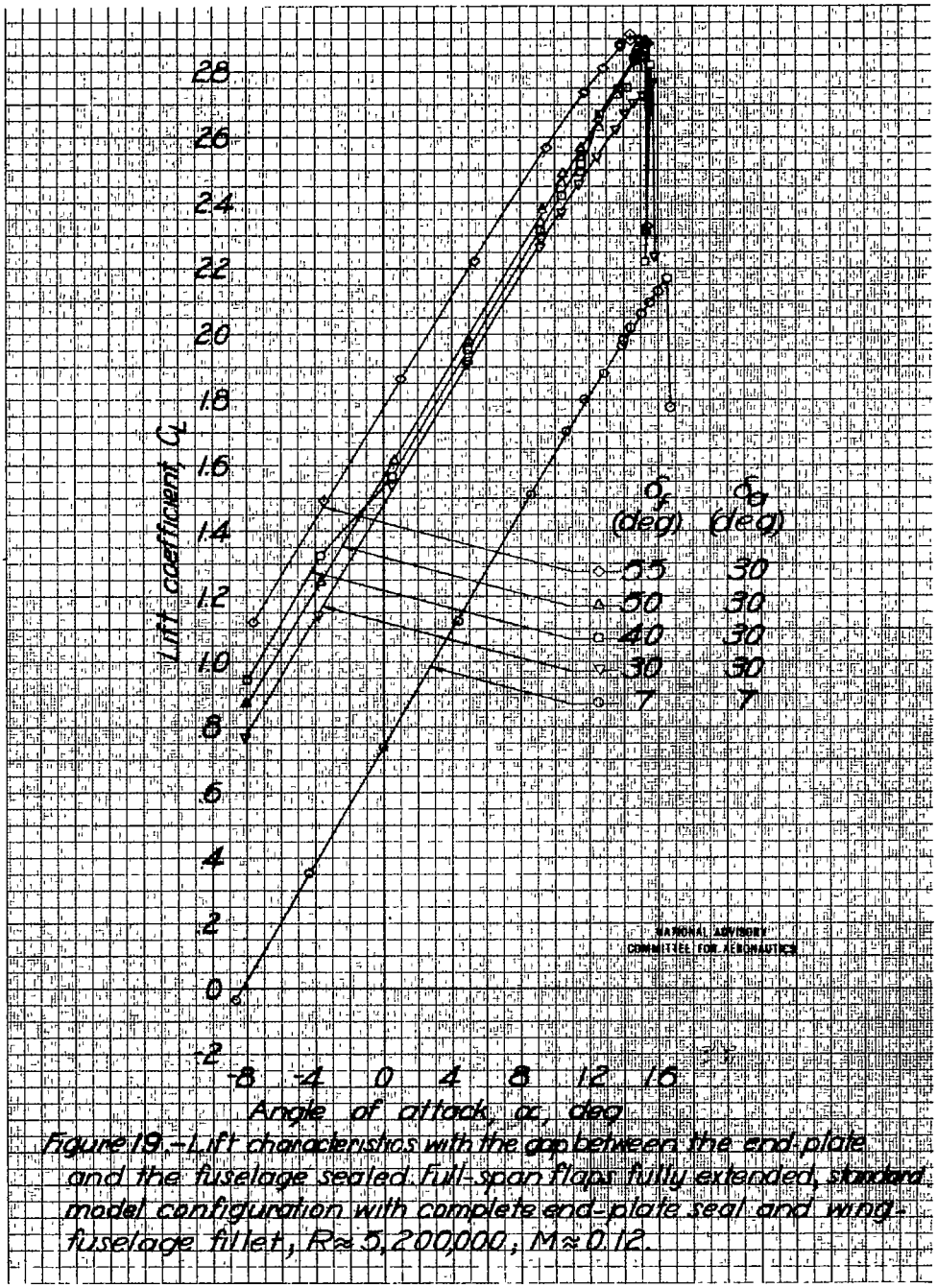

Figure 19.–Lift characteristics with the gap between the end plate and the fuselage sealed. Full-span flaps fully extended, standard model configuration with complete end-plate seal and wing-fuselage fillet, $R \approx 5,200,000$, $M \approx 0.12$.

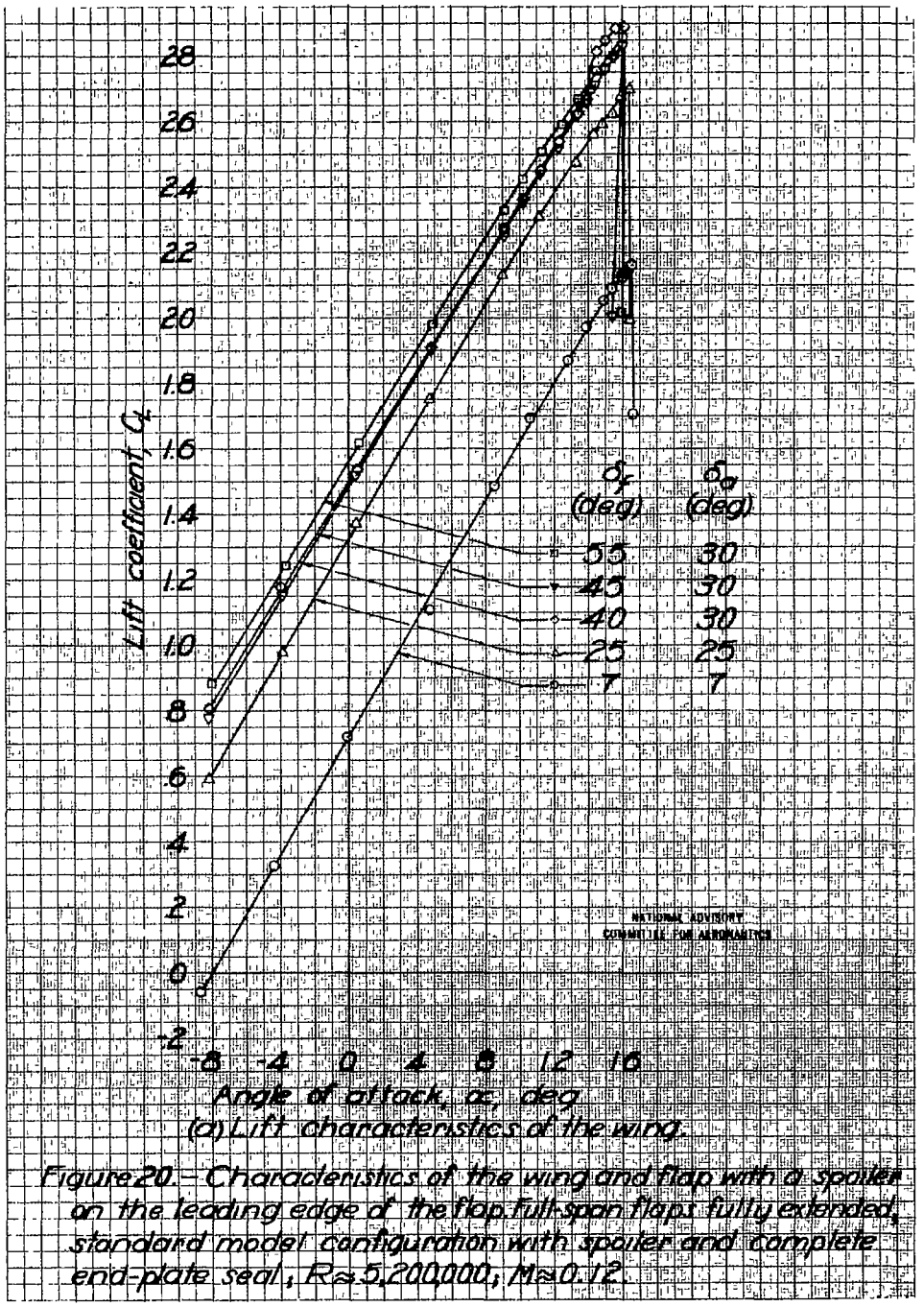

(a) Lift characteristics of the wing.

Figure 20.- Characteristics of the wing and flap with a spoiler on the leading edge of the flap, full-span flaps fully extended, standard model configuration with spoiler and complete end-plate seal, $R \approx 5,200,000$, $M \approx 0.12$.

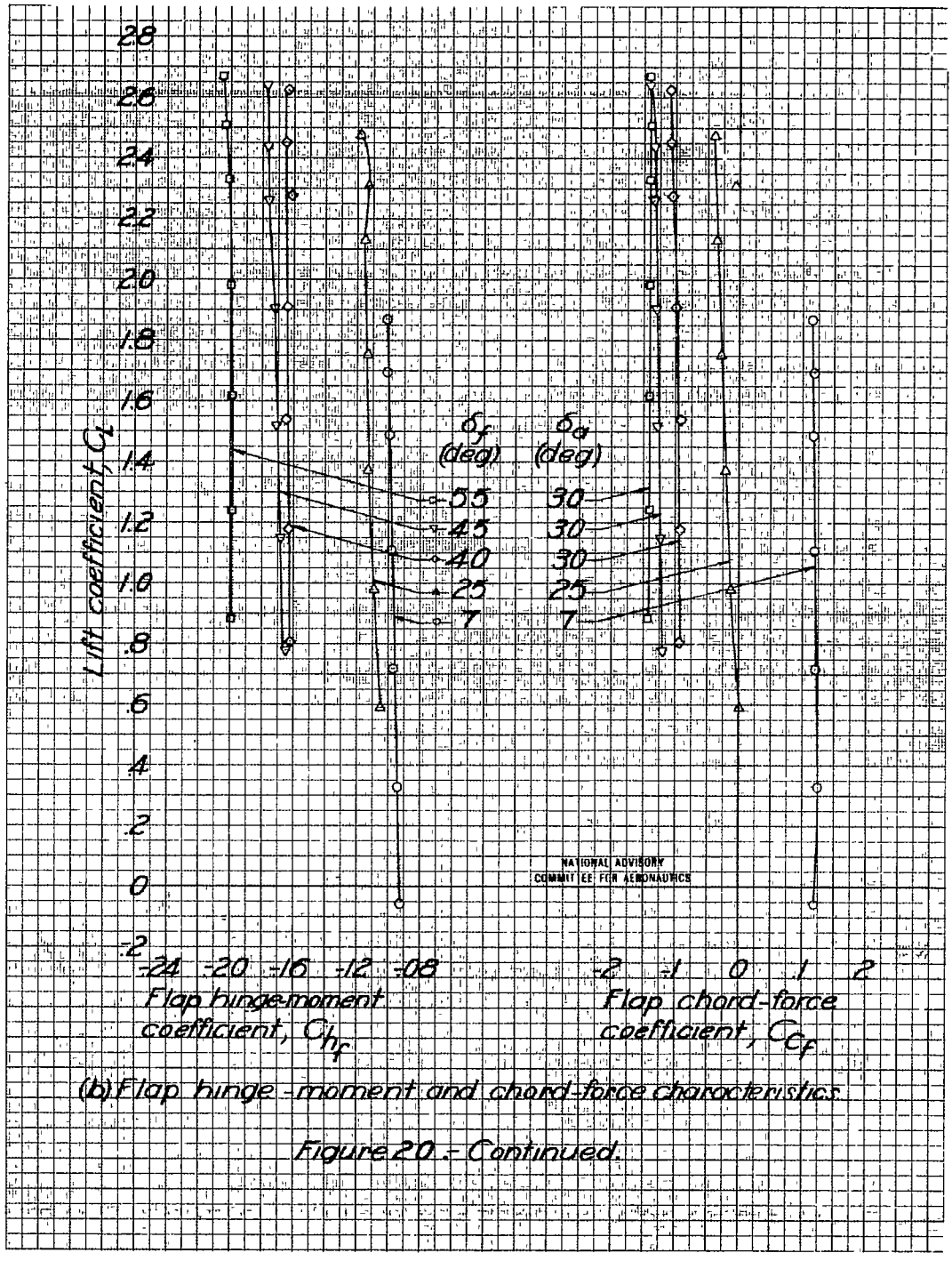

(b) Flap hinge-moment and chord-force characteristics.

Figure 20.- Continued.

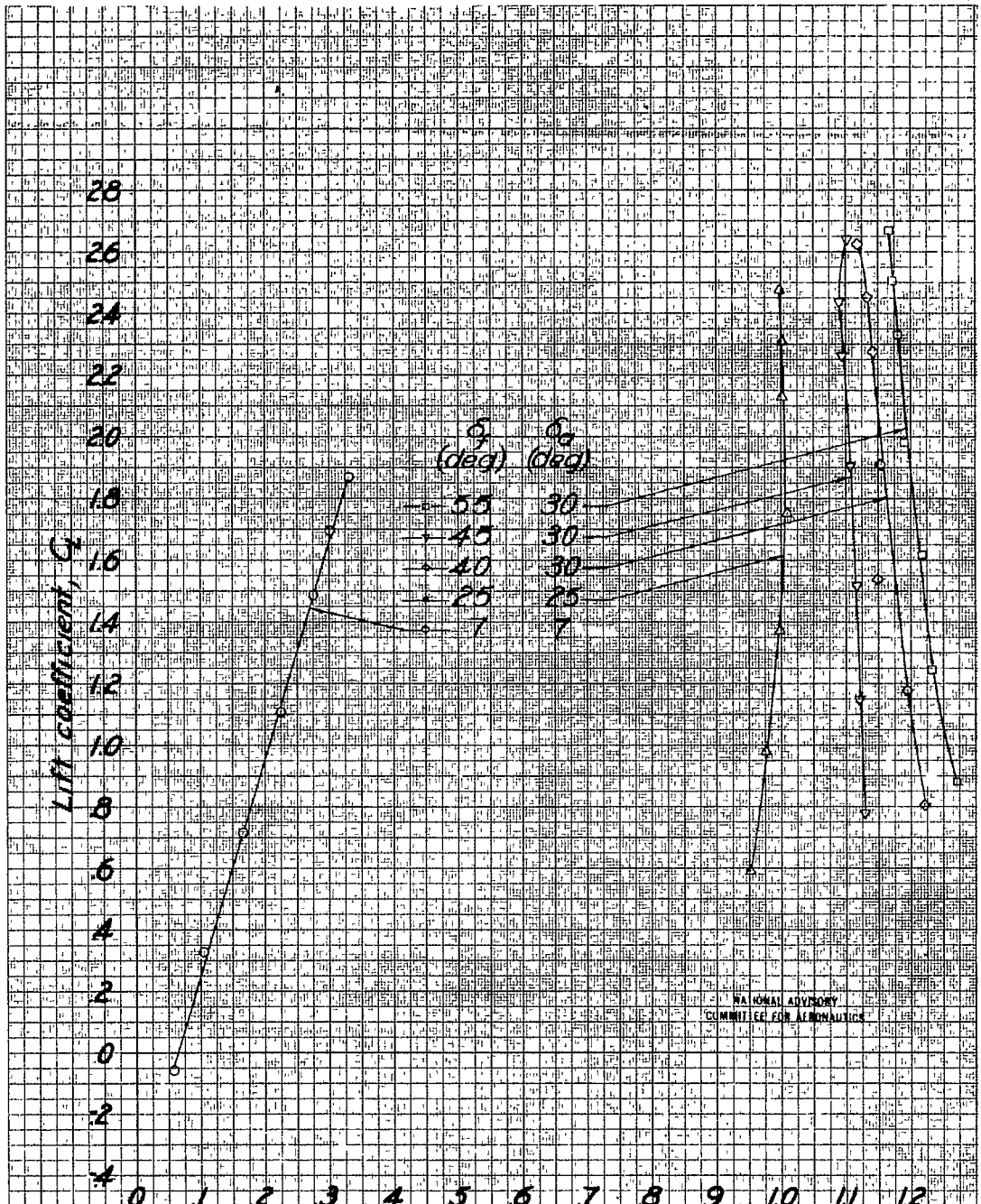

(c) Flap normal-force characteristics.

Figure 20.- Concluded.

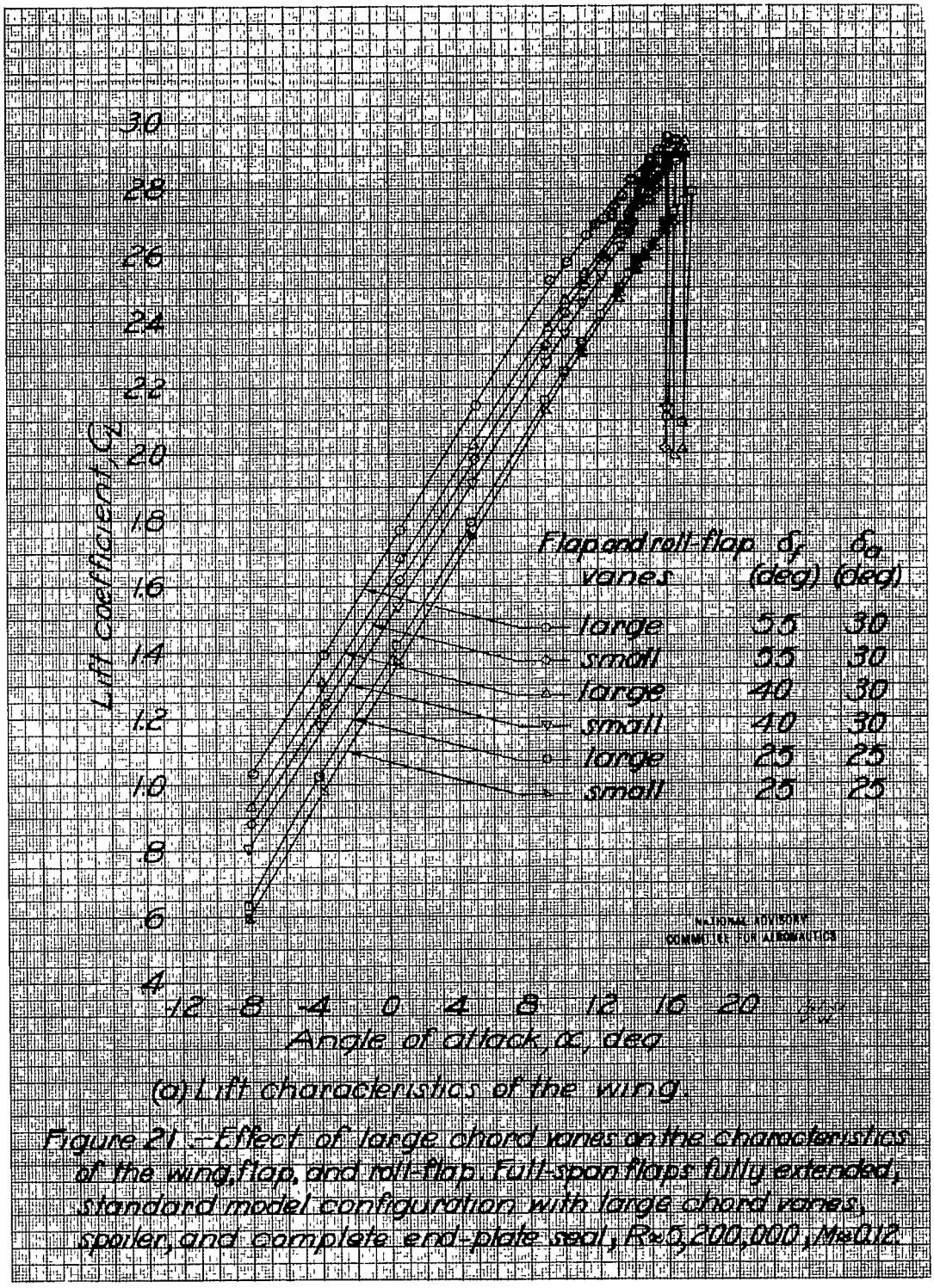

(a) Lift characteristics of the wing.

Figure 21.- Effect of large chord vanes on the characteristics of the wing, flap, and roll-flap. Full-span flaps fully extended, standard model configuration with large chord vanes, spoiler, and complete end-plate seal, $R \approx 5,200,000$, $M \approx .12$.

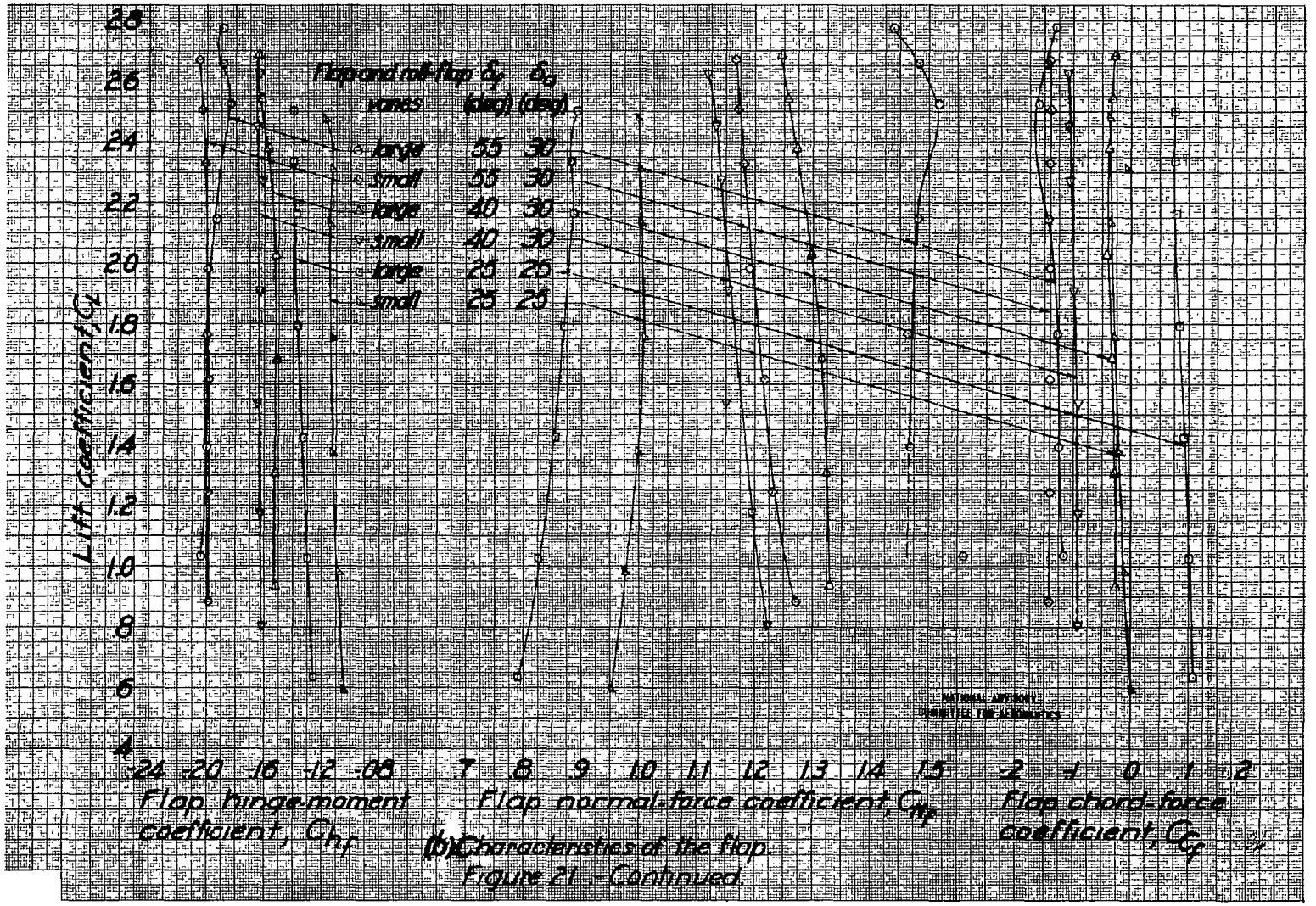

(b) Characteristics of the flap.

Figure 21.- Continued.

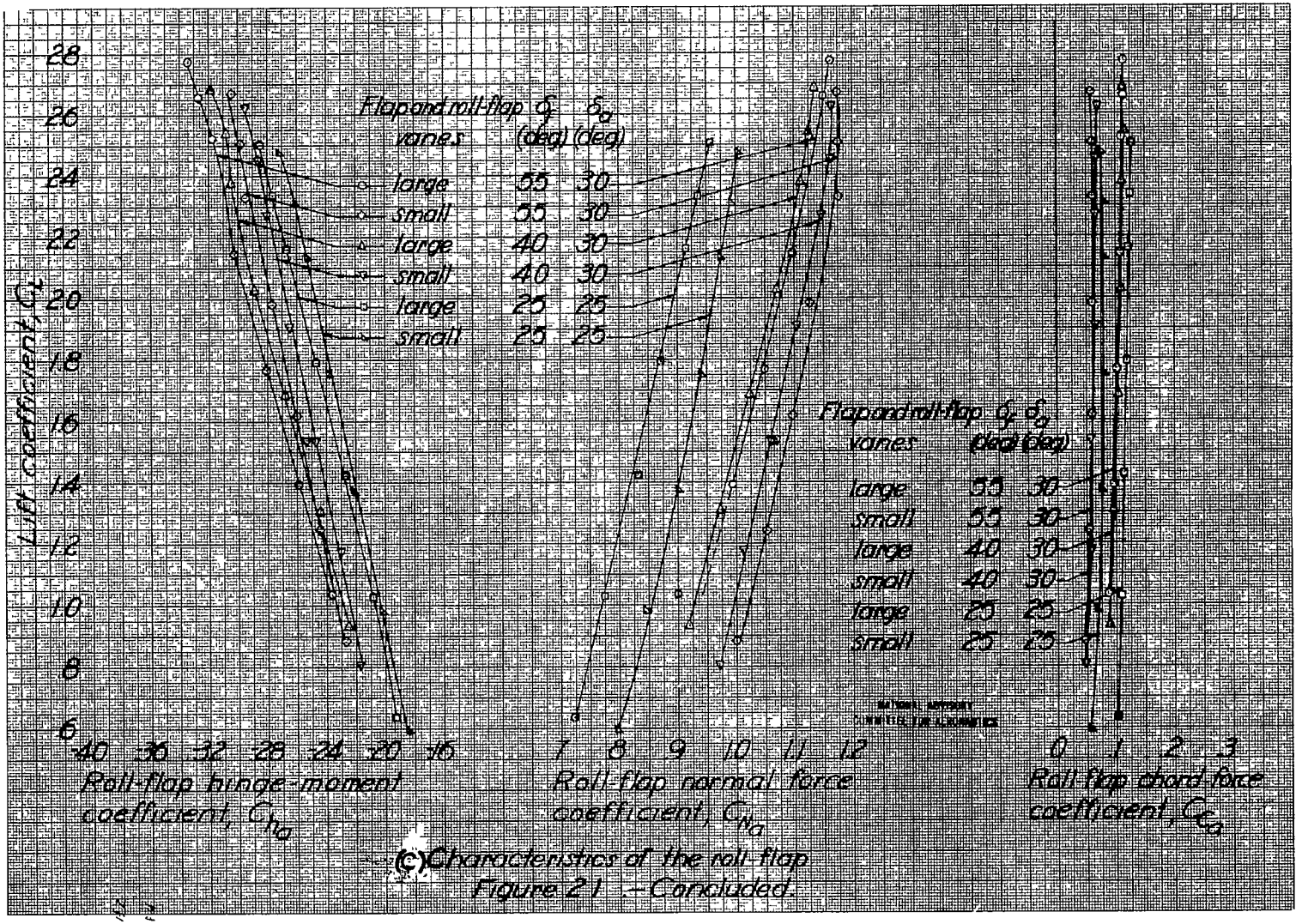

(c) Characteristics of the roll-flap

Figure 21.- Concluded.

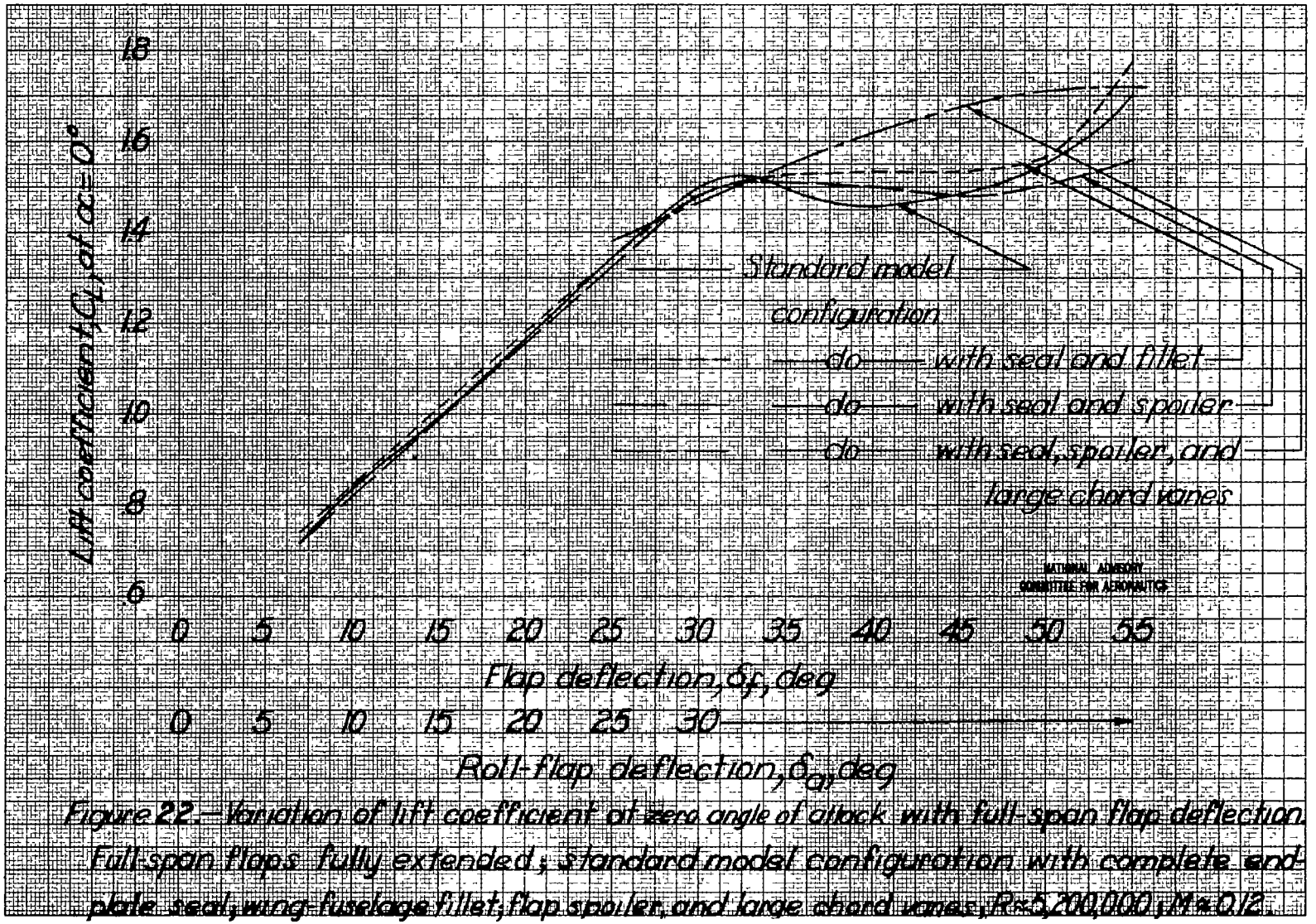

Figure 22.—Variation of lift coefficient at zero angle of attack with full-span flap deflection. Full-span flaps fully extended; standard model configuration with complete end-plate seal, wing-fuselage fillet, flap spoiler, and large chord vanes; $R = 5{,}200{,}000$; $M = 0.12$.

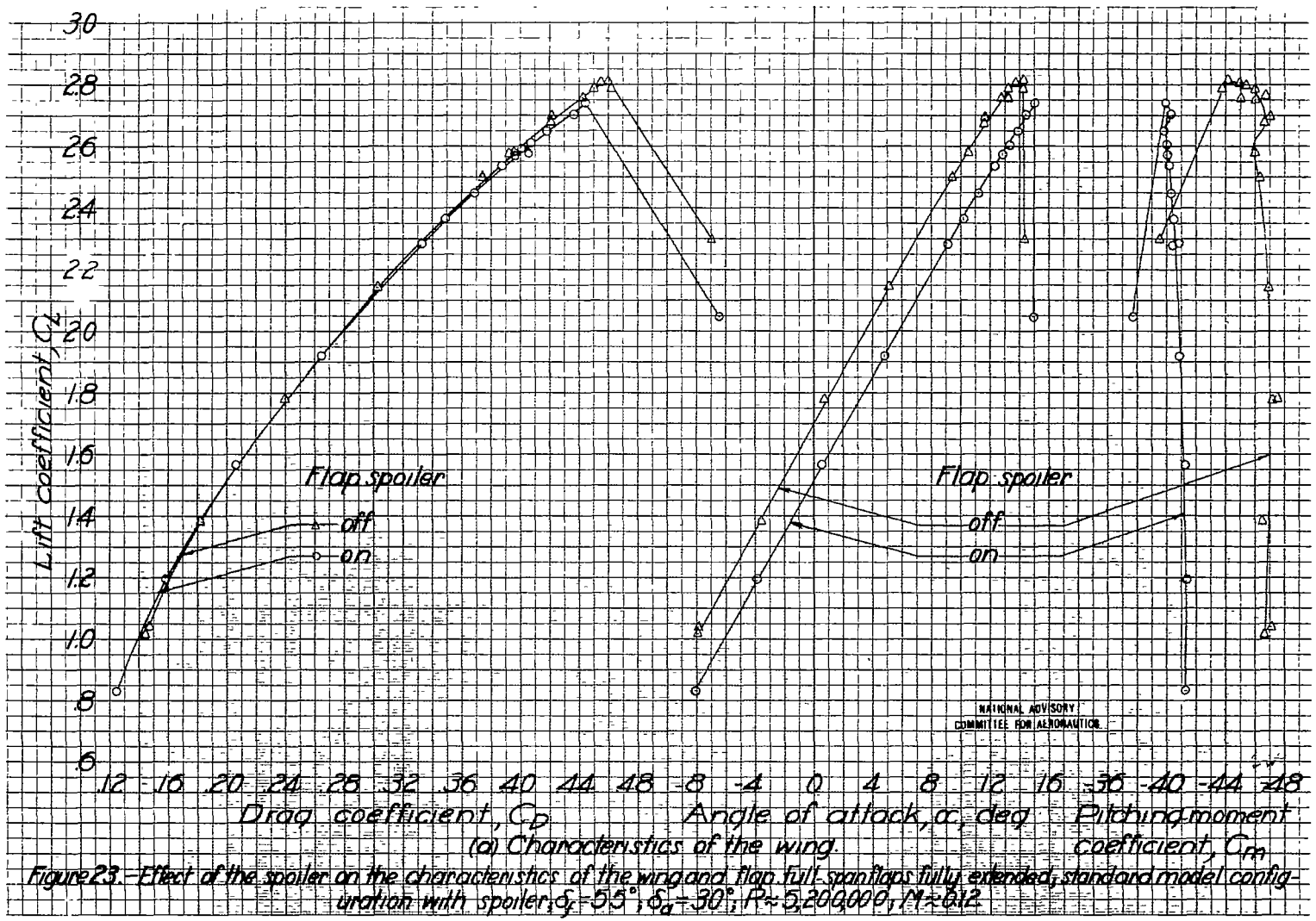

(a) Characteristics of the wing.

Figure 23.- Effect of the spoiler on the characteristics of the wing and flap full-span flaps fully extended, standard model configuration with spoiler; $\delta_f = 55°$; $\delta_a = 30°$; $R \approx 5,200,000$; $M \approx .212$

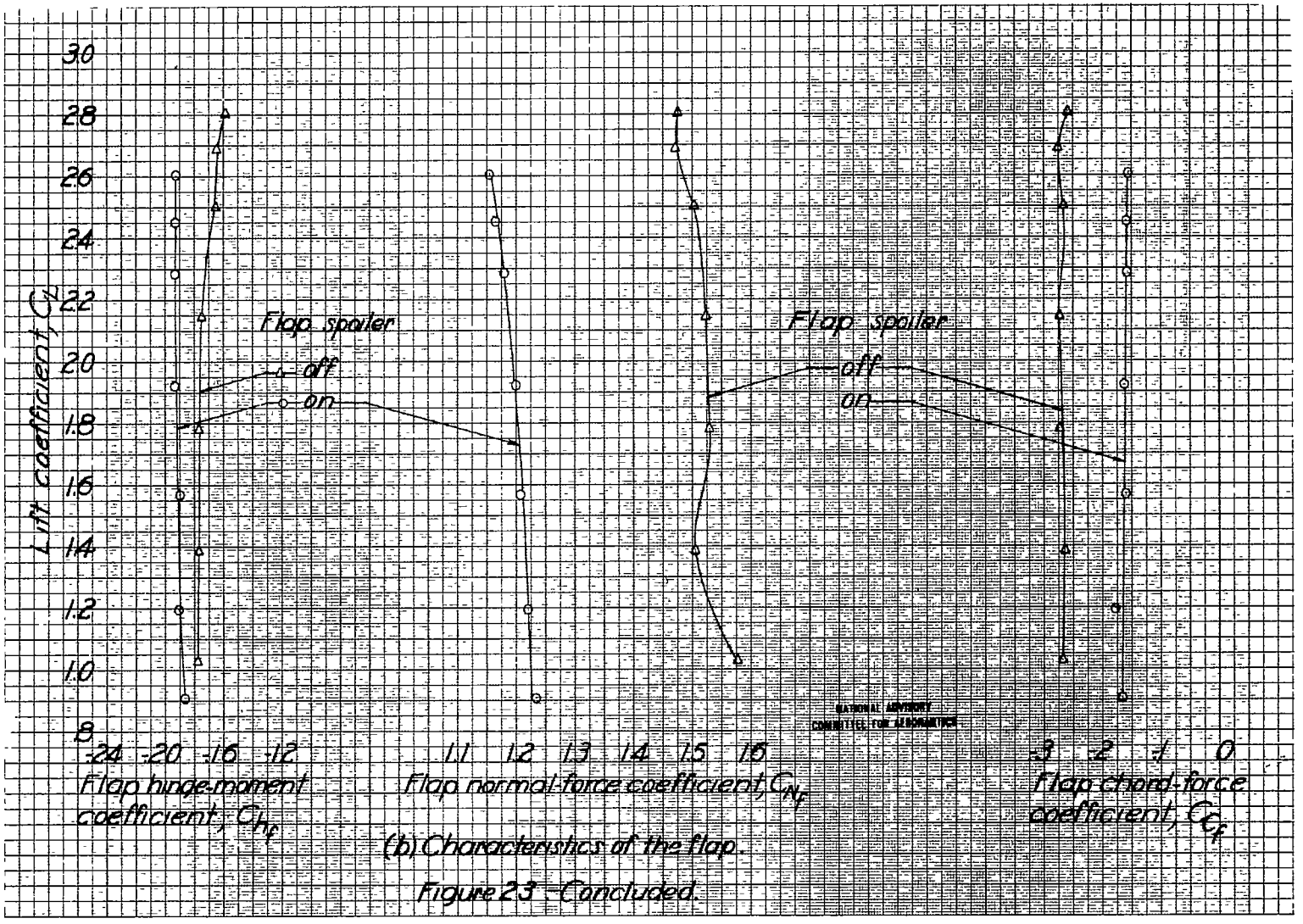

(b) Characteristics of the flap.

Figure 23.—Concluded.

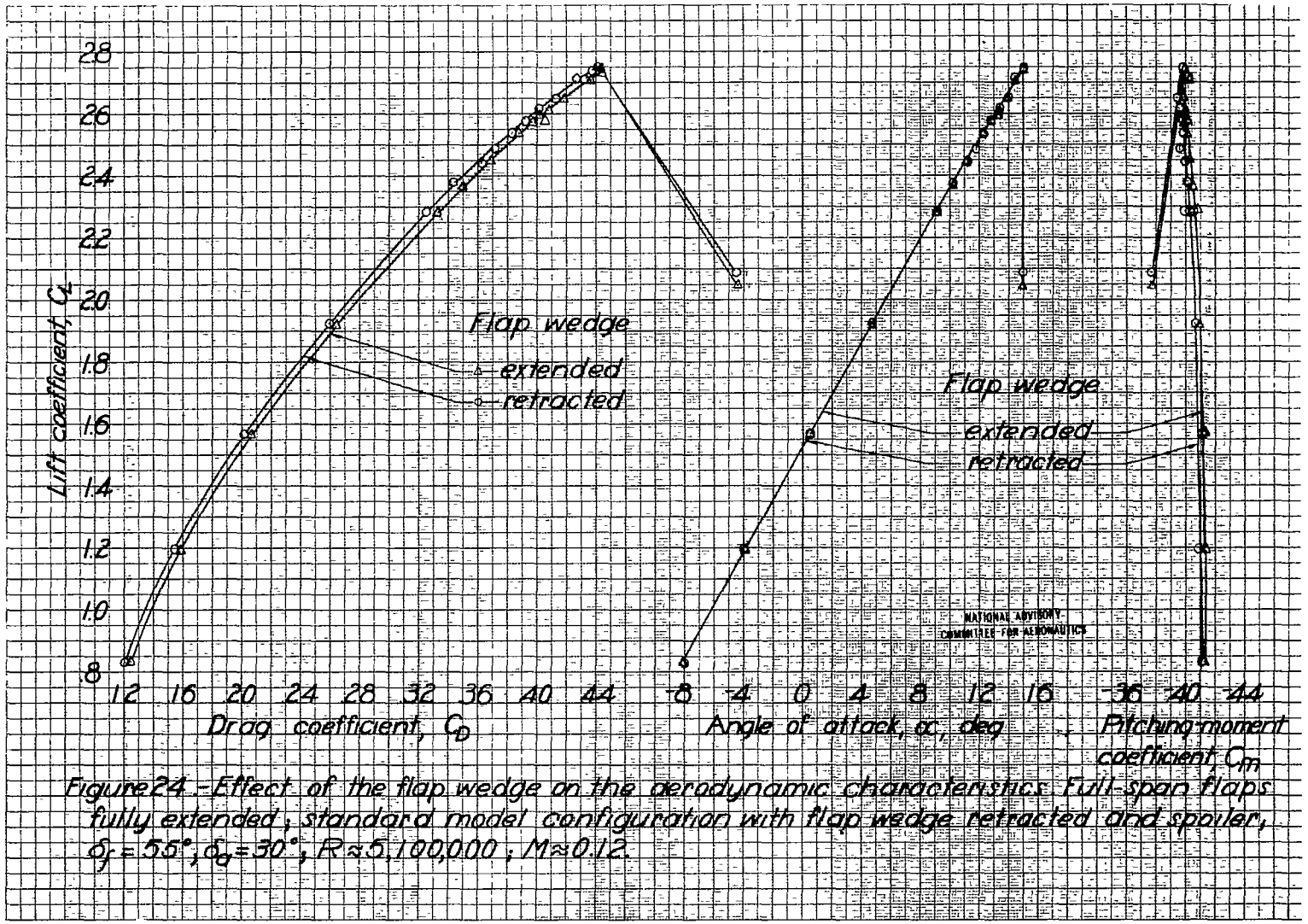

Figure 24 - Effect of the flap wedge on the aerodynamic characteristics. Full-span flaps fully extended; standard model configuration with flap wedge retracted and spoiler; $\delta_f = 55°$; $\delta_a = 30°$; $R \approx 5,100,000$; $M \approx 0.12$.

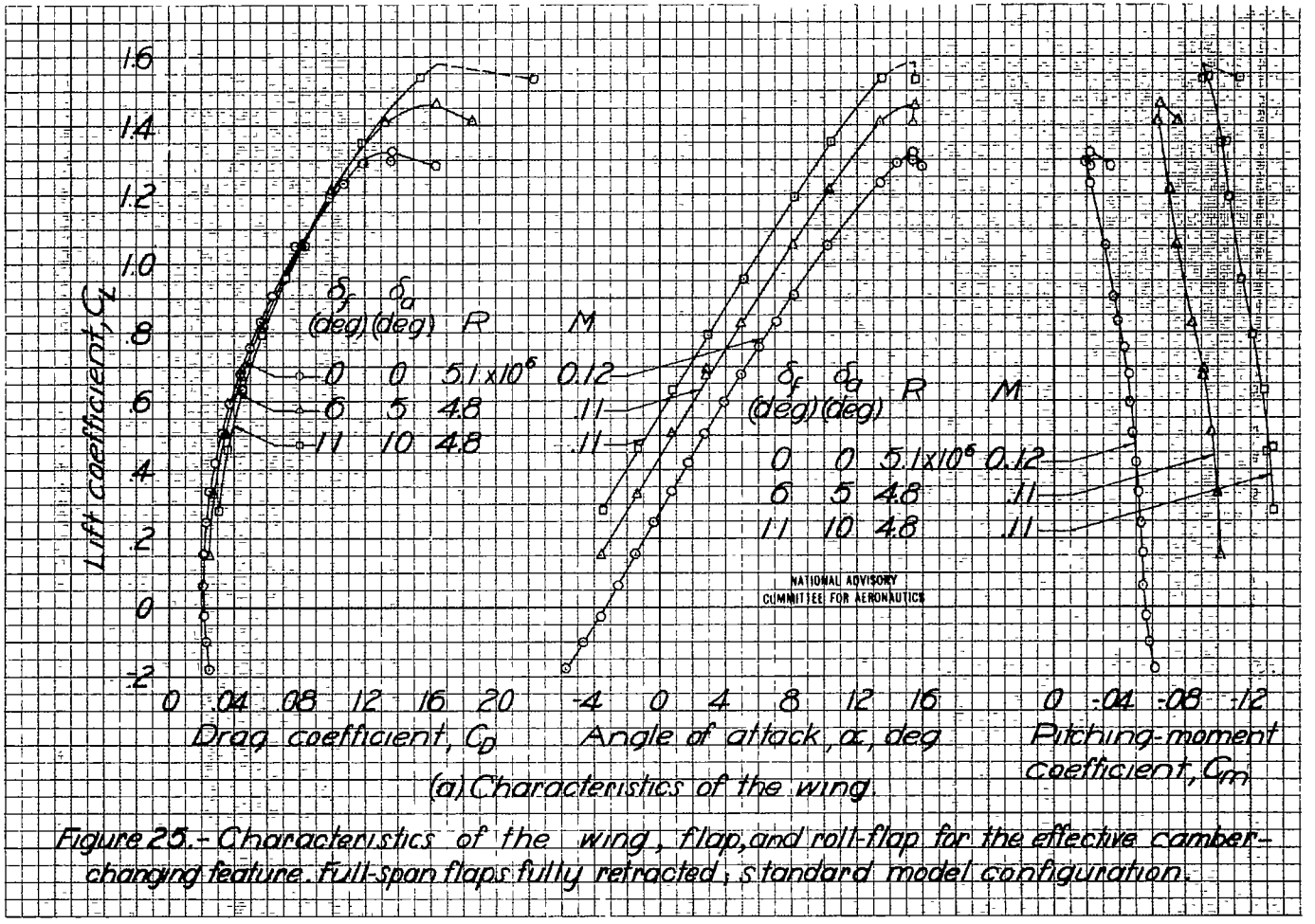

(a) Characteristics of the wing.

Figure 25.- Characteristics of the wing, flap, and roll-flap for the effective camber-changing feature. Full-span flaps fully retracted; standard model configuration.

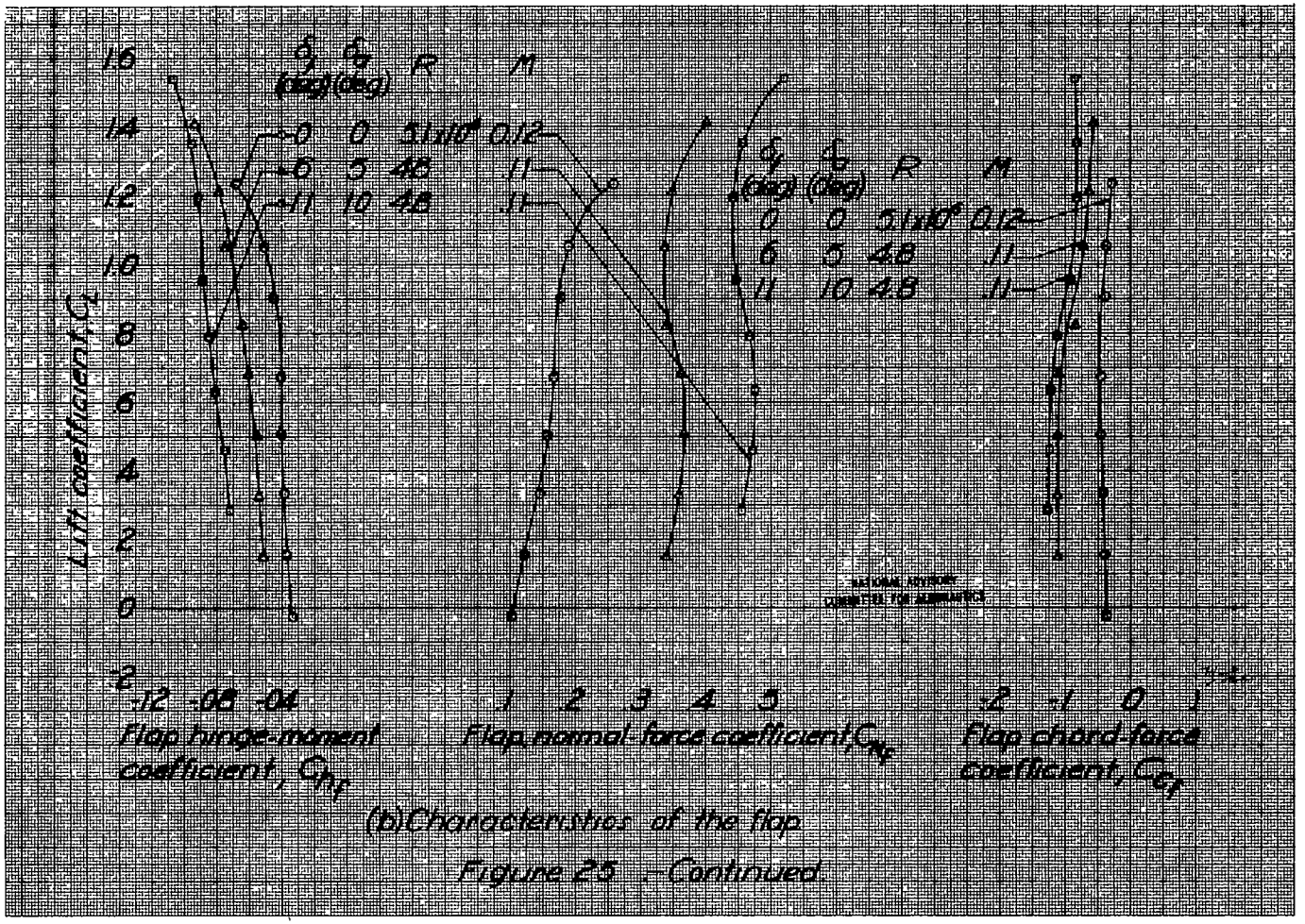

(b) Characteristics of the flap

Figure 25.—Continued

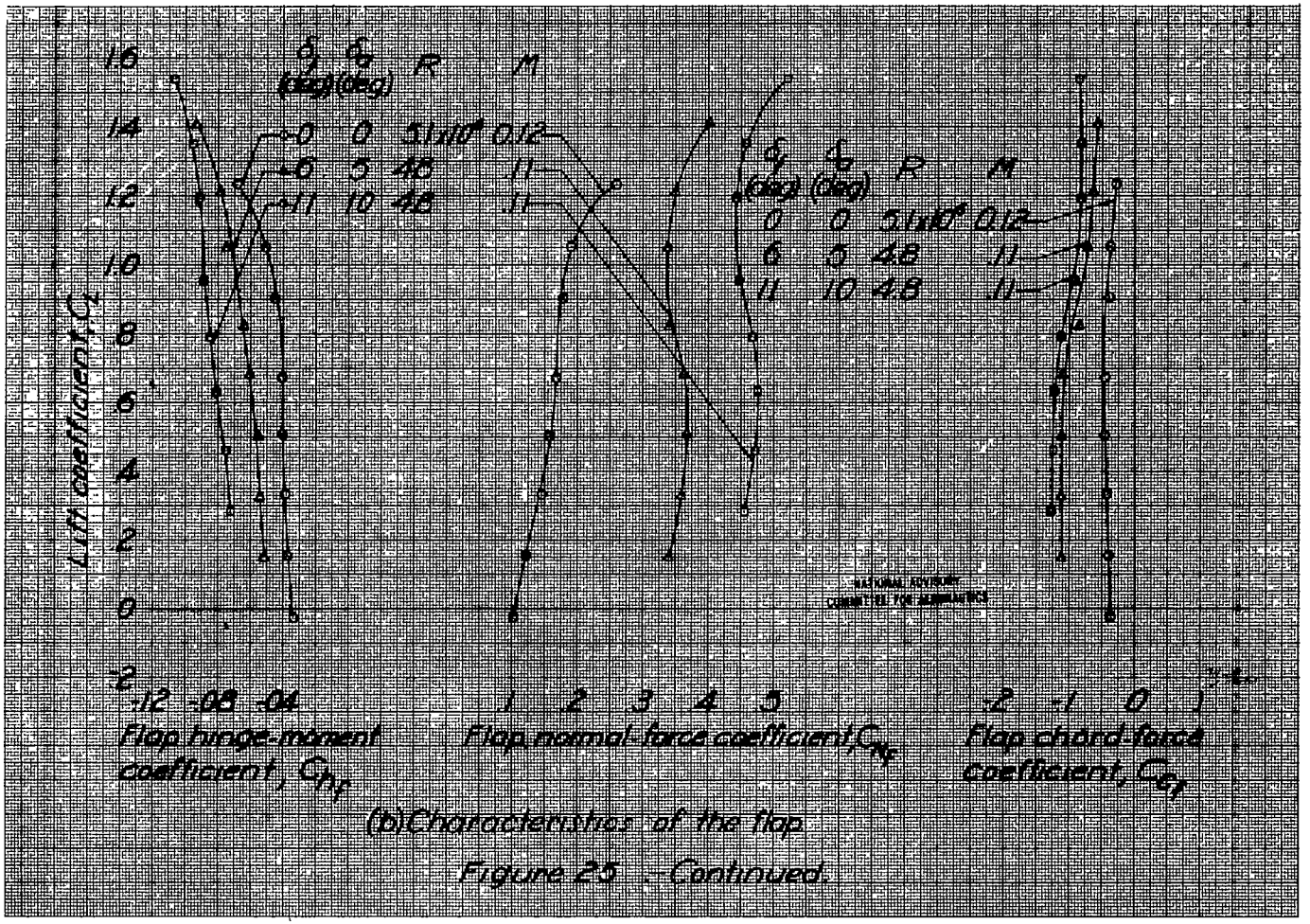

(b) Characteristics of the flap.

Figure 25.—Continued.

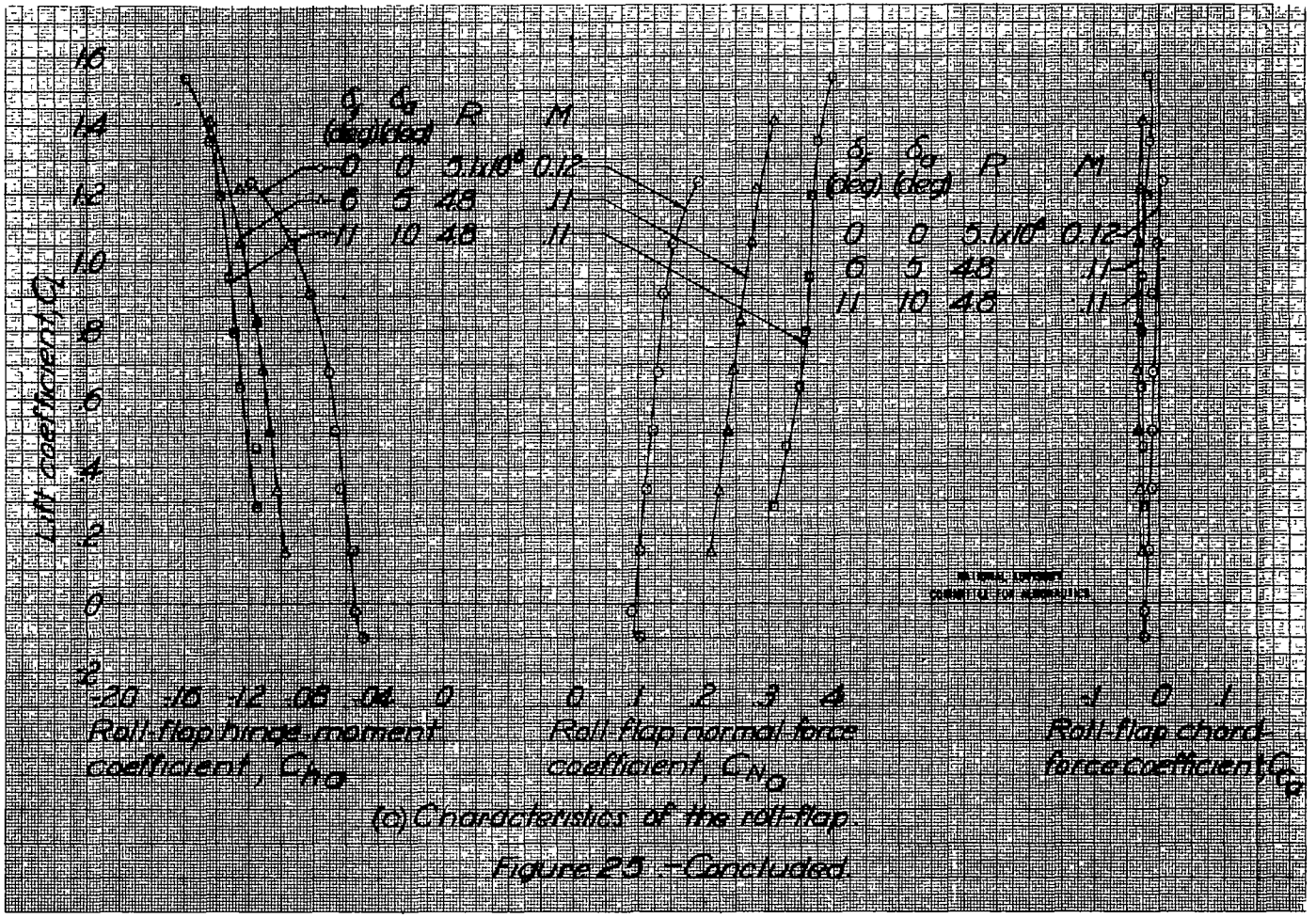

(c) Characteristics of the roll-flap.

Figure 23.—Concluded.

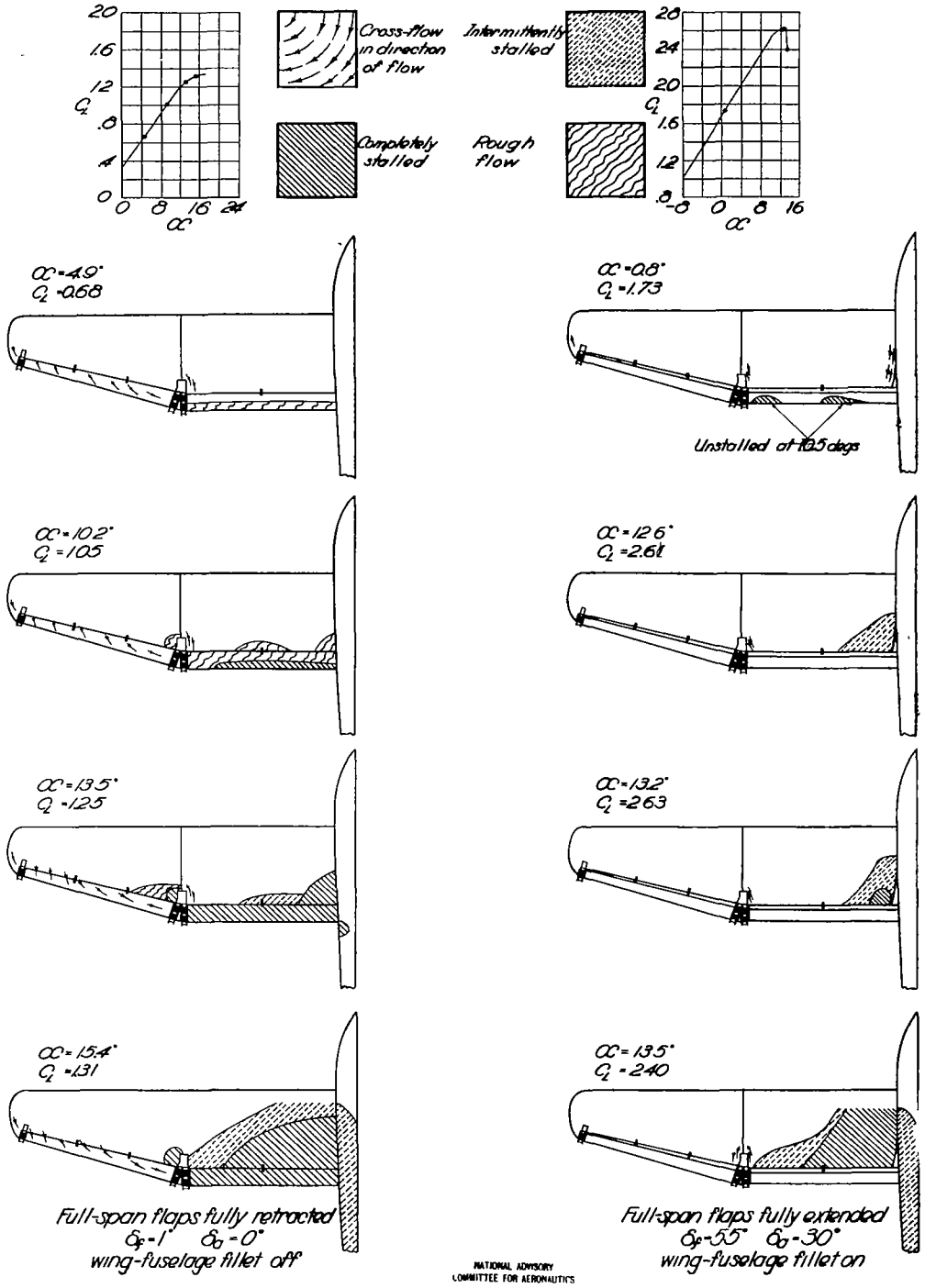

Figure 26.- Stall diagrams of the 0.30-scale XTB2D-1 semispan model at several angles of attack and two flap conditions; standard model configuration with wing-fuselage fillet; $R \approx 5,200,000$; $M \approx 0.12$.

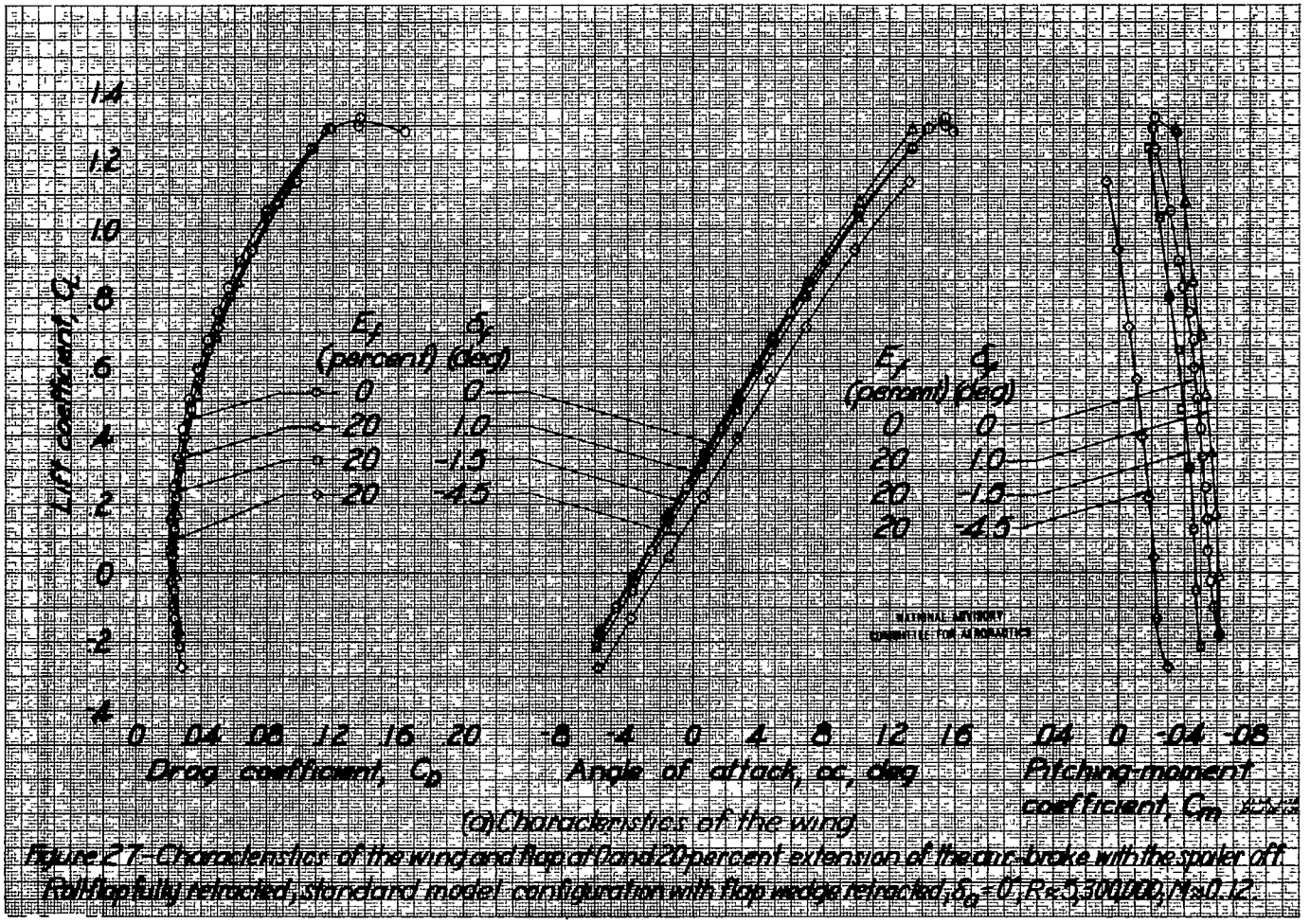

(a) Characteristics of the wing.

Figure 27.- Characteristics of the wing and flap at 0 and 20 percent extension of the arc brake with the spoiler off. Roll flap fully retracted, standard model configuration with flap wedge retracted, $\delta_a = 0$, $R \approx 5,300,000$, $M \approx 0.12$.

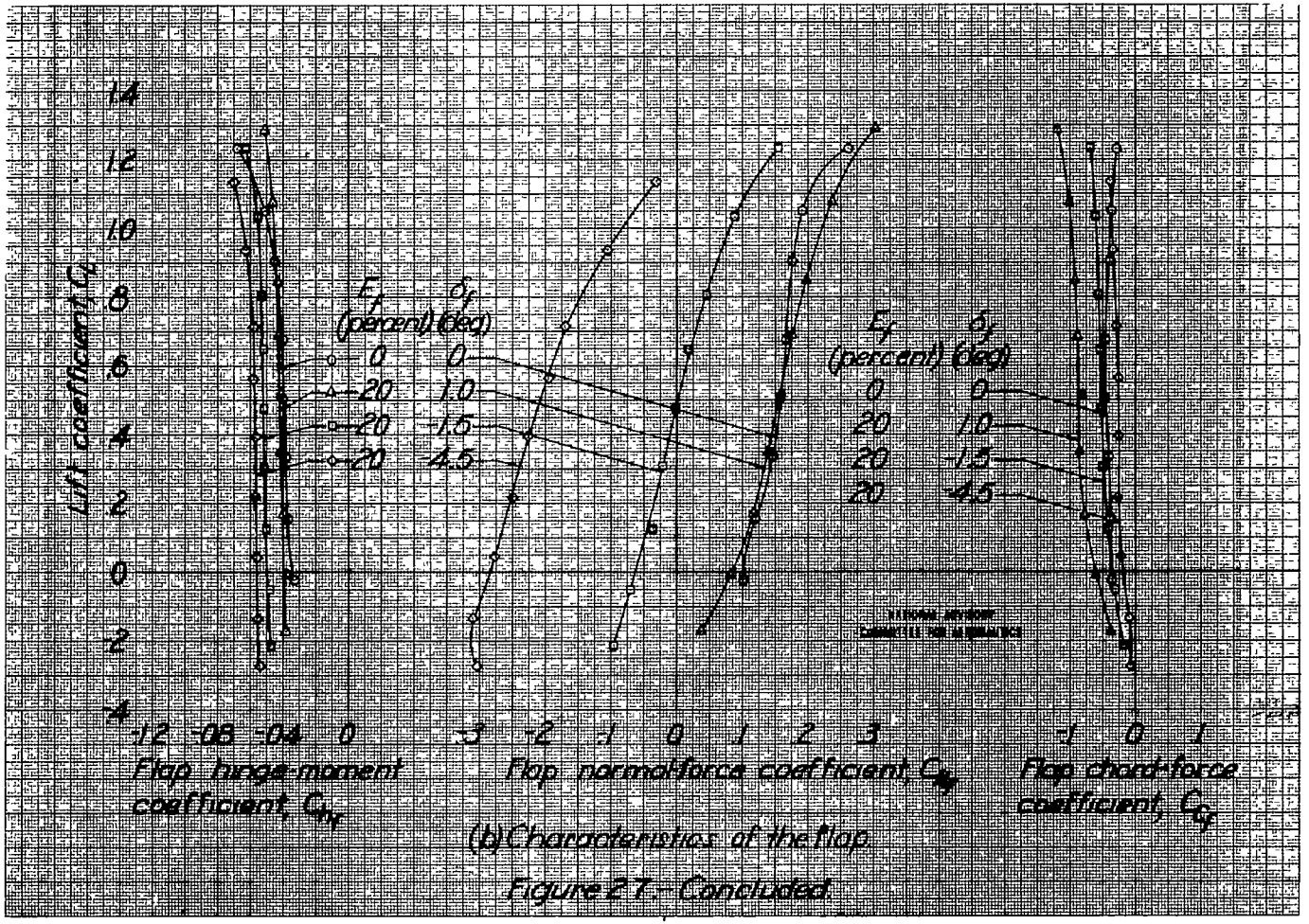

(b) Characteristics of the flap.

Figure 27.- Concluded.

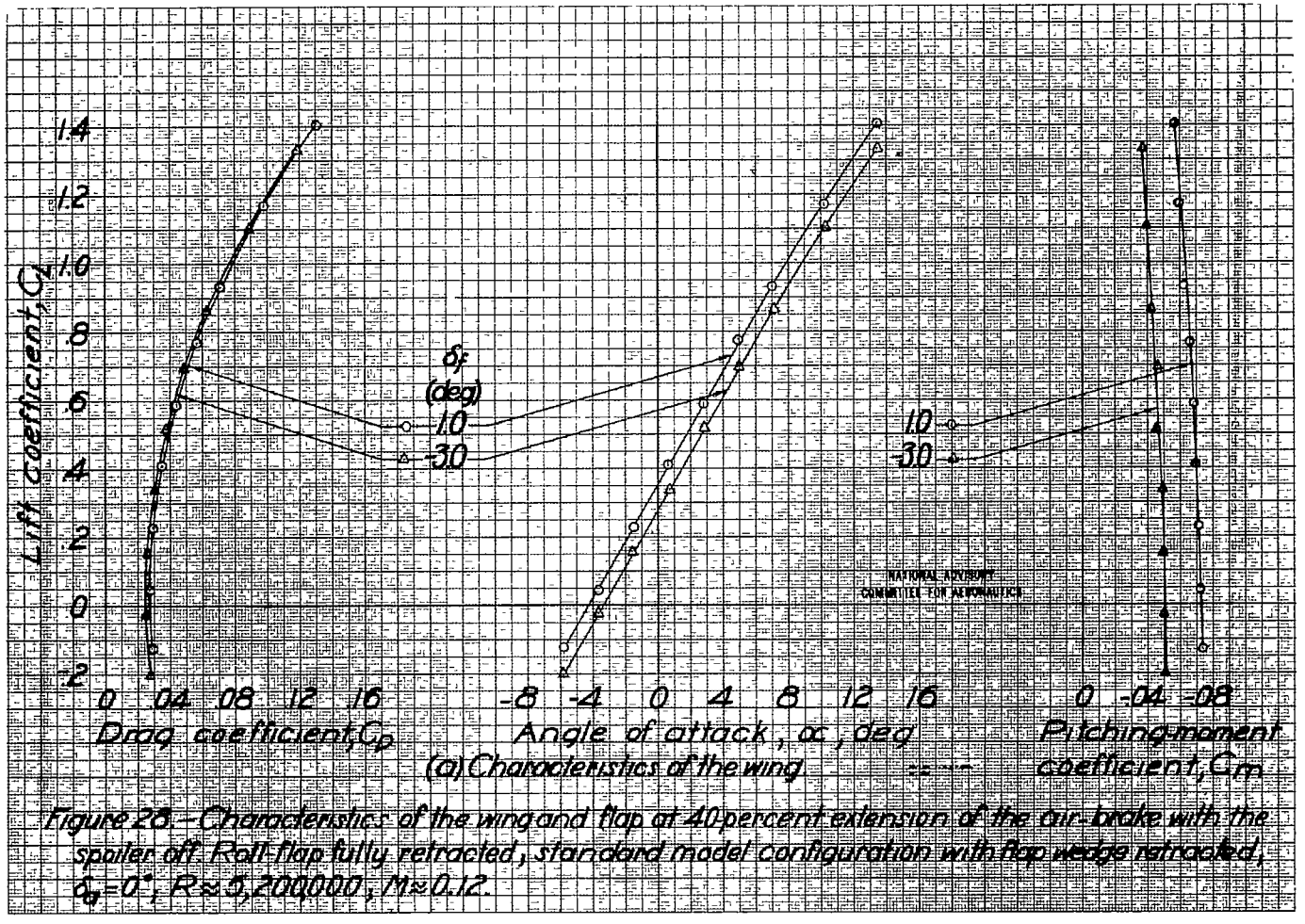

Figure 20.- Characteristics of the wing and flap at 40-percent extension of the air brake with the spoiler off. Roll flap fully retracted, standard model configuration with flap wedge retracted, $\delta_a = 0°$; $R \approx 5{,}200000$; $M \approx 0.12$.

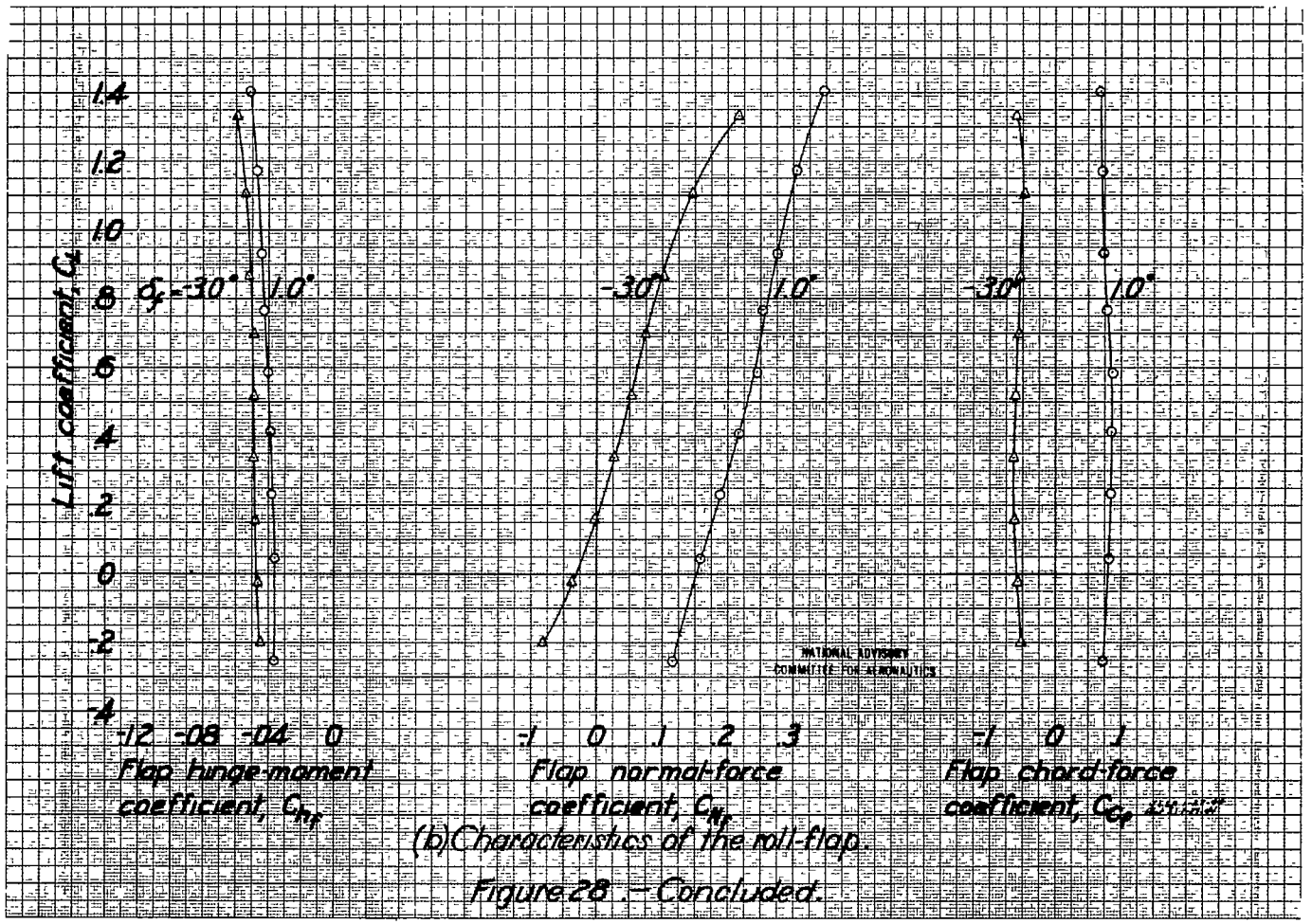

(b) Characteristics of the roll-flap.

Figure 28.—Concluded.

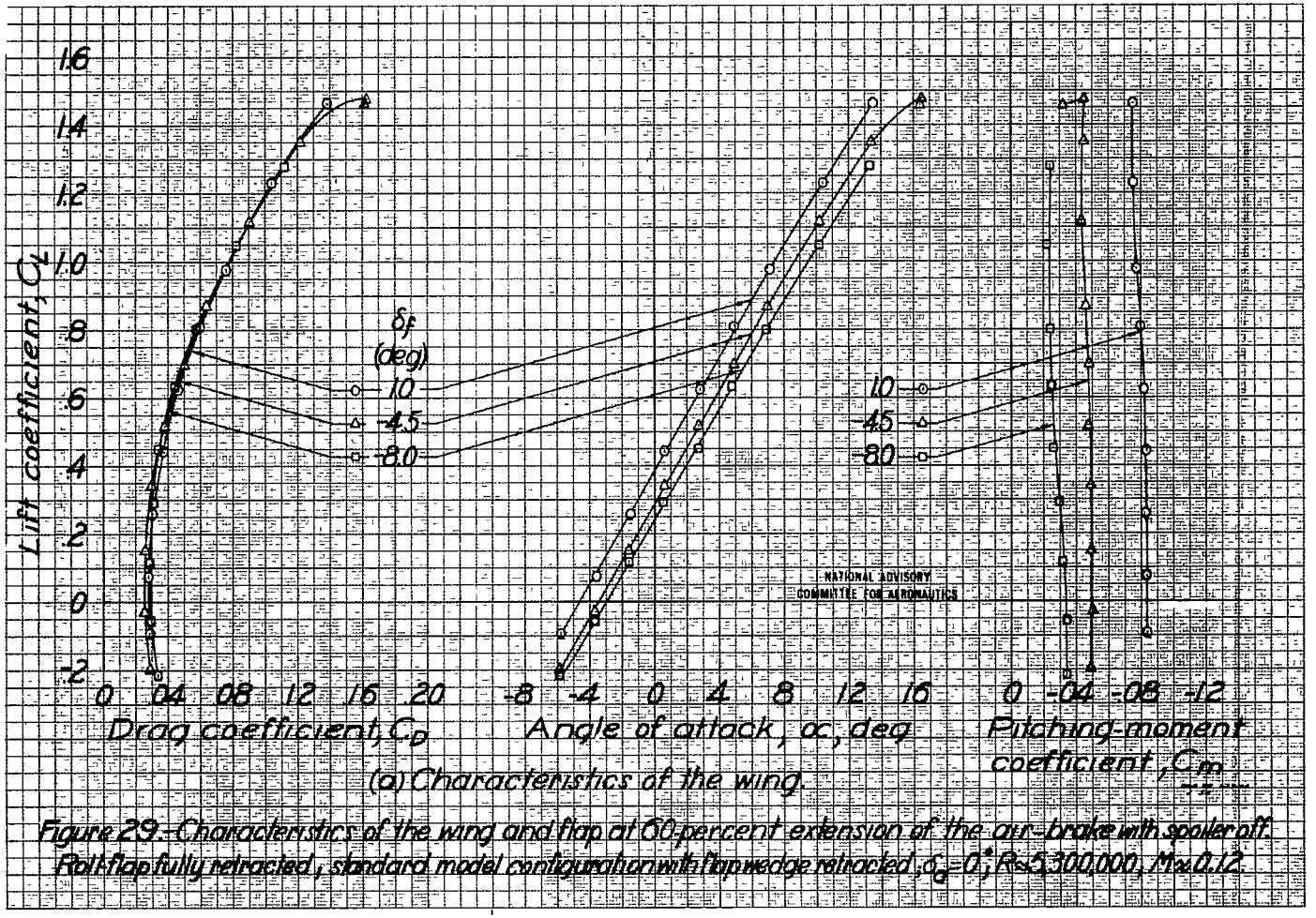

(a) Characteristics of the wing.

Figure 29.- Characteristics of the wing and flap at 60 percent extension of the air-brake with spoiler off. Roll flap fully retracted, standard model configuration with flap wedge retracted, $\delta_a = 0°$; R=5,300,000, M=0.12.

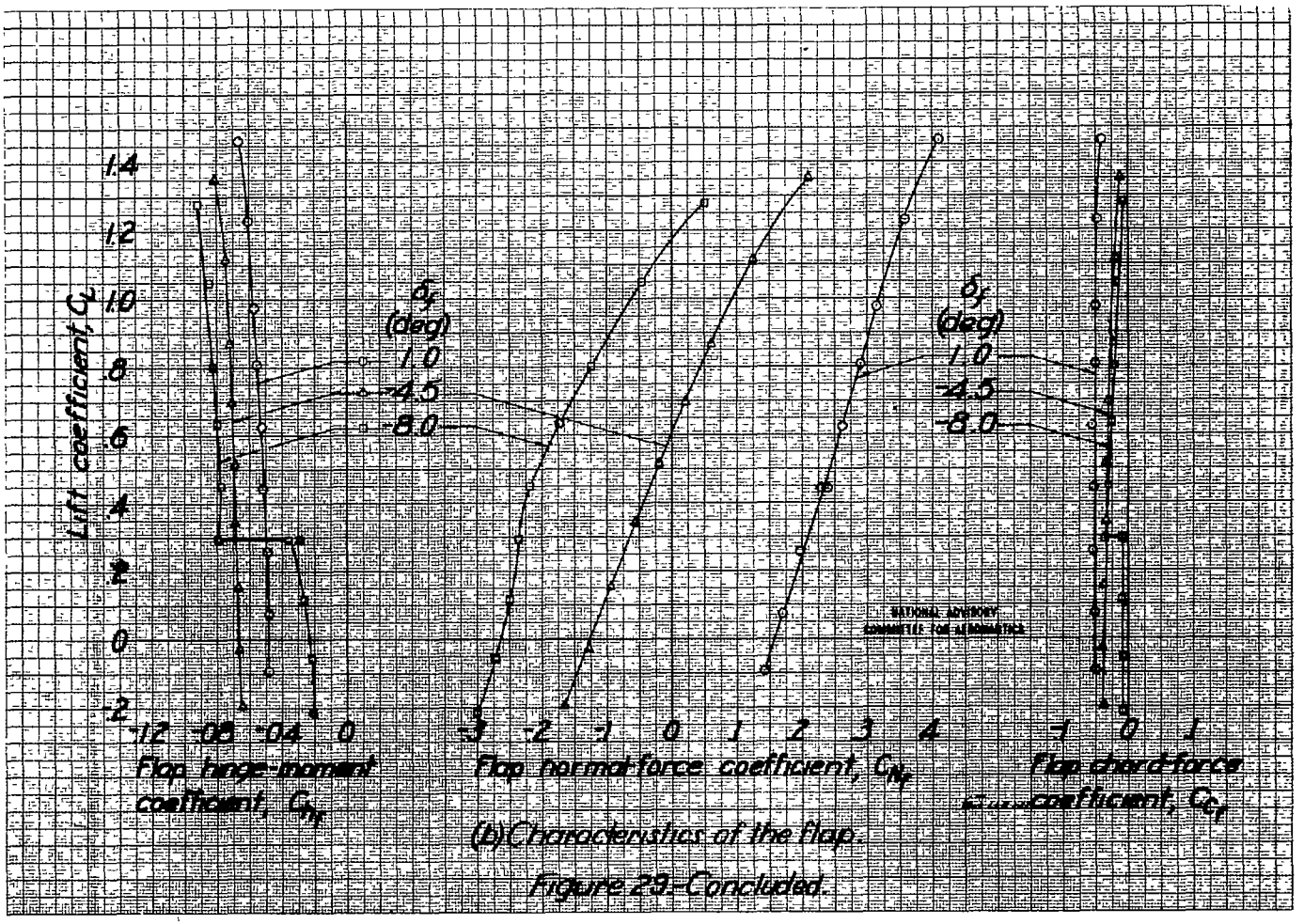

(b) Characteristics of the flap.

Figure 29.- Concluded.

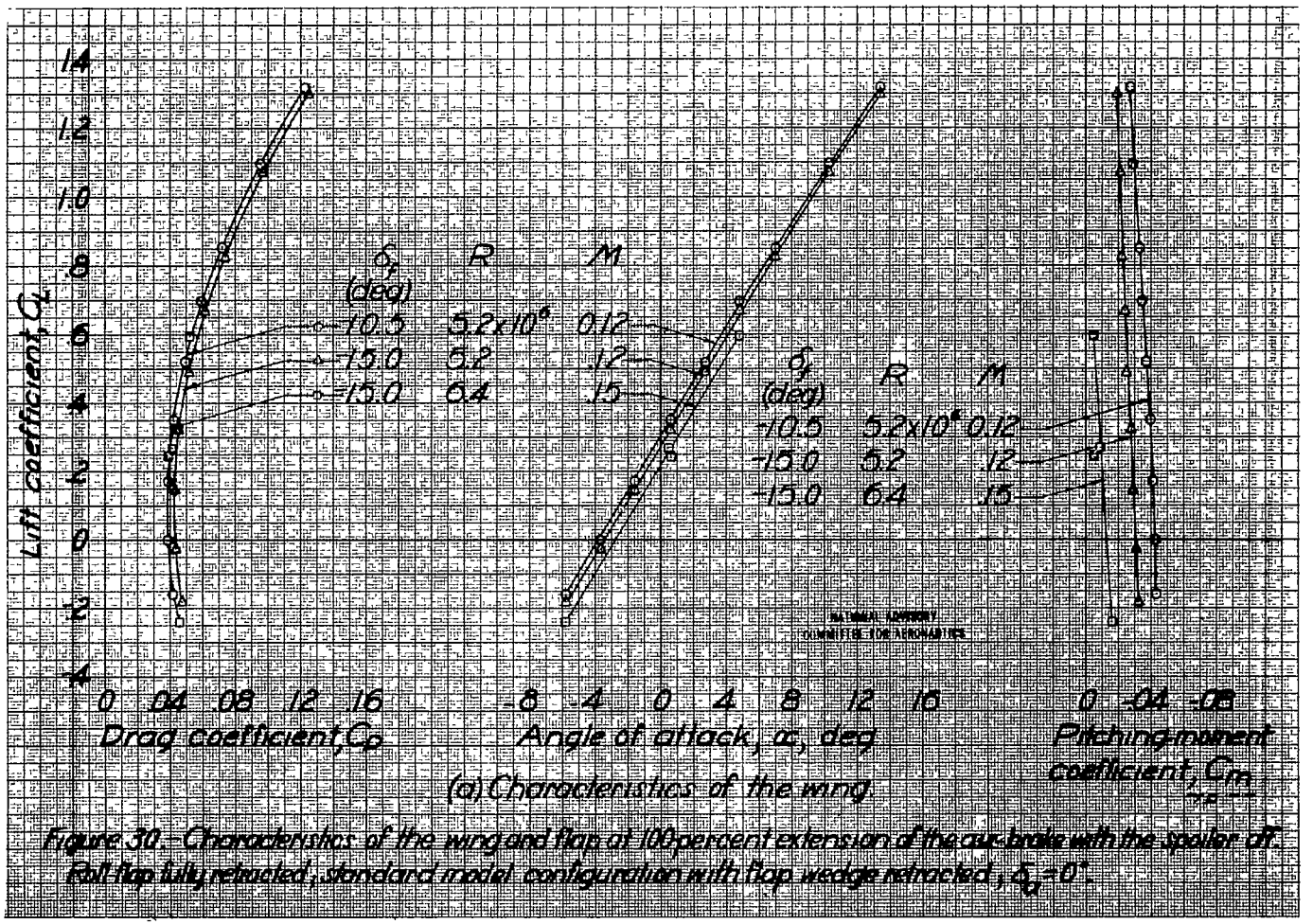

Figure 30.- Characteristics of the wing and flap at 100 percent extension of the aux brake with the spoiler off. Roll flap fully retracted, standard model configuration with flap wedge retracted, $\delta_a = 0°$.

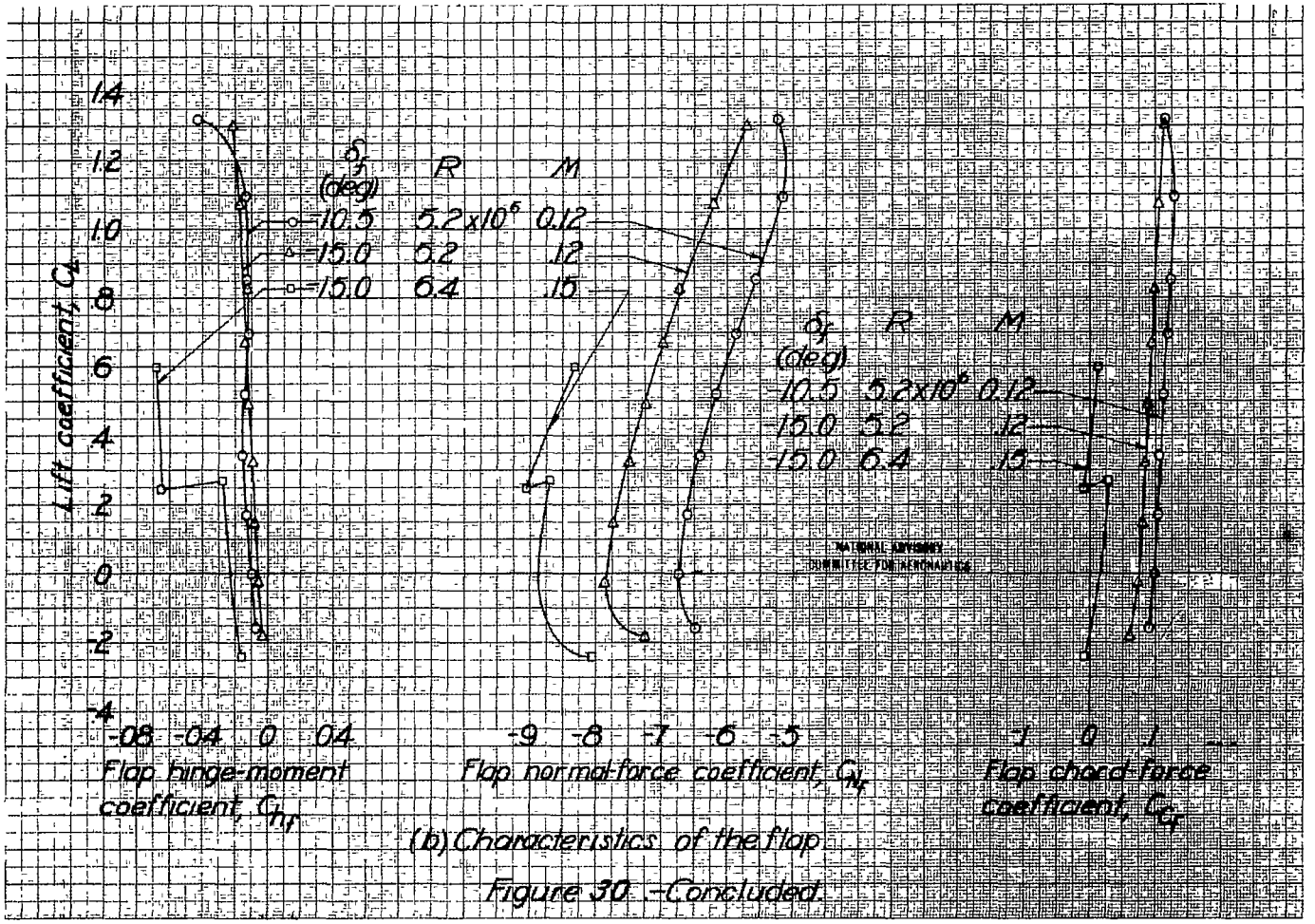

(b) Characteristics of the flap

Figure 30.—Concluded.

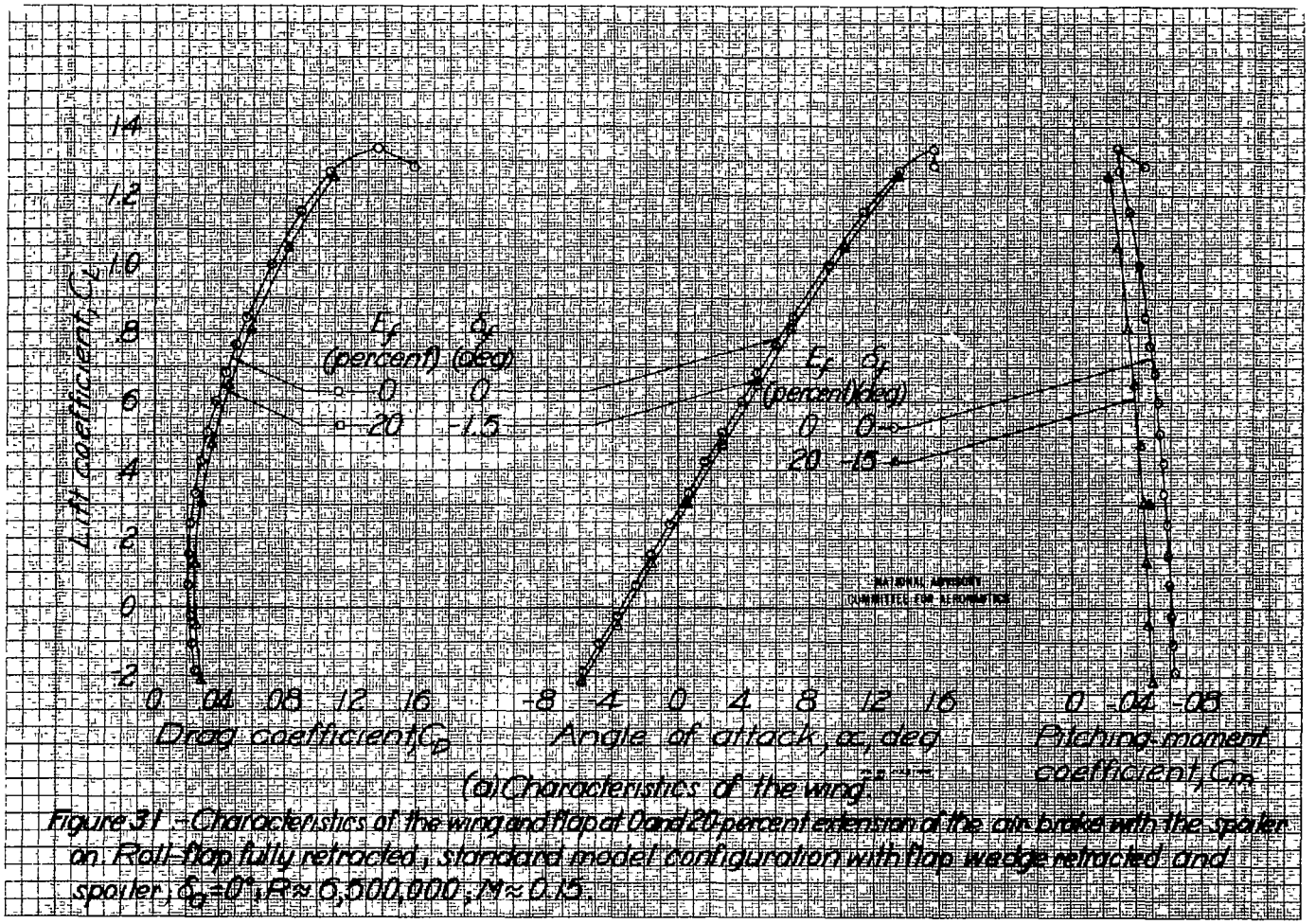

(a) Characteristics of the wing.

Figure 31.- Characteristics of the wing and flap at 0 and 20 percent extension of the air brake with the spoiler on. Roll-flap fully retracted, standard model configuration with flap wedge retracted and spoiler, $\delta_a = 0°$; $R \approx 6{,}500{,}000$; $M \approx 0.15$.

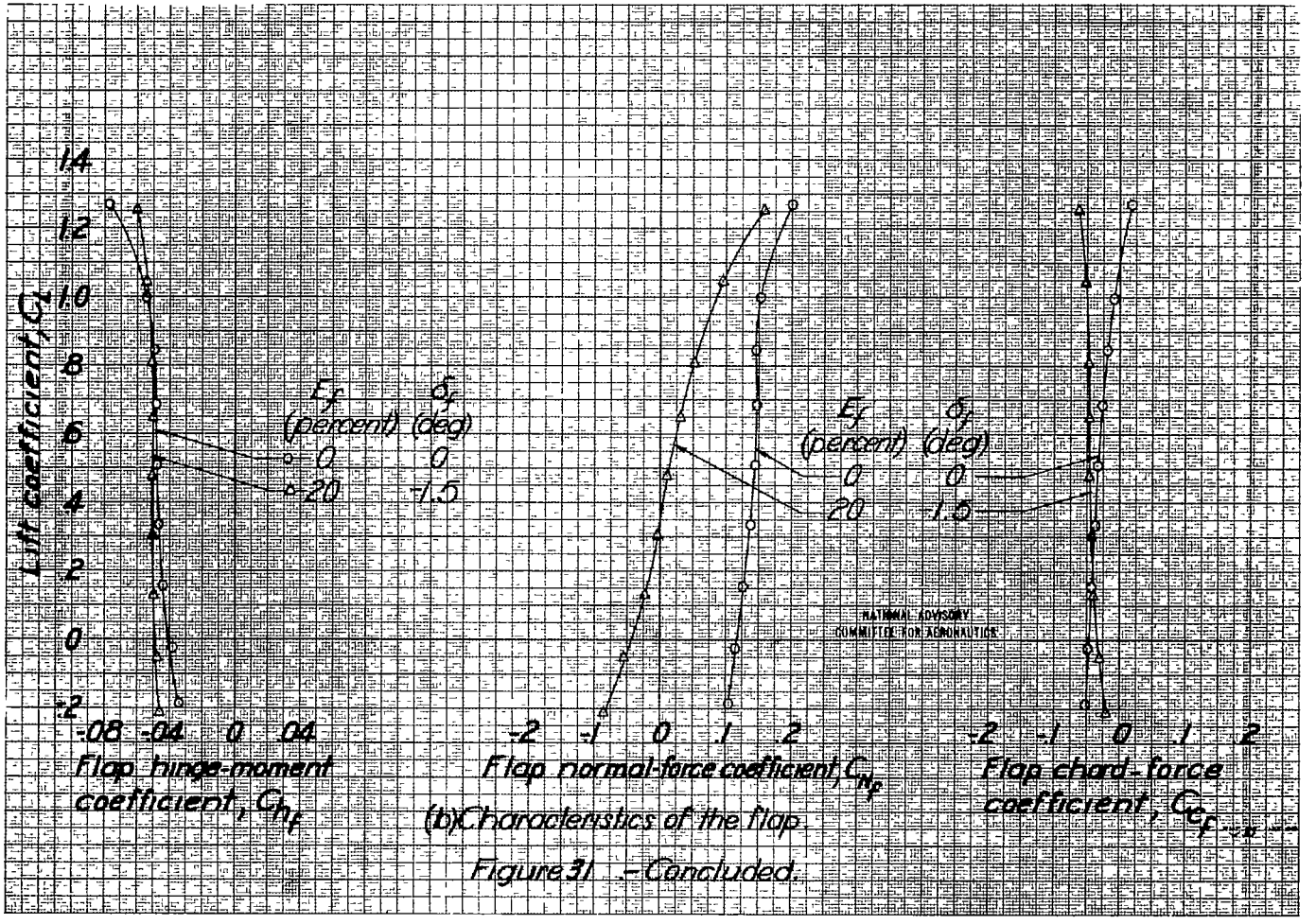

(b) Characteristics of the flap.

Figure 31.—Concluded.

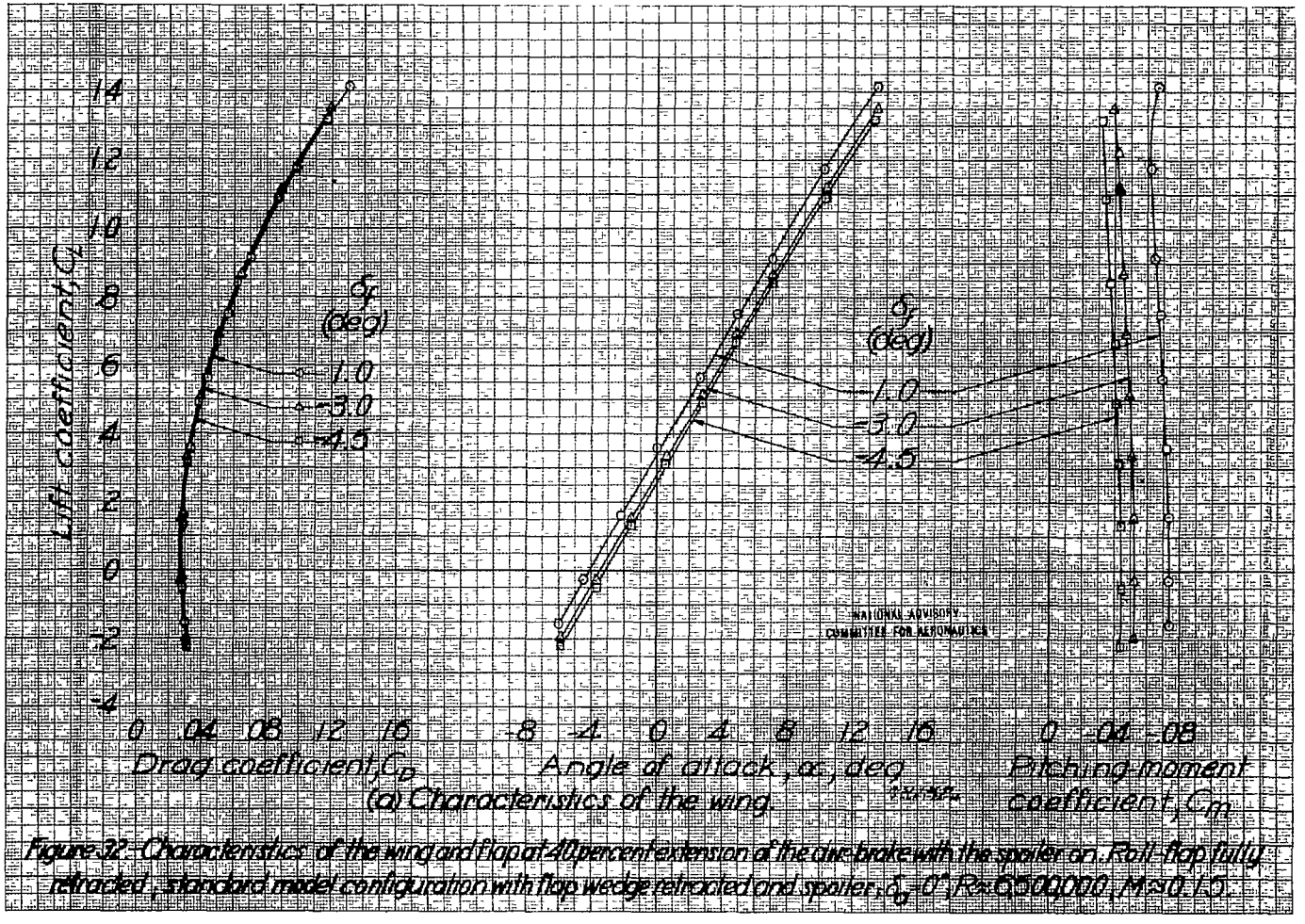

(a) Characteristics of the wing.

Figure 32.- Characteristics of the wing and flap at 40 percent extension of the dive brake with the spoiler on. Roll flap fully retracted; standard model configuration with flap wedge retracted and spoiler, $\delta_s = 0°$; $R = 6{,}500{,}000$; $M = 0.15$.

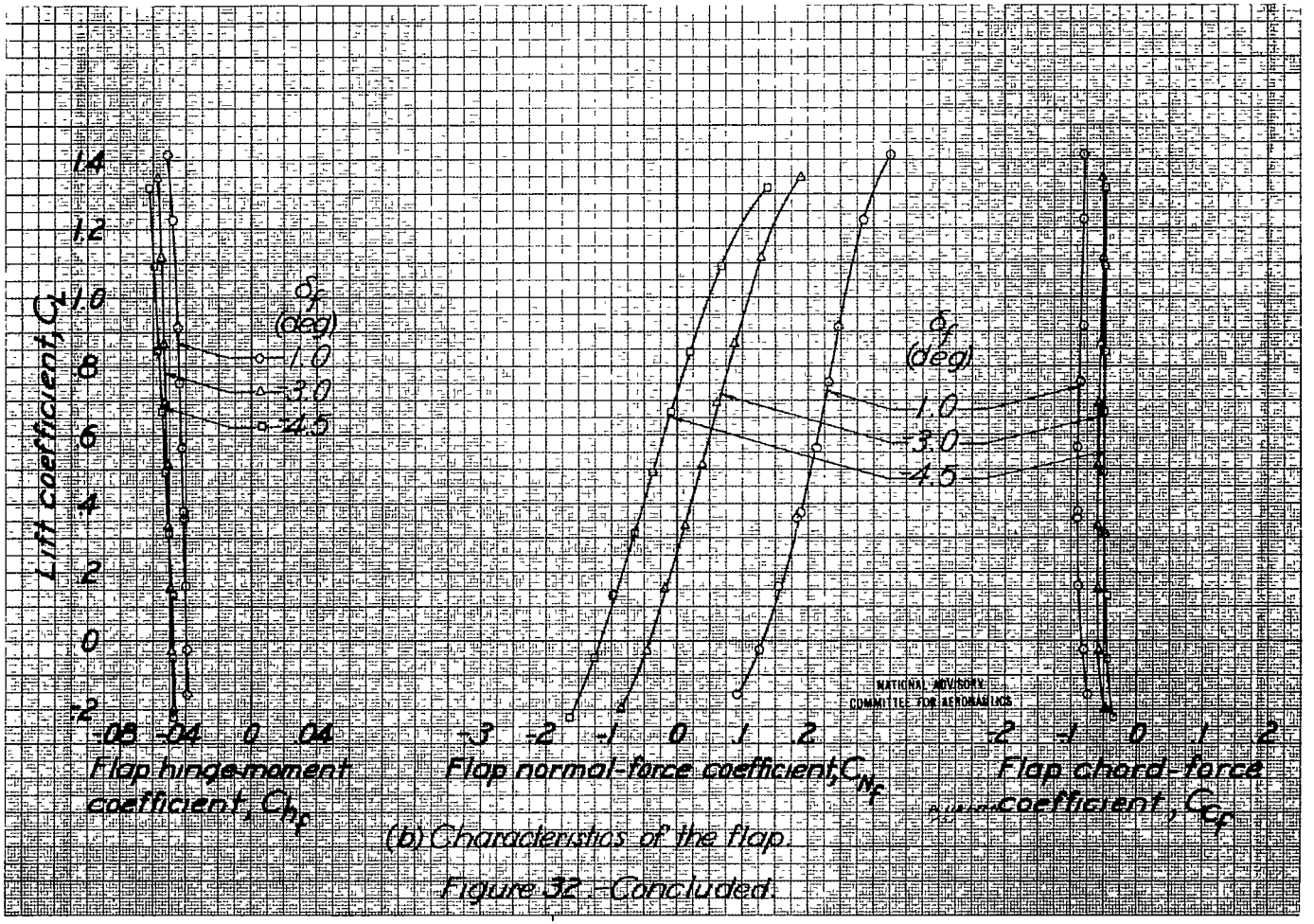

(b) Characteristics of the flap.

Figure 32.—Concluded.

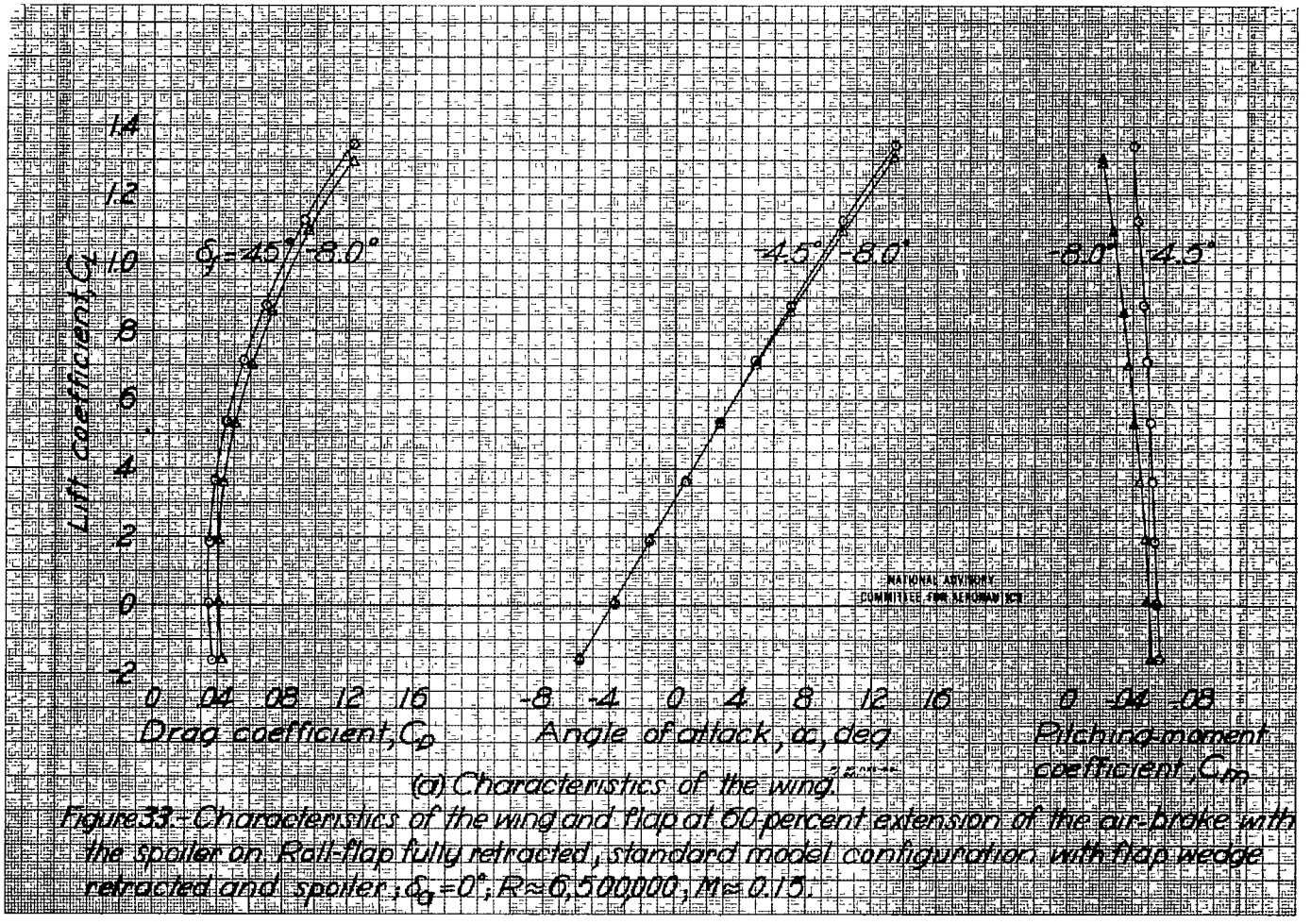

(a) Characteristics of the wing.

Figure 33.- Characteristics of the wing and flap at 60 percent extension of the air brake with the spoiler on. Roll flap fully retracted, standard model configuration with flap wedge retracted and spoiler; $\delta_a = 0°$; $R \approx 6{,}500{,}000$; $M \approx 0.15$.

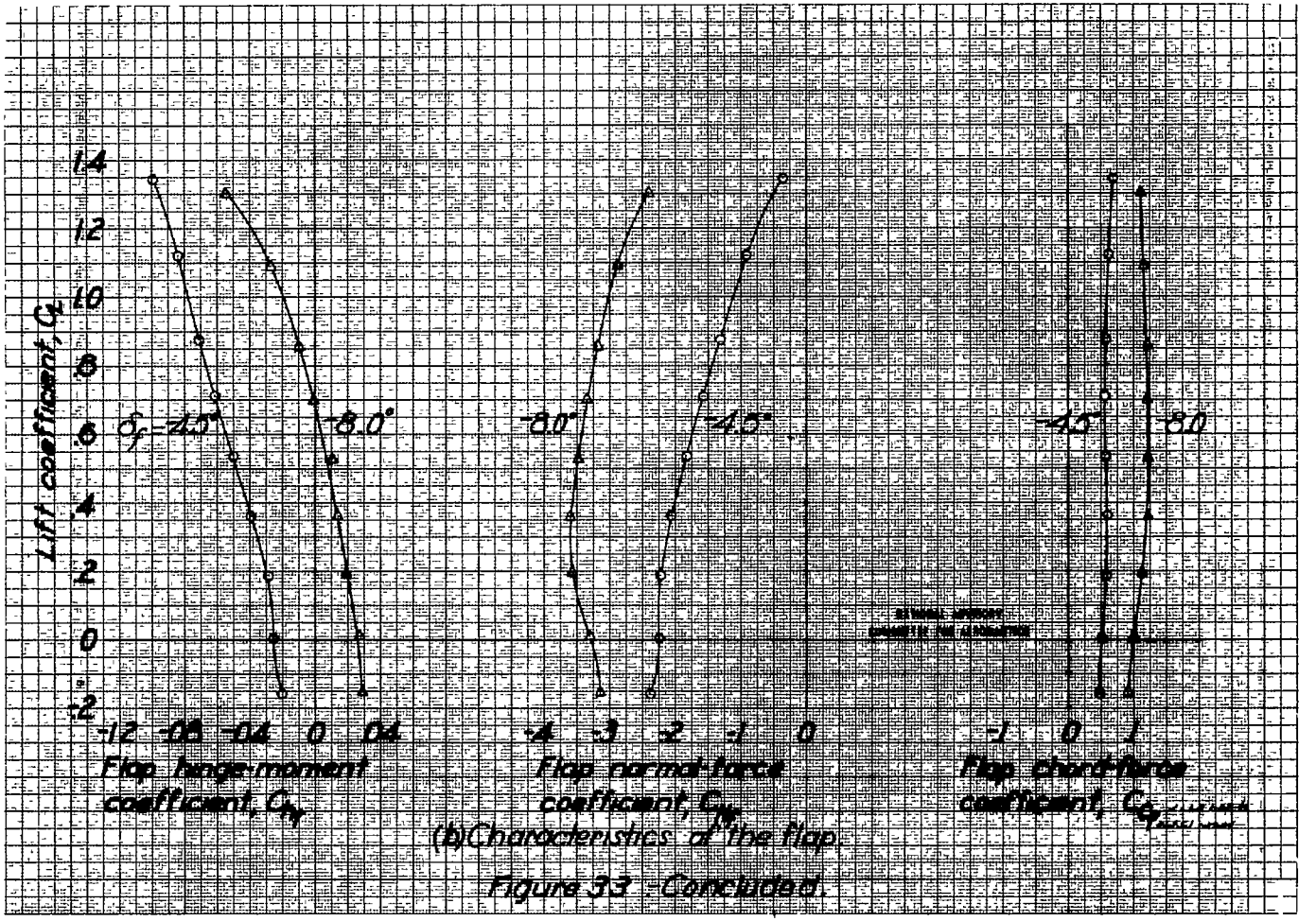

(b) Characteristics of the flap.

Figure 33.- Concluded.

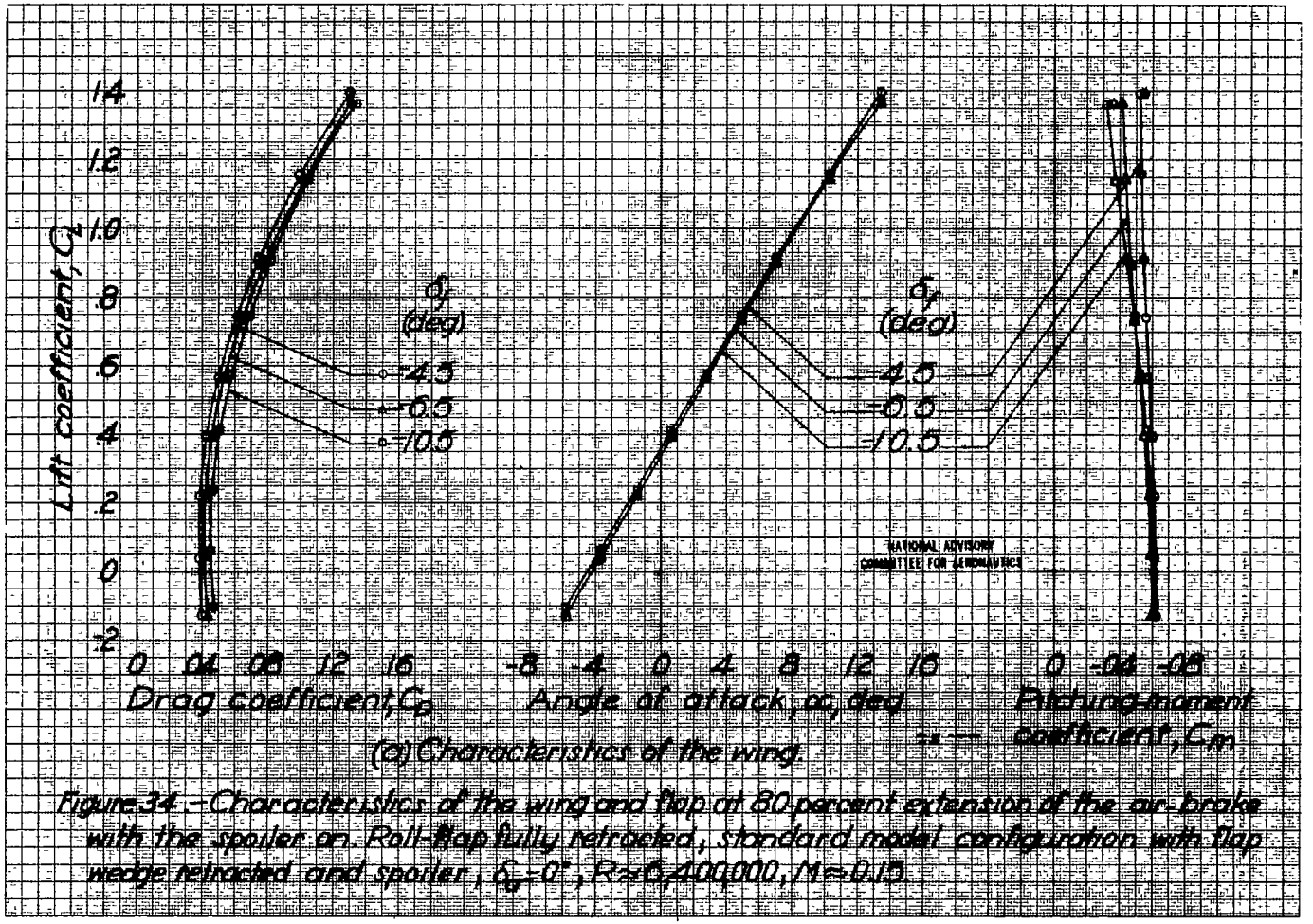

(a) Characteristics of the wing.

Figure 34.- Characteristics of the wing and flap at 80 percent extension of the air-brake with the spoiler on. Roll-flap fully retracted, standard model configuration with flap wedge retracted and spoiler, $\delta_s = 0°$; $R = 6,400,000$, $M = 0.15$.

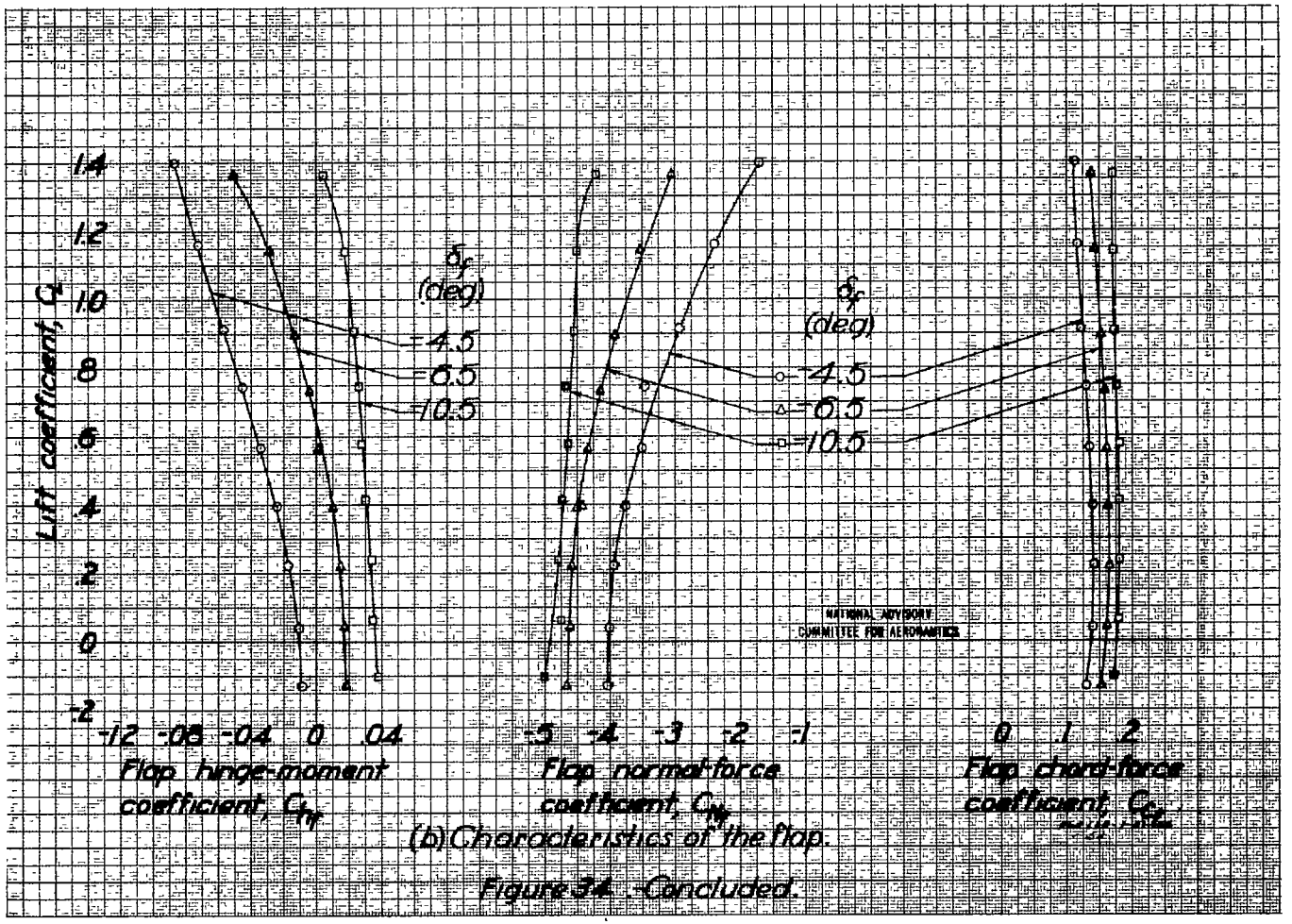

(b) Characteristics of the flap.

Figure 34.- Concluded.

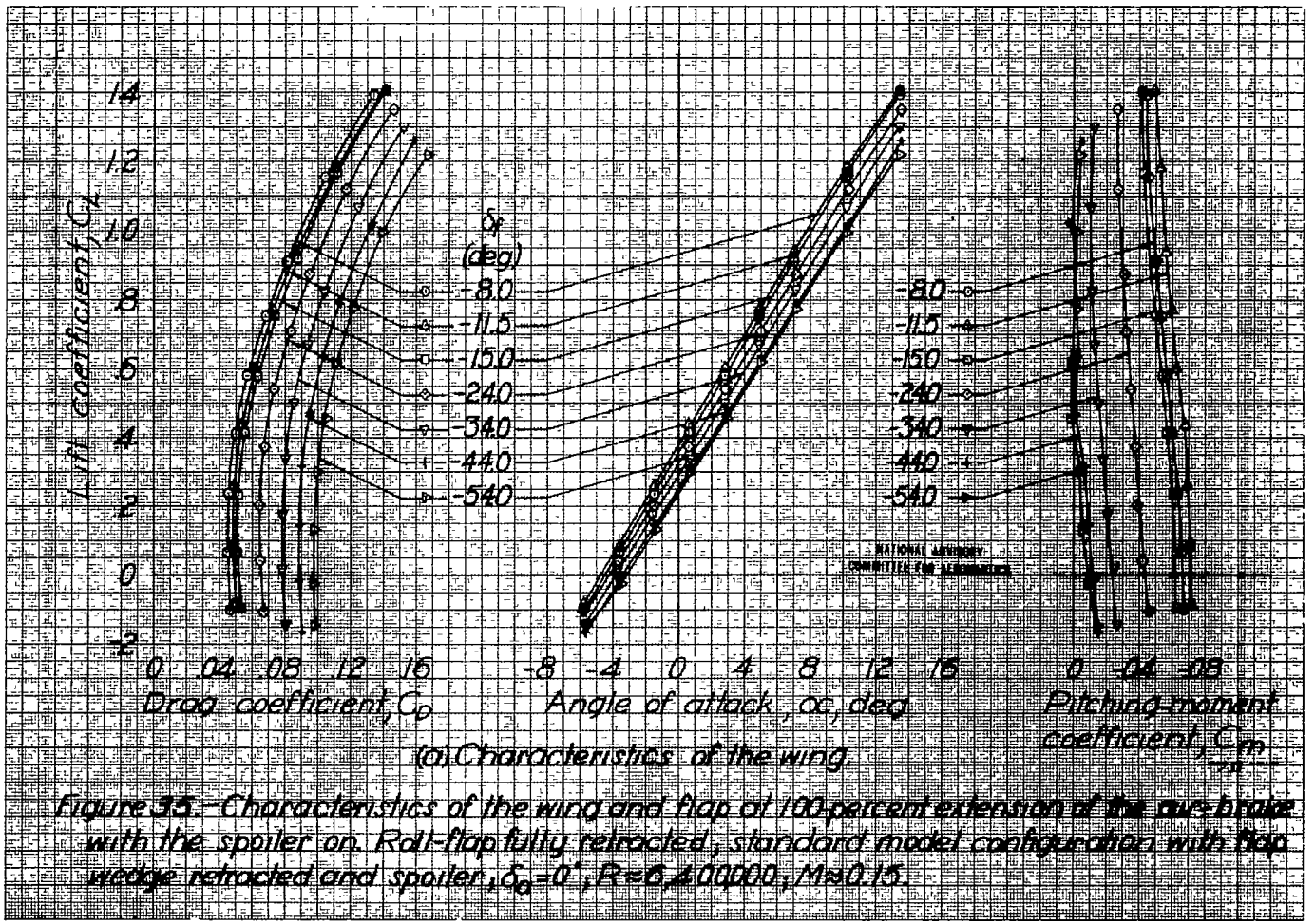

(a) Characteristics of the wing.

Figure 35.- Characteristics of the wing and flap at 100 percent extension of the auto-brake with the spoiler on. Roll-flap fully retracted, standard model configuration with flap wedge retracted and spoiler, $\delta_s = 0°$; $R \approx 6,400000$; $M \approx 0.15$.

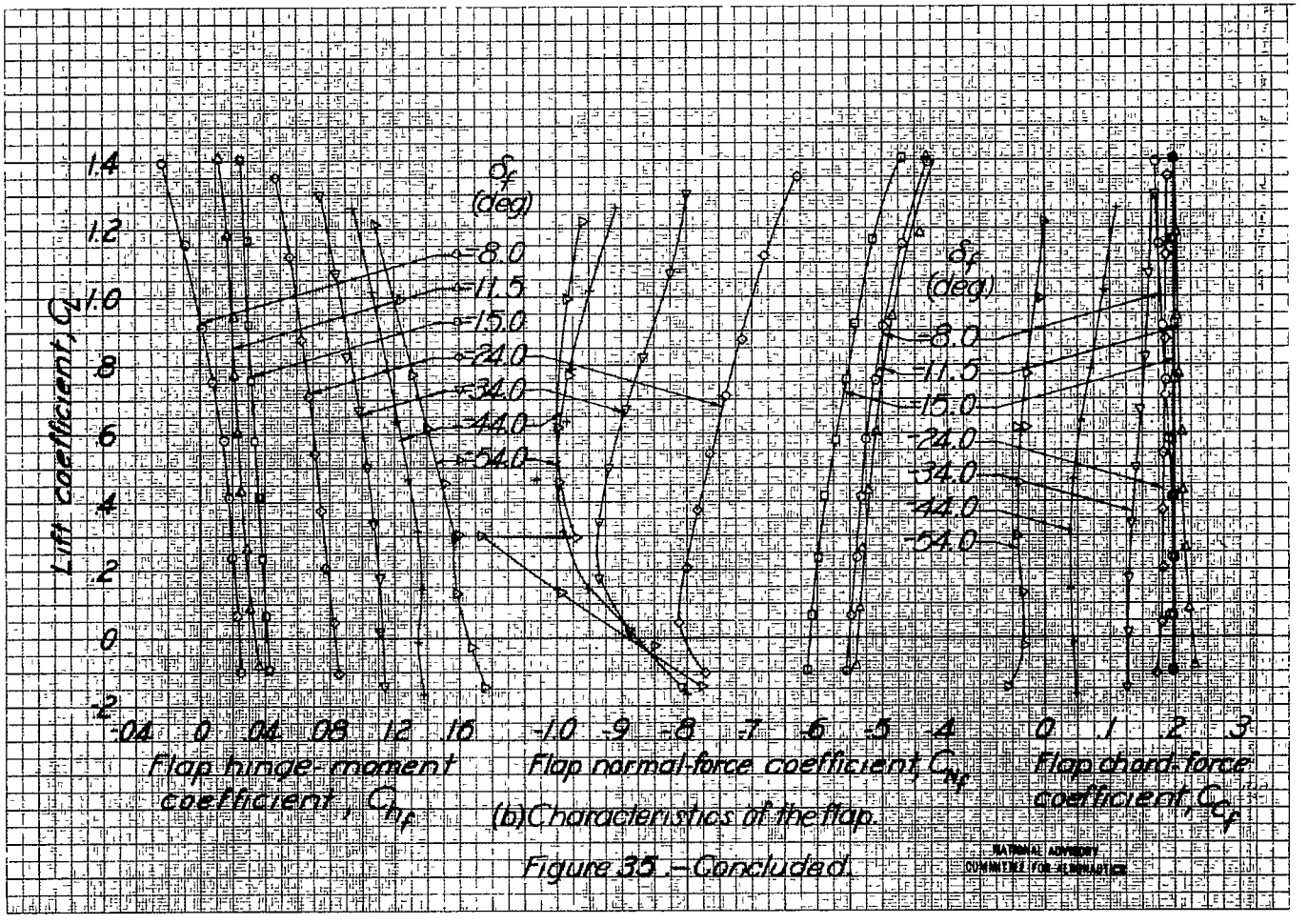

(b) Characteristics of the flap.

Figure 35.—Concluded.

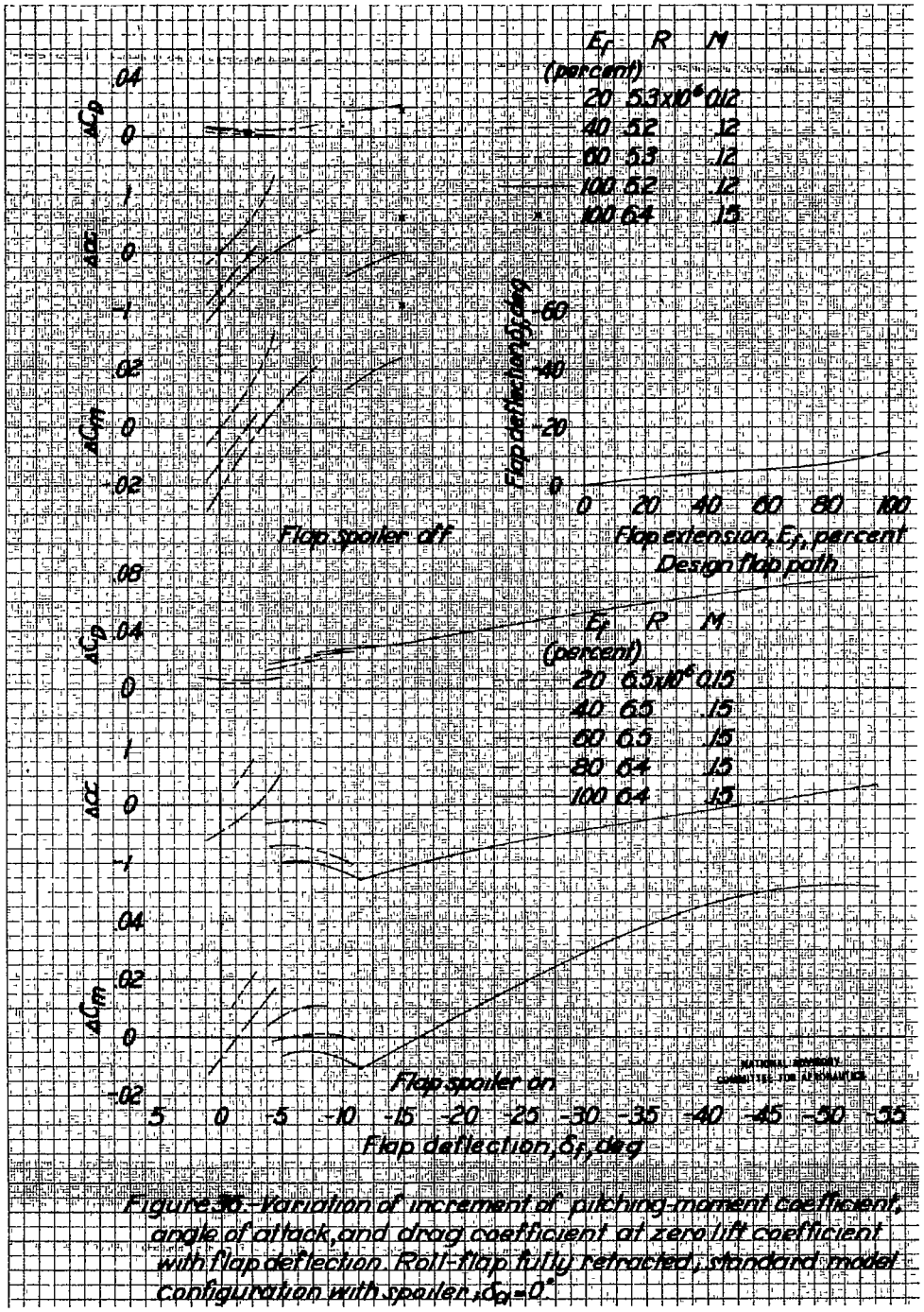

Figure 36.- Variation of increment of pitching-moment coefficient, angle of attack, and drag coefficient at zero lift coefficient with flap deflection. Roll-flap fully retracted; standard model configuration with spoiler, $\delta_a = 0°$.

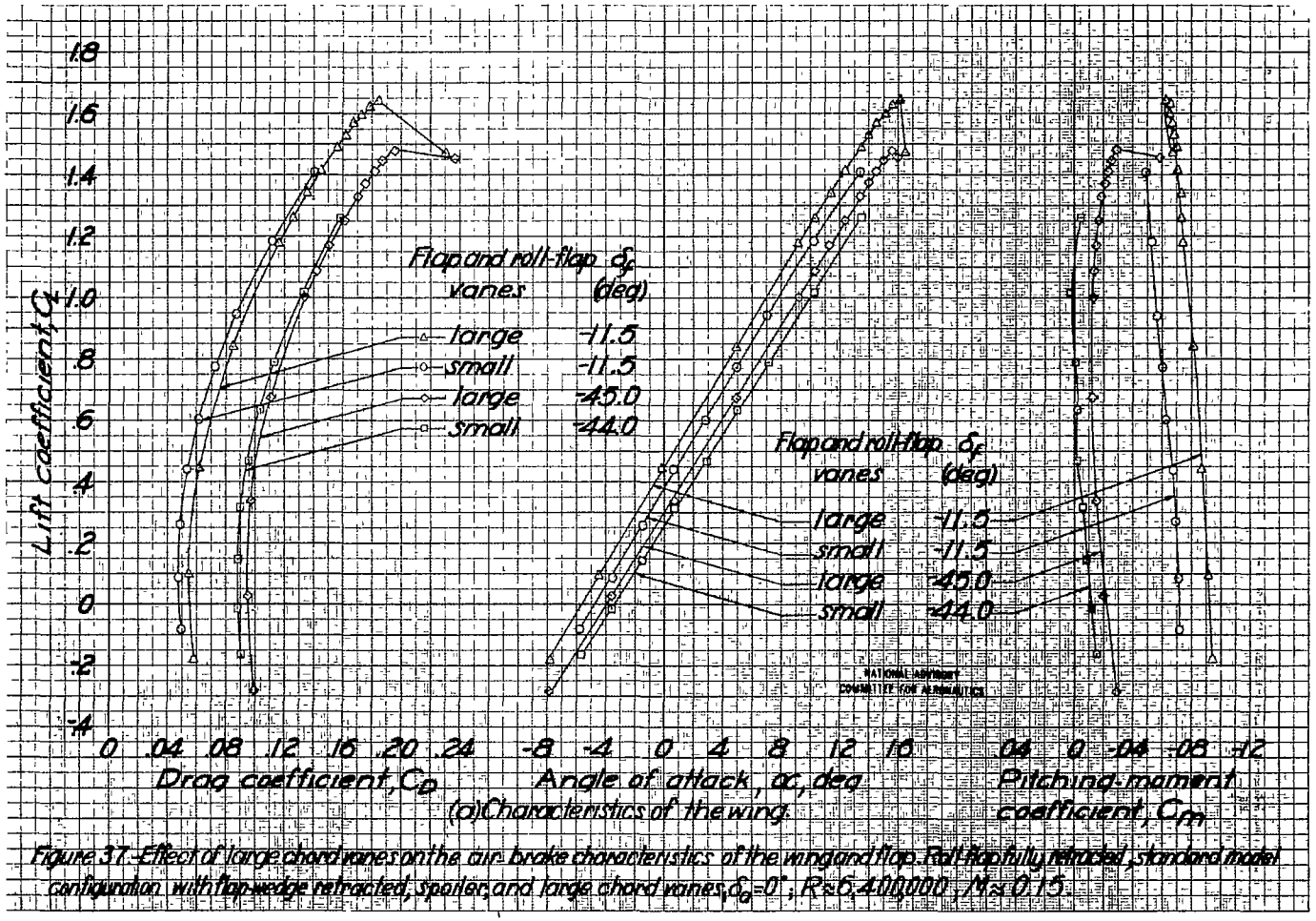

(a) Characteristics of the wing.

Figure 37.- Effect of large chord vanes on the air-brake characteristics of the wing and flap. Roll flap fully retracted; standard model configuration with flap wedge retracted, spoiler, and large chord vanes; $\delta_a = 0°$; $R \approx 6,400,000$; $M \approx 0.15$.

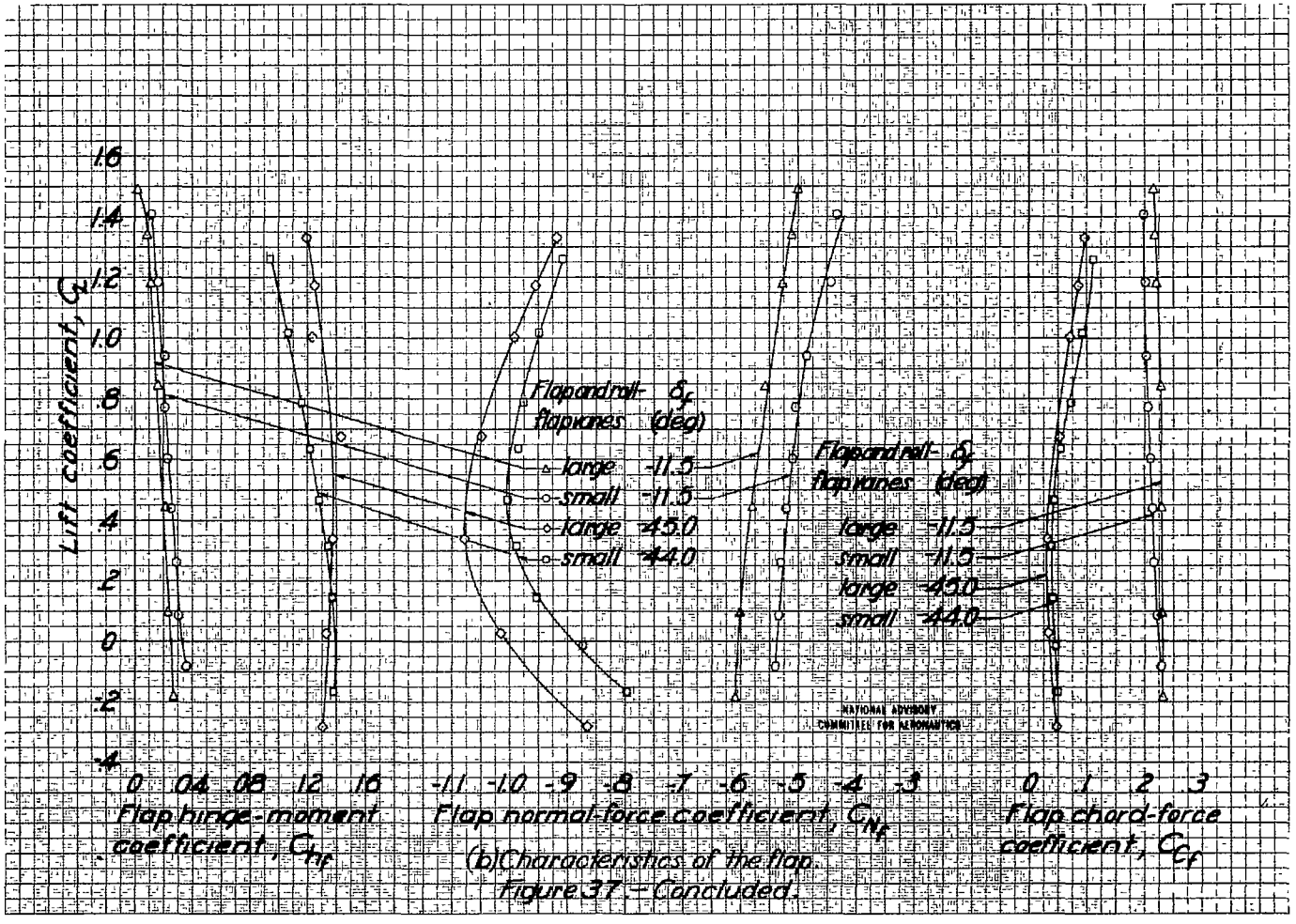

(b) Characteristics of the flap.

Figure 37.—Concluded.